NUREG/CR-6017
SAND93-0528

# Fire Modeling of the Heiss Dampf Reaktor Containment

Prepared by

V. F. Nicolette
Sandia National Laboratories

K. T. Yang
University of Notre Dame

Prepared for
U.S. Nuclear Regulatory Commission

9510310360 950930
PDR NUREG
CR-6017 R PDR

## AVAILABILITY NOTICE

Availability of Reference Materials Cited in NRC Publications

Most documents cited in NRC publications will be available from one of the following sources:

1. The NRC Public Document Room, 2120 L Street, NW., Lower Level, Washington, DC 20555-0001

2. The Superintendent of Documents, U.S. Government Printing Office, P. O. Box 37082, Washington, DC 20402-9328

3. The National Technical Information Service, Springfield, VA 22161-0002

Although the listing that follows represents the majority of documents cited in NRC publications, it is not intended to be exhaustive.

Referenced documents available for inspection and copying for a fee from the NRC Public Document Room include NRC correspondence and internal NRC memoranda; NRC bulletins, circulars, information notices, inspection and investigation notices; licensee event reports; vendor reports and correspondence; Commission papers; and applicant and licensee documents and correspondence.

The following documents in the NUREG series are available for purchase from the Government Printing Office: formal NRC staff and contractor reports, NRC-sponsored conference proceedings, international agreement reports, grantee reports, and NRC booklets and brochures. Also available are regulatory guides, NRC regulations in the *Code of Federal Regulations*, and *Nuclear Regulatory Commission Issuances*.

Documents available from the National Technical Information Service include NUREG-series reports and technical reports prepared by other Federal agencies and reports prepared by the Atomic Energy Commission, forerunner agency to the Nuclear Regulatory Commission.

Documents available from public and special technical libraries include all open literature items, such as books, journal articles, and transactions. *Federal Register* notices, Federal and State legislation, and congressional reports can usually be obtained from these libraries.

Documents such as theses, dissertations, foreign reports and translations, and non-NRC conference proceedings are available for purchase from the organization sponsoring the publication cited.

Single copies of NRC draft reports are available free, to the extent of supply, upon written request to the Office of Administration, Distribution and Mail Services Section, U.S. Nuclear Regulatory Commission, Washington, DC 20555-0001.

Copies of industry codes and standards used in a substantive manner in the NRC regulatory process are maintained at the NRC Library, Two White Flint North, 11545 Rockville Pike, Rockville, MD 20852-2738, for use by the public. Codes and standards are usually copyrighted and may be purchased from the originating organization or, if they are American National Standards, from the American National Standards Institute, 1430 Broadway, New York, NY 10018-3308.

## DISCLAIMER NOTICE

This report was prepared as an account of work sponsored by an agency of the United States Government. Neither the United States Government nor any agency thereof, nor any of their employees, makes any warranty, expressed or implied, or assumes any legal liability or responsibility for any third party's use, or the results of such use, of any information, apparatus, product, or process disclosed in this report, or represents that its use by such third party would not infringe privately owned rights.

NUREG/CR-6017
SAND93-0528

# Fire Modeling of the Heiss Dampf Reaktor Containment

Manuscript Completed: August 1995
Date Published: September 1995

Prepared by

V. F. Nicolette
Sandia National Laboratories
Albuquerque, NM 87185-0835

K.T. Yang
University of Notre Dame
Notre Dame, IN 46556

W. Gleaves, NRC Project Manager

**Prepared for**
**Division of Engineering Technology**
**Office of Nuclear Regulatory Research**
**U.S. Nuclear Regulatory Commission**
**Washington, DC 20555-0001**
**NRC Job Code L1330**

# Abstract

This report summarizes Sandia National Laboratories' participation in the fire modeling activities for the German Heiss Dampf Reaktor (HDR) containment building, under the sponsorship of the United States Nuclear Regulatory Commission. The purpose of this report is twofold: 1) to summarize Sandia's participation in the HDR fire modeling efforts, and 2) to summarize the results of the international fire modeling community involved in modeling the HDR fire tests.

Calculations were conducted for an HDR oil fire test using the COMPBRN zone model, and the University of Notre Dame fire field model. COMPBRN had difficulty simulating the fire environment beyond the first 4 minutes following ignition due to instabilities resulting from high wall, ceiling, and hot gas layer temperatures. The Notre Dame fire model results indicate reasonable (and, in some cases, excellent) agreement with the experimental data. Discrepancies between calculation and experiment are explainable in terms of leakage around the doorway of the fire room.

Calculations were also conducted for an HDR cable fire test using the COMPBRN model. Results were obtained for the first 9 minutes of the fire (up to the point at which the door to the fire room was opened in the test). The strengths of COMPBRN are seen to be its ability to model the transient ignition and burning of cable tray fires in pre-flashover compartments.

Additional comments on the state of fire modeling and trends in the international fire modeling community are also included. It is noted that although the trend internationally in fire modeling is toward the development of the more complex fire field models, each type of fire model has something to contribute to the understanding of fires in nuclear power plants.

# Table of Contents


Abstract ..... iii
Table of Contents ..... v
List of Tables and Figures ..... vi
Acknowledgements ..... vii

Executive Summary ..... 1

1 Introduction and Background ..... 3
1.1 HDR Fire Experiments ..... 3
1.2 HDR Fire Modeling History ..... 3
1.3 Sandia's Role in HDR Fire Tests ..... 4
1.4 Brief Overview of Fire Modeling of Nuclear Power Plants ..... 4

2 E41.7 Fire Experiment ..... 8
2.1 Overview of E41.7 Experiment ..... 8
2.2 E41.7 Zone Model Calculations Using COMPBRN ..... 8
2.2.1 E41.7 COMPBRN Assumptions and Input ..... 8
2.2.2 E41.7 COMPBRN Results ..... 9
2.3 E41.7 Field Model Calculations ..... 12
2.3.1 E41.7 Field Model Assumptions and Input ..... 13
2.3.2 E41.7 Field Model Results ..... 14

3 E42.2 Fire Experiment ..... 18
3.1 Overview of E42.2 Experiment ..... 18
3.2 E42.2 Zone Model Calculations Using COMPBRN ..... 18
3.2.1 E42.2 COMPBRN Assumptions and Input ..... 18
3.2.2 E42.2 COMPBRN Results ..... 19

4 Other HDR Fire Modeling Efforts ..... 28
4.1 E41.7 Participants ..... 28
4.2 E41.7 Calculations by Other Participants ..... 29
4.3 E42.2 Participants ..... 29
4.4 E42.2 Calculations by Other Participants ..... 31

5 Summary ..... 35
5.1 E41.7 Lessons Learned ..... 35
5.2 E42.2 Lessons Learned ..... 35
5.3 General Observations from HDR Fire Modeling ..... 36

6 References ..... 38

Appendix A: Brief Description of Fire Models Used by Other HDR Participants ... A-1

Appendix B: University of Notre Dame Field Model Calculations for HDR test E41.7 ..... B-1

Appendix C: University of Notre Dame Field Model Calculations for HDR test E41.5 ..... C-1

# List of Tables

Table 1: COMPBRN Results for E41.7 Test ..... 11
Table 2: Additional E41.7 Calculations ..... 13
Table 3: Cable Tray Ignition/Temperature ..... 25
Table 4: E41.7 Participants ..... 28
Table 5: HDR E4[illegible] 2 Calculation Participants
(Originally Interested) ..... 32
Table 6: Fire Models for ISP ..... 33

# List of Figures

Figure 1: The HDR Containment Building ..... 4
Figure 2: Zone Fire Model Example ..... 6
Figure 3: Control Volume Fire Model Example ..... 7
Figure 4: Fire Field Model Example ..... 7
Figure 5: E41.7 COMPBRN Input Deck ..... 10
Figure 6: NDFM E41.7 Geometric Model ..... 13
Figure 7: E41.7 CT5204 Temperature ..... 16
Figure 8: E41.7 CT5246 Temperature ..... 16
Figure 9: E41.7 CT5290 Temperature ..... 17
Figure 10: E41.7 CT5294 Temperature ..... 17
Figure 11: E42.2 Cable Tray Layout Diagram ..... 19
Figure 12: E42.2 COMPBRN III Input Deck ..... 20
Figure 13: COMPBRN E42.2 Fire Power Output ..... 26
Figure 14: COMPBRN E42.2 Fire Total Energy Output ..... 26
Figure 15: COMPBRN E42.2 Fuel Mass Loss Rate ..... 27
Figure 16: COMPBRN E42.2 Hot Gas Layer Temperatures ..... 27
Figure 17: E41.7 Comparison of Models to Experiment ..... 30
Figure 18: E42.2 Comparison of Models to Experiment ..... 34

# Acknowledgements

The authors wish to thank Steve Nowlen, of Sandia National Laboratories for managing this project.

This work has been funded entirely by the United States Nuclear Regulatory Commission (USNRC) under FIN L1330. The authors are especially grateful to Bill Farmer (USNRC, ret.), who provided much support and enthusiasm for this international cooperative program.

The German nuclear safety research institutions were very gracious in permitting and encouraging us to join in this unique opportunity. 'Vielen dank' to Herr K. Müller (KfK), Herr Liemersdorf (GRS), and Herr L. Wolf (Battelle, Frankfurt), and all of their colleagues. A special thank you goes to Herr K. Müller (KfK) for arranging all of the meetings and coordinating the many researchers around the world involved in this project.

The authors would like to take this opportunity to thank the many fire modeling researchers involved in this effort for their interest and helpful discussions related to fire modeling of the HDR containment.

The authors gratefully acknowledge the efforts of graduate students Q. Xia and H. J. Huang at the University of Notre Dame for performing the field model calculations referred to herein.

# Executive Summary


The Heiss Dampf Reaktor (HDR) is a decommissioned experimental nuclear reactor in the Federal Republic of Germany. The German nuclear reactor safety authority, Gesellschaft für Anlagen und Reaktorsicherheit (GRS), has recognized the unique opportunity that the HDR containment represents for reactor safety research, and has conducted a series of large-scale fire tests in the HDR containment.

The HDR fire tests are the only fire tests that have been conducted inside an actual nuclear reactor containment building. As a result, there has been much interest in using fire models to simulate these fire tests within the international nuclear reactor safety community. Many different countries have participated over the past 5 years in a cooperative effort to model these tests using the latest fire models available.

Sandia National Laboratories (Sandia) has served as technical consultants to the United States Nuclear Regulatory Commission (USNRC) concerning the HDR fire tests. The purpose of this report is twofold: 1) to summarize Sandia's participation in the HDR fire modeling efforts, and 2) to summarize the results of the international fire modeling community involved in modeling the HDR fire tests.

As part of Sandia's support of the HDR fire modeling activities, a fire zone model (COMPBRN) and a fire field model (the Notre Dame Fire Model, or NDFM) have been used to simulate some of the HDR tests. HDR test E41.7 was a large oil pool fire test in a small room in the containment. The E41.7 COMPBRN calculations could not be obtained beyond 4-7 minutes into the fire (depending on the input parameters) due to instabilities in the COMPBRN code. The calculations become unstable due to the large radiative heat fluxes that are calculated to exist. These results indicate that COMPBRN cannot model very large fires in small rooms (it was not developed for fires of this type).

The E41.7 test Notre Dame Fire Model calculations demonstrate the capabilities of a fire field model. The fire heat release rate used for the field model calculations was based on COMPBRN results. All of the temperatures obtained in the calculations compared reasonably well with experimental data. For some of the data locations, the agreement is excellent. Discrepancies between the calculated and measured temperatures are explainable in terms of leakage around the doorway of the fire room. Such good agreement of the NDFM calculations with data was somewhat surprising in view of the fact that only a few calculations were performed with the model, and that the heat release estimates were obtained using the COMPBRN code.

The results of the other E41.7 participants indicate that the level of agreement of the different model results with the test measurements is a strong function of location in the containment. Even within the fire room itself, only two of the models were consistently within 250 C of the measured gas temperatures. This poor agreement was heavily influenced by the fact that the fire room was virtually a fireball, which most fire models are not designed to model. In general, the agreement became worse (and the disparity wider) as rooms farther removed from the fire room were examined.

HDR test E42.2 was selected as an international standard problem (ISP). This test involved a cable tray fire that spread from tray to tray. The E42.2 COMPBRN results demonstrate that COMPBRN can yield reasonable results for small to medium-sized fires. Note that results were only obtained early in the fire, before the door to the fire room was opened. The strengths of COMPBRN are seen to be its ability to model the transient ignition and burning of cable tray fires in a pre-flashover compartment.

Agreement of the COMPBRN E42.2 results with experimental data is reasonable, but hot gas layer temperatures and cable

tray mass loss rates are significantly underpredicted during the initial stages of the fire. The timing and sequence of cable tray ignition were well-predicted with the exception of the very early stages of the fire. Unfortunately, the COMPBRN results were very sensitive to the user's choice of input parameters.

The results of the other E42.2 participants indicate similar (or worse) descrepancies with the experimental data. The need for better models of the cable insulation burning and charring was seen to be a major research need by all of the participants.

Fire modeling continues to grow and develop in maturity. However, compared to many other areas of science, it is still relatively immature. Its development has been hindered by the complexity and tight coupling of the non-linear phenomena involved. In many respects, there is still somewhat of an art to making accurate fire modeling calculations. Experience with a particular fire model is essential to determine its weak areas and potential pitfalls. Many models require the input of parameters which are not well known, and to which the results are very sensitive, unfortunately.

Just a few years ago, fire modeling efforts were dominated by zone models and control volume models. With advances in computers and computational fluid dynamics (CFD), many of the fire modeling efforts world wide are moving in the direction of field model development. It is not expected that fire field models will replace the other types of fire models, but rather will serve to complement the suite of fire analysis tools available for fire safety analyses.

Validation of fire models remains an important issue. The HDR comparisons have demonstrated that fire models perform poorly when used outside of the realm for which they were designed and validated. Thus, validation of the models against more fire data representative of fires in nuclear power plants is needed.

In conclusion, the HDR fire tests and modeling efforts have contributed a wealth of information regarding actual fires in nuclear power plant containments, and the strengths and weaknesses of present day fire models for simulating these fires.
Based on the experiences with the HDR fire modeling efforts, fire models can potentially contribute to improved fire safety of nuclear power plants, when they are used within their realm of applicability. Defining this realm of applicability, and the sensitivities inherent in today's fire models, is a task that remains to be completed.

# 1 Introduction and Background

## 1.1 HDR Fire Experiments

The Heiss Dampf Reaktor (HDR) is a decommissioned experimental nuclear reactor in the Federal Republic of Germany. Since the HDR reactor has been decommissioned, the containment building is available for nuclear reactor safety studies. The German nuclear reactor safety authority (Gesellschaft für Anlagen und Reaktorsicherheit, or GRS) has recognized the unique opportunity that the HDR containment represents for reactor safety research, and has conducted a series of large-scale tests in the HDR containment building. To date, seismic tests, hydrogen transport tests, blowdown tests, and fire tests have all been conducted inside the HDR containment building.

The HDR test programs have been conducted by the nuclear research center Kernforschungszentrum in Karlsruhe, Germany (or KfK). Both the GRS and Battelle-Frankfurt have provided oversight and management functions for the tests. The HDR itself is located in the town of Kahl, just outside of Frankfurt.

The goal of the HDR tests has been to generate large-scale experimental data for seismic, hydrogen transport, blowdown, and fire phenomena inside an actual nuclear reactor containment. This test data can then be used to evaluate the state-of-the-art in modeling techniques and tools for these phenomena. Areas of uncertainty in present modeling techniques can then be identified, and future research directed toward reducing these uncertainties.

Since the focus of this report is on the HDR fire tests (and the application of fire modeling tools to these tests), only the HDR fire tests and modeling efforts will be discussed in this report.

## 1.2 HDR Fire Modeling History

The HDR fire tests represent a unique contribution to the existing large-scale fire test database. These tests are the only fire tests that have been conducted inside an actual nuclear reactor containment building. As a result, there has been much interest in these tests within the international nuclear reactor safety community.

Because of this interest, KfK organized fire modeling efforts among any countries that were interested in participating. Many different countries have participated over the past 5 years in a cooperative effort to model these tests using the latest fire models available.

These fire modeling efforts usually have several stages associated with them: 1) a pre-test calculation, 2) a blind post-test calculation (before most of the experimental results are released, but including the experimentally measured mass loss rate), and 3) an open post-test calculation (in which all of the experimental results have been previously released for comparison). Also, one international standard problem (ISP) has been formulated for one of the fire tests.

The HDR containment bulding is relatively small in comparison to United States (U.S.) power generating reactors. The containment is 20 m in diameter by 60 m high. The inside surface area is about 10,000 m2, with a volume of 11,000 m3. As shown in Figure 1, it is also highly compartmentalized, without many of the large open rooms present in U.S. power reactors.

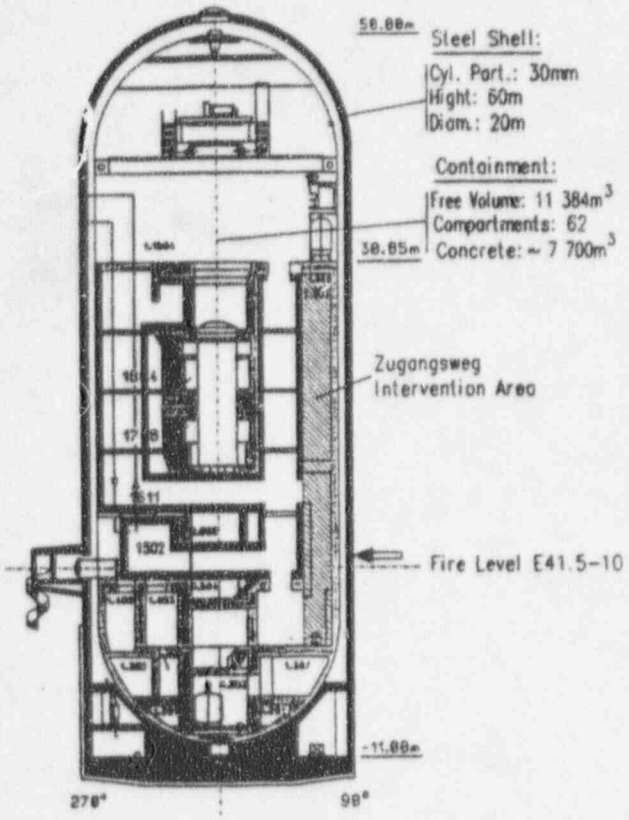


**Figure 1 : The HDR Containment Building**

## 1.3 Sandia's Role in HDR Fire Tests

Sandia has been involved in the HDR fire test program since 1990 as technical consultants to the United States Nuclear Regulatory Commission (USNRC). The formal USNRC name for this program was the HDR/KfK Cooperative Fire Research Effort.

The objectives of this program were as follows: 1) to follow the progress of the fire testing efforts being conducted by the Germans in the HDR test facility, 2) to provide technical support for the development of test plans by the German researchers, 3) to participate in the international fire model assessment efforts being coordinated in conjunction with these tests, and 4) to communicate the results of the German fire tests and the international fire modeling activities to the USNRC.
As the above objectives indicate, Sandia has been involved in the HDR tests in both fire modeling and test support roles. However, the focus of this report is on the HDR fire modeling efforts (as opposed to the test support efforts). The Sandia test support efforts for the HDR are discussed in a separate report (Nowlen, 1993).

The purpose of this report is twofold: 1) to summarize Sandia's participation in the HDR fire modeling efforts, and 2) to summarize the results of the international fire modeling community for the HDR fire tests.
While there were some HDR fire modeling efforts by the international community before Sandia's involvement in this program (namely, the E41.1 test calculations), these will not be discussed herein. Rather, this report will focus on the last two HDR fire tests for which fire modeling calculations have been performed in the international community (including Sandia). These two HDR tests have been given the names E41.7 and E42.2.

## 1.4 Brief Overview of Fire Modeling of Nuclear Power Plants

In this section, a brief overview of fire modeling of nuclear power plants will be given. The intent is to familiarize the reader with some of the terms used later on in the report. A more detailed

discussion can be found in Nicolette and Nowlen (1991).

Fire models are useful for predicting the consequences of a fire inside a nuclear power plant. They can be used to determine how large a fire will grow, and what equipment might be damaged in a fire. They can also be used to assess evacuation procedures and inhabitability of the control room. As such, they might potentially be used to provide a basis for licensing and regulatory decision-making, and are often coupled into a fire risk assessment as part of the suite of evaluation tools.

The value of fire modeling can be seen from the above discussion. The questions then arise: How good (accurate) are these fire models? What types of fire models are best? What is the state-of-the-art in fire modeling, and in what direction is the international fire modeling community moving?

It is with these questions in mind that the HDR fire modeling studies were conducted. Fire science is relatively young compared to other fields of science. The complexity of the fire environment (involving the interaction of combustion, fluid mechanics, heat transfer, and turbulence) has hindered progress in the development of accurate models. The non-linearity of the phenomena involved has also made progress slow. In spite of these impediments, a number of fire models have been developed over the years which can be applied to the analysis of nuclear power plant fires.

Generally speaking, there are three basic types of fire models: zone models, hybrid (control volume) models, and field models, in increasing order of complexity. Zone models (e.g., COMPBRN, CFAST, BRI2) are the simplest fire models, and typically divide the fire room into four regions: flame, plume, hot gas layer, and ambient (Figure 2). Some zone models also allow for the inclusion of secondary targets and combustible fuel elements. They are relatively easy to use, and require little computer (CPU) time. Their main disadvantages are that: 1) many of them are limited to the calculation of only one room, 2) they are based on experimental data and correlations to a great extent, which limits their applicability to fires for which data exists, and 3)they generally only provide spatially-averaged results for each region of interest (e.g. temperatures are averaged throughout the hot gas layer).

A hybrid (or control volume) fire model (e.g., GOTHIC/FATHOMS) is more sophisticated than a zone model, and allows for many rooms or compartments to be interconnected. Additionally, a given room can be subdivided to the level of interest. The control volume approach is shown in Figure 3. In the control volume model approach, mass, heat and momentum transfer occur between the compartments via pipelines or pathways. Their main advantage is that they can handle complex geometries easily. They are also very well suited to include systems models of complex phenomena found inside reactor containments (such as water sprays, or fan coolers).

The main disadvantages of the hybrid model approach are: 1) the pathway flow coefficients from room to room (or compartment to compartment) must be specified, 2) they generally only provide spatially-averaged results, and 3) the CPU requirements can be very large.

Fire field models (e.g. NDFM, KAMELEON Fire, CFDS-FLOW3D) are generally the most complex models available (although hybrid models with many different systems models incorporated may surpass them). Field models gain their name from the fact that they solve the governing differential equations for mass, heat, and momentum transport throughout the entire field (at discrete locations, or nodes). A typical field model calculational grid is shown in Figure 4.

The main advantages of field models are: 1) they provide very detailed information about the fire environment, 2) of all the models, they have the fewest assumptions built into them, and 3) they are not limited to the modeling of fires for which experimental data exists. This last point implies that field models can be used to predict fires for which no

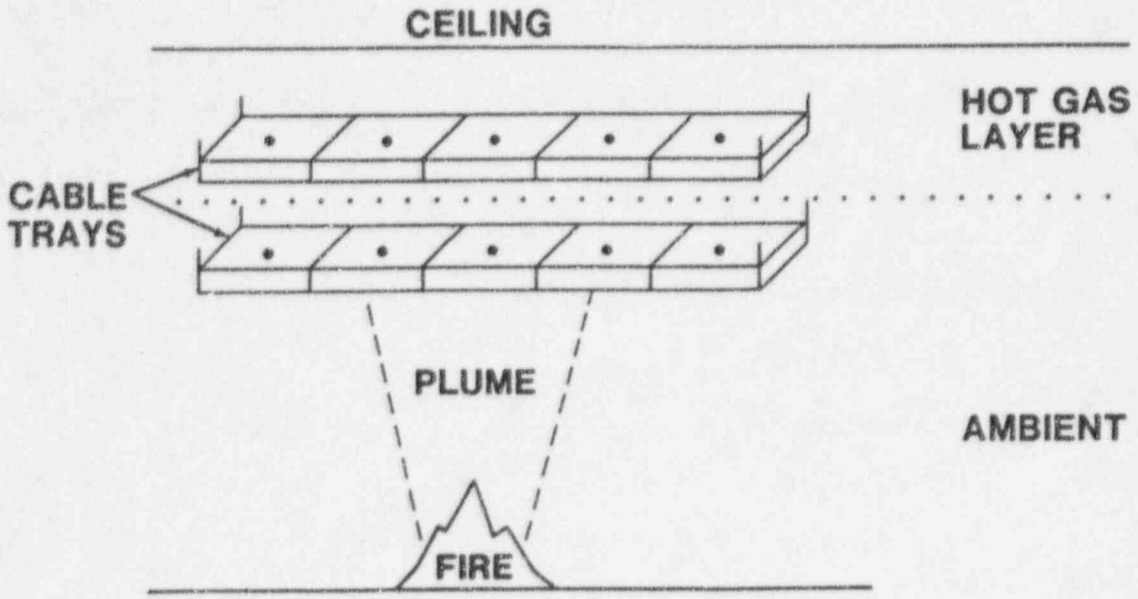


**Figure 2: Zone Fire Model Example**

representative experimental data exists, because field models are based on a 'first-principles' approach that solves the fundamental governing equations, with very few assumptions.

There are generally three major disadvantages to fire field models. First, they require very extensive CPU time to perform a calculation (although this restriction is diminishing as computer speeds and storage increase). Several hours of CPU time on a CRAY XMP computer would not be uncommon with a field model. Second, the input requirements can be more complex for a field model, because the user must specify a detailed numerical grid for the calculations. Third, field models generally lack the extensive validation of the other types of fire models. This last point is mainly due to the immaturity of field modeling relative to the other models, and to the general difficulty of obtaining the detailed field data needed for the validation.

The above discussion is not meant to single out one type of model that should be used exclusive of the others. Each of the different types of models has a role to play in nuclear power plant fire modeling. The type of model employed to solve a particular problem should be based on the information that is required from the model, as well as the scenario the model is applied to. If detailed information is required for a fire which is greatly different than those represented in the experimental data base, a field model is the best choice. If a very large number of fire scenarios must be investigated (such as for a fire risk assessment), and a sufficient experimental database exists for fires of this type, a zone model is the best selection. Finally, if multi-room transport and complex geometries are important considerations, a hybrid control volume model may be the best of all three.

Unfortunately, with all of the different types of fire models there is a strong sensitivity to the input parameters and/or grid selected by the user. Fire model results are, therefore, a function of the knowledge and experience base of the user regarding fire modeling in general, and also with the specific model being applied. In this light, fire model results must always be interpreted in view of the experience of the person who generated them, as well as with regard to the model that produced them.

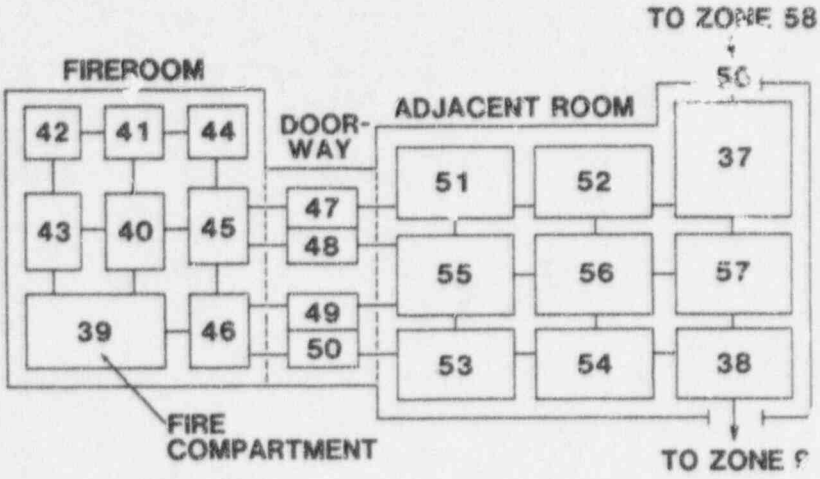


Figure 3: Control Volume Fire Model Example

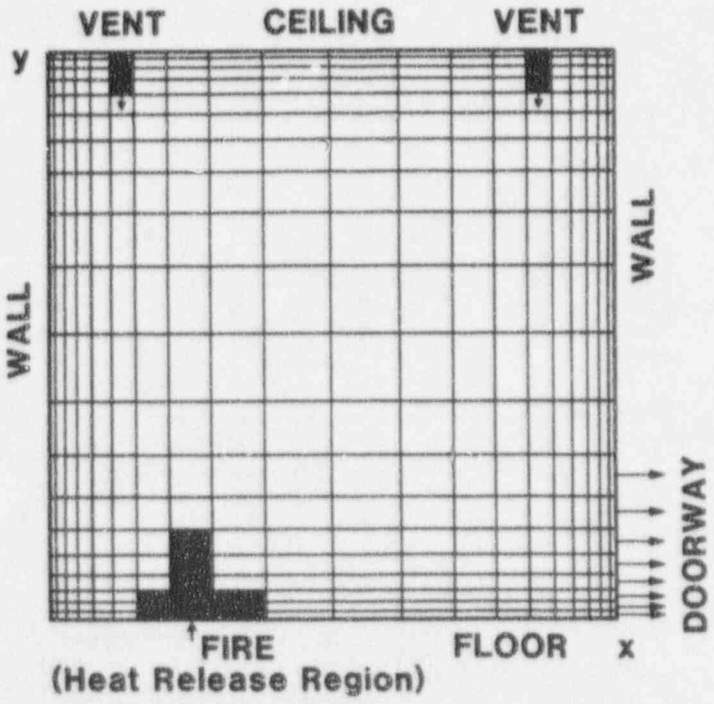


Figure 4: Fire Field Model Example

# 2 E41.7 Fire Experiment

## 2.1 Overview of E41.7 Experiment

The details of the E41.7 test specification are contained in the problem specification report (Müller and Max, 1991). Test E41.7 was an oil pool fire test with high forced ventilation at the 1500 level of the HDR containment building. The ventilation rate for the fire room was specified as 30 air changes per hour (ACH) for the first 15 minutes of the test. During this time period, the doors to the fire room were closed. After 15 minutes, the doors were opened and the ventilation rate was reduced to 10 ACH. The focus herein is only on the first 15 minutes.

The fire room has a volume of 100 $m^3$ (approximate ceiling height of 4.7 m, and floor area of 22 $m^2$). The floor and side walls are made of concrete. The side walls are protected with Alsiflex mats (2.5 cm thick).The ceiling is protected with Promatec (5.0 cm thick). The material properties for these materials can be found in the problem specification report (Müller and Max, 1991).

The fuel was burned in a 2m x 1m pan located near the center of the fire room. The initial fuel loading was 40 liters of Shell SOLT oil. This fuel has a density of 0.756 kg/l and a calorific value of 42,500 kJ/kg. When the initial fuel load was consumed, oil was supplied at a rate of 0.12 kg/s for the duration of the test.

## 2.2 E41.7 Zone Model Calculations Using COMPBRN

The goal of the E41.7 COMPBRN calculations was two-fold: 1) Perform blind post-test calculations with COMPBRN to generate results for later comparison to the test data, and 2) Based on the COMPBRN results, estimate the heat release rate for this test for use in the Notre Dame Fire Model calculations being performed by the University of Notre Dame. Because no heat release rate information was given in the problem specification, it had to be calculated as part of the results.

A modified version of the COMPBRN III fire model (Ho, et al., 1985) was applied to the E41.7 test. This version (Nicolette, et. al., 1989) was modified for the USNRC-sponsored Fire Risk Scoping Study (Lambright, et al., 1989).

COMPBRN III is a zone fire model that models the growth and consequences of a fire in a single room. It has been used in several nuclear power plant fire risk assessment efforts to assess the fire vulnerability of safety-related equipment (see for example, Lambright and Bohn, 1989a and 1989b). COMPBRN III was selected for this study because of Sandia's extensive experience in applying it to nuclear power plant fire scenarios.

### 2.2.1 E41.7 COMPBRN Assumptions and Input

Because COMPBRN III is a zone model, it will output values for parameters of interest that are spatially-averaged over a region of the fire compartment. For this experiment, the results of interest are the hot gas layer temperatures as a function of time, the fire heat release rate, and the length of time required for the initial pool of oil to be consumed. First, some preliminary calculations must be performed to determine appropriate input parameters.

The ventilation rate of 30 ACH corresponds to 0.85 $m^3/s$ into the fire room. The amount of fuel initially is 30.2 kg. For conduction into the walls, floor, and ceiling, the composite layers are converted into an equivalent thickness of Alsiflex by ratioing the thermal diffusivities of the materials (including concrete). Thus, the walls are represented by 27.5 cm of Alsiflex, the ceiling by 10.5 cm of Alsiflex, and the

floor by 62.5 cm of Alsiflex. The thermal diffusivity of all surfaces was varied over the range 1.5 - 2.0E-6 $m^2/s$. The absorptivity of all surfaces was varied from 0.7-0.9 with little impact on the results.

COMPBRN requires the user to input burning parameters that describe the fuel and the fire. For these calculations, the assumption is made that the SOLT oil behaves similarly to kerosene fuel. An efficiency of 70-80% is assumed for the burning process (i.e., 70% of the oil that is vaporized undergoes complete combustion). Half of the energy released in the combustion process is assumed to be in the form of thermal radiation (since these flames are sooty). A surface-controlled burning rate of 0.039 $kg/m^2s$ is used based on information in the SFPE (Society of Fire Protection Engineers, 1988) handbook. This burning rate is considered to have a heat flux augmentation factor of 1.3E-6 $kg/m^2$-J, which is related to the inverse of the latent heat of vaporization (0.77 kJ/g). An initial temperature of 300 K is assumed for all surfaces.
Only the case with a surface emissivity of 0.7, an efficiency of 70%, and a thermal diffusivity of 2.0E-6 $m^2/s$ will be discussed. These input parameters are believed to be the most reasonable for the cases that were run. The input deck is shown in Figure 5.

### 2.2.2 E41.7 COMPBRN Results

COMPBRN calculations were performed for the ranges of parameters specified above. The size of the calculated fire (on the order of megawatts (MW)) is very large relative to the volume of the fire room. This agrees with the observation during the test that most of the room was filled with flames (i.e., a fireball). Consequently, the surfaces of the fire room heat up to very high temperatures very quickly in the simulations.

As a result of these high wall and ceiling temperatures, the COMPBRN calculations become unstable within 4 - 7 minutes from the beginning of the fire. This is due to the manner in which COMPBRN models the radiative heat input into a surface. The fact that thermal radiation is a highly nonlinear process (varying as the fourth power of absolute temperature) exacerbates this instability. Therefore, the calculations could not be carried out for long times.

The COMPBRN results are shown in Table 1 for the first 4 minutes of the calculation, along with some experimental results. The COMPBRN-calculated mass loss rate agrees quite well with the measured values over the first 2 minutes. The COMPBRN-calculated values are lower by about 20%. Note that there is some discrepancy in the test data at time equal to zero. It is not clear why the test data shows 0.11 kg/s as the mass loss rate before ignition occurs. At 3 minutes, COMPBRN calculates a mass loss rate of 0.1535 kg/s. This is about 50% larger than the measured value. The reason for this result is two-fold. First, COMPBRN calculates that the hot gas layer results in substantial heat fluxes back to the pool of fuel, which results in more vaporization and more combustion. Second, COMPBRN assumes that the air entrained by the fire is not diminished in oxygen concentration. In the actual test, some depletion of the oxygen may have been occurring, as evidenced by the monotonic decrease in the measured mass loss rate. By 4 minutes, COMPBRN predicts that the fire has become limited by the amount of oxygen available (ventilation controlled burning). It no longer burns at a rate solely dependent on the amount of fuel surface area (surface controlled burning). The mass loss rate drops substantially at this time as a result.

The initial pool fire is calculated to be approximately 2.8 MW in size. This calculated fire size agrees well (within 20%) with the size predicted by using equations and parameters out of the SFPE handbook. The COMPBRN calculated initial pool fire size is 20% larger than that obtained from the SFPE correlation because thermal radiation back to the pool surface augments the amount of fuel vaporized compared to the free-pool fire correlations.

During the initial pool fire burning, COMPBRN calculates that the surrounding surfaces heat up quickly and provide

```
NJOB, NTIME, DELT
 1   5    60.
NSM, NCOM, NFUEL,NNCOM,NPILOT, IROOM,INITG
 6   0    3    0   1     1    0
HDR E41.7 TEST (FIRST 15 MINUTES)
SMX, SMY, SMZ, SLNG, SWID, SDEP $OIL POOL FIRE (2x1 m2) SM #1
1.3 1.4  .6  2.  1.  .1
  SMASS,SPOR,SLOSS,NFCL,IORNT,IDIREC,IFTYP $END OIL POOL FIRE
   43.1   1.  1.   1   3     1    1
SMX, SMY, SMZ, SLNG, SWID, SDEP $CEILING SM #2
2.33 2.33 4.67 4.66  4.66  .105
  SMASS,SPOR,SLOSS,NFCL,IORNT,IDIREC,IFTYP $END CEILING
   1.   1.  1.   1   3     1    2
SMX, SMY, SMZ, SLNG, SWID, SDEP $WALL 1, Y-Z, X=0  SM #3
0.  2.33 2.34 4.67  4.66  .275
  SMASS,SPOR,SLOSS,NFCL,IORNT,IDIREC,IFTYP $END WALL 1
   1.   1.  1.   1   1     3    3
SMX, SMY, SMZ, SLNG, SWID, SDEP $WALL 2, Y-Z, X=4.66M  SM #4
4.66 2.33 2.34 4.67  4.66  .275
  SMASS,SPOR,SLOSS,NFCL,IORNT,IDIREC,IFTYP $END WALL 2
   1.   1.  1.   1   1     3    3
SMX, SMY, SMZ, SLNG, SWID, SDEP $WALL 3, X-Z, Y=0  SM#5
2.33  0.  2.34 4.67  4.66  .275
  SMASS,SPOR,SLOSS,NFCL,IORNT,IDIREC,IFTYP $END WALL 3
   1.   1.  1.   1   2     3    3
SMX, SMY, SMZ, SLNG, SWID, SDEP $WALL 4, X-Z, Y=4.66  SM #6
2.33 4.66 2.34 4.67  4.66  .275
  SMASS,SPOR,SLOSS,NFCL,IORNT,IDIREC,IFTYP $END WALL 4
   1.   1.  1.   1   2     3    3
IPIL, JPIL, IPFUEL, PMASS
1     1     1     .01
IFUEL,      DENS,          SPHT
1,41,21    756.,2*130.     3*1000.
THK         HEAT           EFF
.1,2*0.2    4.25E7,2*1.    .7,2*0.1
FIGTP       FTDAM          FIGTS
573.,2*2000. 573.,2*2000.  573.,2*2000.
BRATV       BRATS0         BRATS1
.025,2*0.   .039,2*0.      1.3E-6,2*0.
GAMMA       EABSRP         REFL
3*.5        3*1.4          3*.1
RTEMP   FLCF   HROOM   CALTEM
300.    23.    10.     0.
IPOOL, ESIGN, EPIGN,   EDAMG,   QCRITS,  QCRITP, QCRITD
1    1.E12   1.E12    1.E12    1.E9     1.6E9   7.2E9
SEE: IV=I,J,K,L
NSEE: NV=I,J,K,L
 ROOM DATA: DCFIN,DCFOUT,DHGT,DWID,FC,FH,GABSRP,HCEIL,PLCF,VFV
        1.0  0.7   0.   0.   0.1.  1.3   10.   0.  0.85
```

**Figure 5: E41.7 COMPBRN Input Deck**

substantial radiative feedback to the fuel pool. Consequently, the fire heat release rate climbs very quickly between 2 and 4 minutes. After 3 minutes, the heat release rate is calculated to be 4.6 MW. By 4 minutes, COMPBRN predicts that the fire has become limited by the amount of oxygen available. The COMPBRN-calculated heat release rate then drops to just under 1 MW.

As shown in Table 1, the COMPBRN-calculated hot gas layer (HGL) temperatures rise to a high level very early in the calculation. This result is influenced by the quasi-steady nature of COMPBRN. COMPBRN always calculates the HGL temperature by assuming that the HGL has reached a steady-state. Obviously, this assumption will be in error during the first few minutes of a fire, when the HGL is developing rapidly. From the 2 minute mark and afterward, the calculated HGL temperatures are within 250 K of the thermocouple data. This is reasonable in view of the quasi-steady nature of COMPBRN. By the 3 minute mark, the HGL temperatures have reached 1135 K. These very high temperatures result in very large radiative heat fluxes back to the fuel pool, and to the walls and ceiling. As a result, the COMPBRN model becomes unstable after the 4 minute mark and does not produce a solution.

It should be noted that thermocouples provide an experimental indication of local gas temperatures, and not the actual gas temperatures. Thermocouples are essentially heat flux sensors, and are influenced by the radiative heat transfer in a fire. Therefore, the degree to which thermocouple data reflect local gas temperatures is a strong function of the radiation environment that they are used in. KfK estimated the experimental error associated with the thermocouple data to be less than 5%. This error estimate is typical for the other data taken by KfK, except velocity (10%).

In order to better quantify when the fire switches to the ventilation controlled burning mode (i.e., was it closer to 3 minutes or to 4 minutes?), some additional calculations were performed. The COMPBRN calculations do not predict what happens between 3 minutes and 4 minutes due to the quasi-steady nature of the code.

Four quantities were calculated: 1) the energy that could be released if all of the available oxygen were consumed (Joules), 2) the amount of fuel (kg) corresponding to that energy (assuming a 70% efficiency), 3) the energy released (Joules) based on the COMPBRN calculations, and 4) the amount of fuel (kg) corresponding to the COMPBRN energy release (again assuming a 70% efficiency). The first calculated quantity assumes that 3,000 kJ of energy are released per kilogram of air

**Table 1: COMPBRN Results for E41.7 Test**

| Time (minutes) | Calculated Mass Loss Rate (kg/s) | Measured* Mass Loss Rate (kg/s) | Calculated Fire HRR (MW) | Calculated HGL Temp (K) | Measured HGL Temp (K) CT5204 |
|---|---|---|---|---|---|
| 0 | 0 | .11 | 0 | 300 | 293 |
| 1 | .09 | .11 | 2.8 | 815 | 450 |
| 2 | .09 | .11 | 2.8 | 962 | 750 |
| 3 | .1535 | .10 | 4.6 | 1135 | 873 |
| 4 | .03 | .10 | 0.9 | 1138 | 925 |

*Measured with a load cell on the pan

combusted, and that all of the air is available to participate in the combustion process. This is probably a reasonable assumption since the fire room gases are relatively well mixed, and HGL temperatures are very high. For the third quantity calculated, the fire was assumed to stay constant at 4.6 MW for the time period between 3 and 4 minutes.

The results of the calculations are shown in Table 2. It was found that at 4 minutes, the amount of fuel consumed was equal to the initial fuel loading in the fire room (30 kg). It can also be seen from Table 2 that virtually all of the available oxygen in the room has been consumed right at 4 minutes. Based on these results, the additional oil fuel flow (0.12 kg/s) is predicted to begin at 4 minutes after fire initiation.

A fuel consumption rate of 0.12 kg/s corresponds to a very large fire (5.1 MW, if 100% efficient). Since the fire has become ventilation controlled following 4 minutes, the heat release rate will be limited by the available oxygen. The method COMPBRN uses to calculate ventilation-controlled burning rates is not straightforward, and depends heavily on the user's input of a ventilation-controlled burning constant. Therefore, the following procedure is used to estimate the ventilation-controlled burning rate.

Additional oxygen enters the fire room in the form of fresh air at a rate of 30 ACH. Again assuming an energy release of 3,000 kJ per kg of air, and assuming that all of the available oxygen is consumed, this would limit the fire to a size of 2.6 MW for all later times (until the doors to the fire room are eventually opened or the ventilation rate is changed). However, because of the very large radiative feedback, all of the added fuel is probably vaporized. The burning efficiency of this ventilation-controlled fire is thus 2.6/5.1 ~ 50%.

The above calculations can be summarized as follows. COMPBRN calculates that the fire size grows from about 2.8 MW during the first 2-3 minutes to 4.6 MW during the 3-4 minute time frame. By 4 minutes, the initial fuel has been consumed as well as most of the initial oxygen supply. Measured mass loss rates are in reasonable agreement during the first 2 minutes of the test, but deviate significantly thereafter. The hot gas layer temperatures are calculated to exceed 1100 K, as compared to approximately 900 K measured. Calculations could not be obtained beyond 4-7 minutes into the fire (depending on the input parameters) due to instabilities in the COMPBRN code. In this time frame, the hot gas layer temperature and the surface temperatures become very high. The calculations become unstable due to the large radiative heat fluxes that are calculated to exist.

These results indicate some of COMPBRN III's limitations. The COMPBRN code is quasi-steady in nature, and cannot be expected to exactly describe the early stages of transient fires. Also, the correlations and models upon which COMPBRN is based do not generally apply for fires that are this large in size. While these results demonstrate some of the limitations of the COMPBRN code, it should be remembered that COMPBRN was not designed to calculate large fires in small rooms.

## 2.3 E41.7 Field Model Calculations

Along with the COMPBRN zone model calculations, field model calculations were also performed for the E41.7 test. The model used is the University of Notre Dame Fire Model (NDFM), developed by Professor K. T. Yang and colleagues. This fire model is a research tool that has been under development since the mid-1970s, and has been used to simulate many different fires (see for example, Liu and Yang, 1978). The calculations discussed herein were performed by Professor Yang and his colleagues at the University of Notre Dame. Other field models could have been used (e.g., the KAMELEON Fire model), but the NDFM was selected due to the authors' familiarity with it.

### 2.3.1 E41.7 Field Model Assumptions and Input

The geometric model of the HDR fire room used in the NDFM E41.7 calculations is sketched in Figure 6. Note that the fire room consists of a larger room (in which there was a pool of fuel) and a smaller room (alcove) that was directly attached. The alcove had doors on the end of it that led to the rest of the containment, but these doors were assumed to be closed. For the model, the ventilation air was introduced into the fire room through a square hole at the actual location of the ventilation inlet in the HDR fire room. This is near the origin in Figure 6. The ventilation rate was maintained at a constant value of 0.85 m3/s.

The calculation domain was divided into cubical cells measuring 0.273 m on each side. The uniform grid used was 28x24x19 cells (IxJxK). A transient 1-D conduction model for the walls (emissivity=0.9) was included. The coefficient of heat transfer at the exterior wall and ceiling surfaces of the fire room (to the

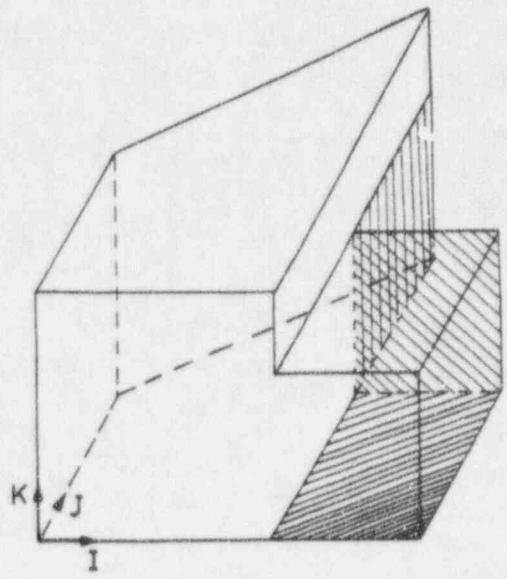


**Figure 6: NDFM E41.7 Geometric Model**

**Table 2: Additional E41.7 Calculations**

| Time (minutes) | Cumulative energy release based on available air (MJ) | Fuel burned based on available air, assuming 70% efficiency (kg) | Cumulative energy release based on COMPBRN fire sizes (MJ) | Fuel burned based on COMPBRN, assuming 70% efficiency (kg) |
|---|---|---|---|---|
| 0 | 300 | 10 | 0 | 0 |
| 0-1 | 453 | 15 | 166 | 6.5 |
| 1-2 | 606 | 20 | 335 | 11 |
| 2-3 | 759 | 26 | 611 | 21 |
| 3-4 | 912 | 31 | 888 | 30 * |

* Initial fuel loading was 30.2 kg.

ambient) was assumed to be 85 W/m2K. The fraction of flame energy radiated away from the flame was assumed to be 0.9. Other physical properties were based on those given in the design specification report (Müller and Max, 1991).
The NDFM does not have a combustion model. Therefore, the user must input a heat release rate, and specify a 'flame volume' over which the energy is distributed. As a result, the model should not be expected to closely predict the temperatures in the flame volume, since they are heavily tied to the assumptions on the size of the flame volume.

For the NDFM calculations of test E41.7, the heat release rate(HRR), in megawatts (MW), was assumed to vary with time (t) according to the following relationship:

HRR = 1.9625 t, for 0 < t < 2 minutes,

HRR = 1.17 t + 1.30, for 2 < t < 4 minutes

This particular form of the relationship was based on the COMPBRN results, and was used to provide a smooth ramp-up of the HRR to reduce any problems with instabilities in the model.

### 2.3.2 E41.7 Field Model Results

The Notre Dame field model results for E41.7 will be summarized briefly here. Details of the calculations can be found in the report attached as Appendix B.

The E41.7 calculations with the NDFM were performed on an IBM RISC 6000 machine. The time steps used were between 0.05 and 0.001 seconds. The total estimated CPU time required to model 4 minutes of the fire was about 50 hours. Because of the large CPU time requirements, only a single set of calculations was performed with the NDFM for the E42.2 test. As a result, there was no 'adjustment of parameters' used to obtain the following results. However, some calculations with the NDFM had been previously performed on another HDR test (E41.5: natural ventilation) to determine an appropriate grid and time step. These calculations are discussed in the report attached as Appendix C.

To begin the NDFM calculations, the model was run with the ventilation turned on, but with no fire load (zero HRR) until a steady-state flow was achieved in the room. Then the fire was assumed to start (time equal to zero in the plots). Calculations were only carried out until 4 minutes was reached, since the COMPBRN results were being used to provide a basis for estimating the HRR for the NDFM calculations.

With a field model such as the NDFM, the HGL is described by many nodes. A rough description of the physical location of each point of interest is given below. A more detailed description can be found in the problem specification report (Müller and Max, 1991).

Thermocouple number 5204 (CT5204) was located directly above the fuel pool, just below the ceiling. The calculated results for this thermocouple are in very good agreement with the measured values, as shown in Figure 7. The slight difference in the shape of the calculated and measured curves could be due to a difference in the rate of heat release used for the calculations, as compared to the test. This agreement is very good, considering the uncertainty in the HRR values and profiles used in the NDFM calculations. As mentioned previously, the error associated with the experimental data is expected to be less than 5%.

Thermocouple number 5246 (CT5246) was located near the closed doors in the alcove, in the vicinity of the ceiling. Figure 8 indicates reasonable agreement between the calculated and measured gas temperatures at this location, with the calculated results underpredicting the test data by about 100 C. The trends in the two curves are very similar, although the calculated temperatures rise more slowly. A possible reason for this discrepancy is that some outflow may have occurred in the test in the vicinity of the doors, whereas the calculations assume a perfectly leak-tight boundary. Leakage around the doors in the test would have resulted in a larger flow of hot gases into this otherwise 'dead' corner, thereby increasing the local gas temperature. There was anecdotal

information that leakage did indeed occur around the doors in the experiment.

Thermocouples 5290 and 5294 were located close to the junction of the main room and alcove. CT5290 was very close to the floor, and CT5294 was very close to the ceiling. For CT5290 (floor), there is excellent agreement during the first 2.5 minutes of the test, as shown in Figure 9. Both the NDFM calculations and the test measurements indicate that the HGL has not descended to this location yet. However, by the 3 minute mark the NDFM results indicate that the HGL has indeed descended almost to the floor, while the test results indicate otherwise. If there is some cold air infiltration near the base of the doors, a fresh supply of cold air would be drawn into the fire room right over CT5290, thus keeping it close to ambient temperature. However, the calculations assume zero infiltration around the closed doors, which allows the HGL to descend more quickly. This is one possible explanation of the discrepancy between the calculated and measured results during the 3 - 4 minute time frame.

Thermocouple 5294 was located directly above CT5290, but very near the ceiling. Excellent agreement between the calculated and the measured HGL temperatures can be seen in Figure 10. The calculated temperatures are within approximately 25 C of the measured values over the 4 minute time period, reaching a maximum value of about 550 C.

In general, the NDFM results show very good agreement with the measured temperatures. Discrepancies between the calculations and the measurements are explainable in terms of gas leakage around the doors. Since only one calculation was performed with the NDFM for test E41.7 (i.e., there was no fine-tuning of the HRR or other input parameters), such good agreement was somewhat of a surprise in view of the uncertainty in HRR.

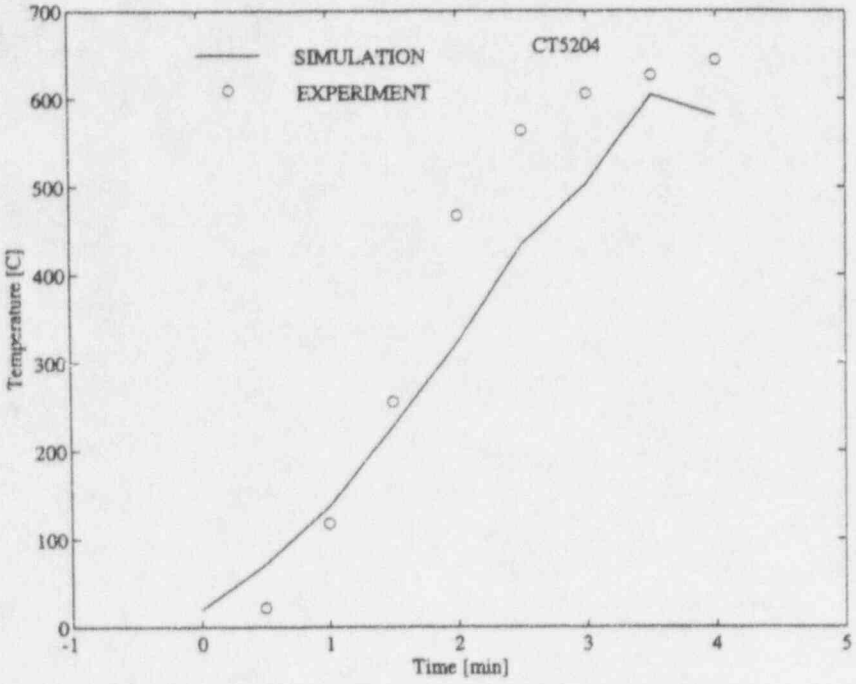


**Figure 7: E41.7 CT5204 Temperature (Solid=NDFM, Circle=Data)**

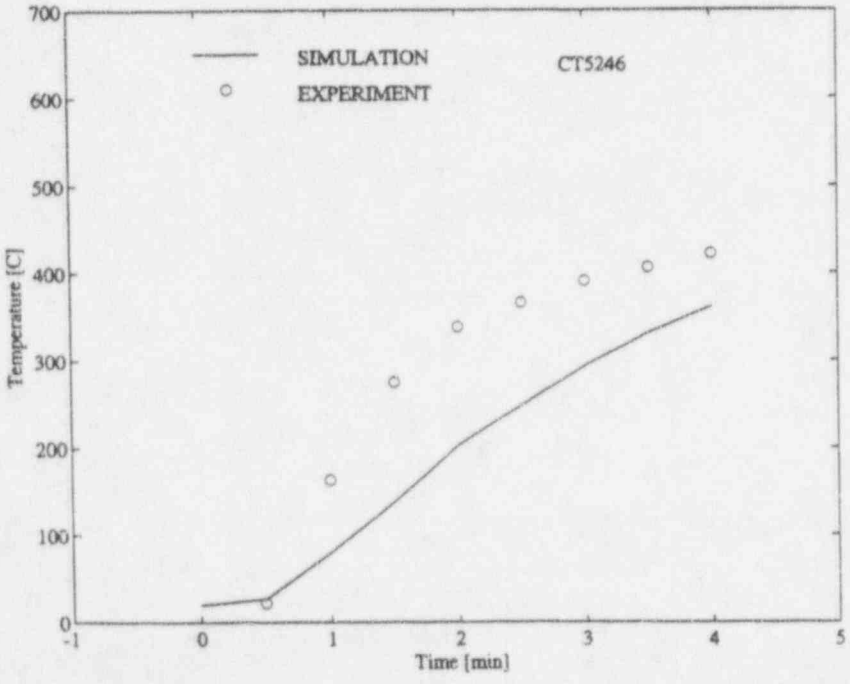


**Figure 8: E41.7 CT5246 Temperature (Solid=NDFM, Circle=Data)**

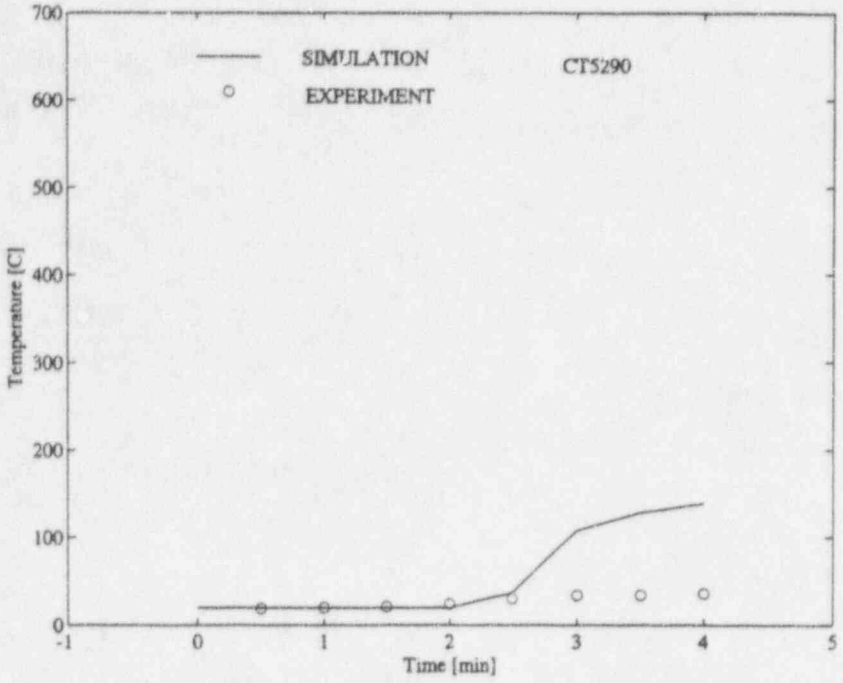


**Figure 9: E41.7 CT5290 Temperature (Solid=NDFM, Circle=Data)**

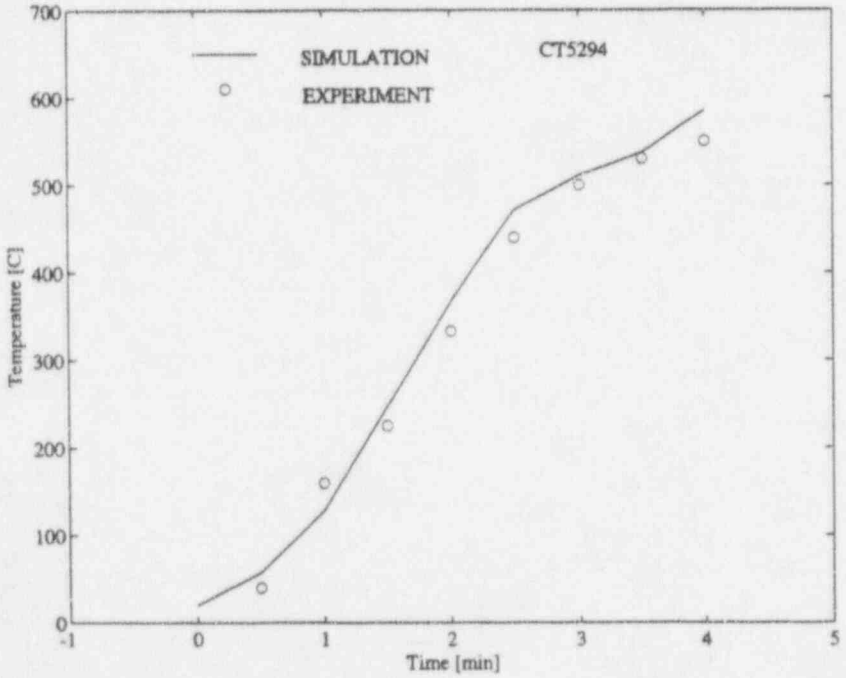


**Figure 10: E41.7 CT5294 Temperature (Solid=NDFM, Circle=Data)**

# 3 E42.2 Fire Experiment

## 3.1 Overview of E42.2 Experiment

The details of the test specification for test E42.2 are contained in the problem specification report (Karwat, et al., 1992). Test E42.2 was a cable fire test with high forced ventilation at the 1500 level of the HDR containment building (the same room that was used for the E41.7 test). The ventilation rate for the fire room was specified as 1700 $m^3$/hr (17 ACH) for the first 22 minutes of the test. According to the test specification, the doors to the fire room were to remain closed until 50% of the fuel was involved in the fire.

The fire room has a volume of 100 $m^3$ (approximate ceiling height of 4.7 m, and floor area of 22 $m^2$). The floor and side walls are made of concrete and concrete blocks, respectively. The side walls are protected with Alsiflex mats (2.5 cm thick). The ceiling is protected with Promatec (5.0 cm thick). The material properties can be found in the problem specification report.

This test differed significantly from test E41.7 in that polyvinyl chloride (PVC) electrical cable insulation served as the source of combustible material in the room. The details of the PVC cable tray fuel loading can also be found in the problem specification report.

There were 3 distinct phases to this experiment: Phase 1 - forced ventilation only; Phase 2 - door is opened, exhaust turned on; and Phase 3 - fire suppression activation. Note that Phase 3 (fire suppression activation) was not included in the problem specification, and no comparisons between calculations and experimental data should be made for this phase of the experiment.

## 3.2 E42.2 Zone Model Calculations Using COMPBRN

The COMPBRN III fire model as modified for the Fire Risk Scoping Study (Lambright, et al. 1989) was also applied to the E42.2 test. The goal of the E42.2 COMPBRN calculations was to perform blind post-test calculations for later comparison to the test data.

Test E42.2 was selected to be an International Standard Problem (ISP). Thus, there were strict guidelines and much formality involved in the problem specification and submission of calculated results.

### 3.2.1 E42.2 COMPBRN Assumptions and Input

The important assumptions necessary to generate a COMPBRN III input deck for test E42.2 will now be stated. A layout of the cable trays is shown in Figure 11.

The cable trays that are covered with Alsiflex mats are not modeled in this simulation. They are included in the calculations, but no heat transfer is allowed to them. In the actual experiment, some of the trays covered with Alsiflex did eventually become involved (ignited), but this was not significant during Phase 1 (which was the only phase of the experiment modeled with COMPBRN III).

The fire room (out to the doors) is modeled as a single square room of appropriate volume and surface area.

No cables in rack III are modeled, since most of them were consumed in previous tests. Material properties assumed for the cables are in the input deck (see Figure 12).

The walls and ceiling are modeled as Alsiflex, with the concrete material converted into an appropriate thickness of Alsiflex for the calculations.

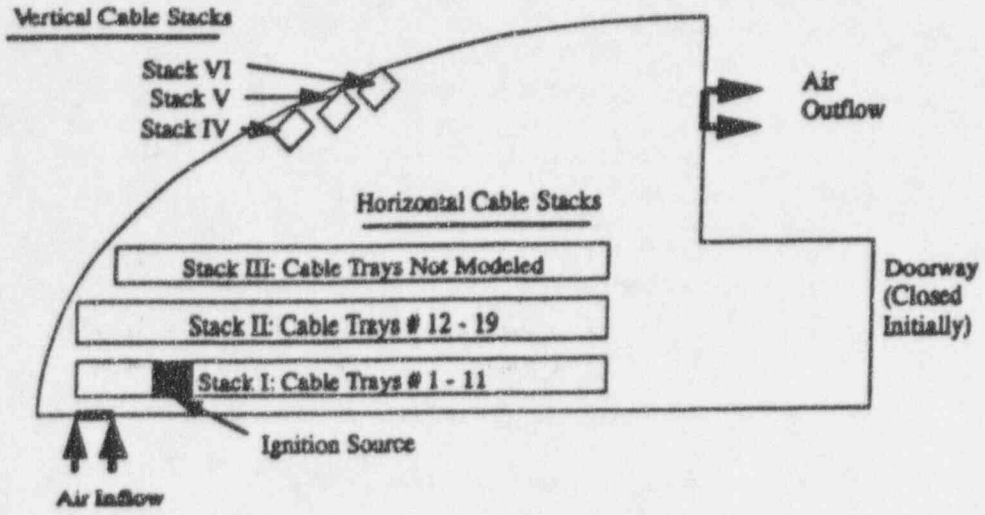


**Figure 11 E42.2 Cable Tray Layout Diagram (Plan View)**

The heat of combustion for the cables was assumed to be 17 MJ/kg (at the upper end of what was measured and reported in the problem specification report). Calculations with 12 MJ/kg (the lower end of that reported in the specification report) did not result in ignition of the surrounding trays.

An ignition temperature of 723 K (450 C) was assumed for the unpowered PVC cables. This value is consistent with the lower limit of Sandia test data on PVC cable (Nowlen, 1989). Each of the cable trays was divided into 4 longitudinal sections for modeling.

There was no radiation shielding of any of the participating cable trays from the hot gas layer. Because of the manner in which COMPBRN models shielding, it is not possible to prohibit thermal radiation to a tray from the hot gas layer without also prohibiting convective heat transfer from the hot gas layer.

COMPBRN requires the user to input burning parameters that describe the fuel and the fire. A surface controlled burning rate of 0.0022 kg/m$^2$s is assumed, with a radiation augmentation factor of 0.186E-06 kg/J. These values are consistent with those used previously in other cable fire simulations (Lambright, et al., 1989).

A combustion efficiency of 0.9 was assumed for the calculations. Although this is unrealistically high for cable insulation, it has been previously determined that such a value is necessary for COMPBRN to correctly predict flame temperatures for cable fires (Nicolette, et al., 1989).

### 3.2.2 E42.2 COMPBRN Results

Because the COMPBRN III fire model is a zone model, the results of interest to us are the hot gas layer temperatures as a function of time, the fire heat release rate, the cable mass loss rate, and the length of time until ignition of the various cable trays. COMPBRN calculations were performed for the parameters specified above. Unfortunately, COMPBRN III does not allow one to simulate the case where a room is initially isolated, and then the doors are opened at a later time. Therefore,

```
NJOB, NTIME, DELT
 1     9     60.
NSM, NCOM, NFUEL,NWCOM,NPILOT, IROOM,INITG
 29    0      4     45    1       1     0
HDR E42.2 CABLE FIRE TEST FOR ISP (FIRST 9 MINUTES, COVERED TRAYS DON'T PARTICIPATE)
SMX, SMY, SMZ, SLNG, SWID, SDEP $SM #1 TOP CABLE TRAY OF STACK 1
 2.3  0.85 2.55   4.   0.3    .013
   SMASS,SPOR,SLOSS,NFCL,IORNT,IDIREC,IFTYP $END TRAY 1 OF STACK 1
    25.3  3.14   1.   4    3      1     1
SMX, SMY, SMZ, SLNG, SWID, SDEP $SM #2 TRAY 2 OF STACK1
2.33 0.85 2.35  4.    0.3  .015
   SMASS,SPOR,SLOSS,NFCL,IORNT,IDIREC,IFTYP $END TRAY 2, STACK1
    25.    3.14   1.  4    3      1     1
SMX, SMY, SMZ, SLNG, SWID, SDEP $SM #3 TRAY 3 OF STACK1
2.33 0.85 2.15  4.    0.3  .015
   SMASS,SPOR,SLOSS,NFCL,IORNT,IDIREC,IFTYP $END TRAY 3, STACK1
    13.9   3.14   1.  4    3      1     1
SMX, SMY, SMZ, SLNG, SWID, SDEP $SM #4 TRAY 4 OF STACK1
2.33 0.85 1.95  4.    0.3  .015
   SMASS,SPOR,SLOSS,NFCL,IORNT,IDIREC,IFTYP $END TRAY 4, STACK1
    27.9   3.14   1.  4    3      1     1
SMX, SMY, SMZ, SLNG, SWID, SDEP $SM #5 TRAY 5 OF STACK1
2.33 0.85 1.75  4.    0.3  .011
   SMASS,SPOR,SLOSS,NFCL,IORNT,IDIREC,IFTYP $END TRAY 5, STACK1
    22.    3.14   1.  4    3      1     1
SMX, SMY, SMZ, SLNG, SWID, SDEP $SM #6 TRAY 6 OF STACK1
1.55 0.85 2.35  4.    0.3  .015
   SMASS,SPOR,SLOSS,NFCL,IORNT,IDIREC,IFTYP $END TRAY 6, STACK1
    30.    3.14   1.  4    3      1     1
SMX, SMY, SMZ, SLNG, SWID, SDEP $SM #7 TRAY 7 OF STACK1
2.33 0.85 1.35  4.    0.3  .015
   SMASS,SPOR,SLOSS,NFCL,IORNT,IDIREC,IFTYP $END TRAY 7, STACK1
    22.3   3.14   1.  4    3      1     1
SMX, SMY, SMZ, SLNG, SWID, SDEP $SM #8 TRAY 8 OF STACK1
2.33 0.85 1.15  4.    0.3  .015
   SMASS,SPOR,SLOSS,NFCL,IORNT,IDIREC,IFTYP $END TRAY 8, STACK1
    20.6   3.14   1.  4    3      1     1
SMX, SMY, SMZ, SLNG, SWID, SDEP $SM #9 TRAY 9 OF STACK1
2.33 0.85 0.95  4.    8.3  .015
   SMASS,SPOR,SLOSS,NFCL,IORNT,IDIREC,IFTYP $END TRAY 9, STACK1
    25.    3.14   1.  4    3      1     1
SMX, SMY, SMZ, SLNG, SWID, SDEP $SM #10 TRAY 10 OF STACK1
2.33 0.85 0.75  4.    0.3  .015
   SMASS,SPOR,SLOSS,NFCL,IORNT,IDIREC,IFTYP $END TRAY 10, STACK1
    29.3   3.14   1.  4    3      1     1
SMX, SMY, SMZ, SLNG, SWID, SDEP $SM #11 TRAY 11 OF STACK1
2.33 0.85 0.55  4.    0.3  .015
   SMASS,SPOR,SLOSS,NFCL,IORNT,IDIREC,IFTYP $END TRAY 11, STACK1
    39.6   3.14   1.  4    3      1     1
SMX, SMY, SMZ, SLNG, SWID, SDEP $SM #12 TRAY 12 OF STACK2
```

**Figure 12: E42.2 COMPBRN III Input Deck**

```
2.33 1.96 1.95  4.    0.3  .015
  SMASS,SPOR,SLOSS,NFCL,IORNT,IDIREC,IFTYP $END TRAY 12, STACK2
   37.2  3.14   1.  4    3      1     1
SMX, SMY, SMZ, SLNG, SWID, SDEP $SM #13 TRAY 13 OF STACK2
2.33 1.96 1.75  4.    0.3  .022
  SMASS,SPOR,SLOSS,NFCL,IORNT,IDIREC,IFTYP $END TRAY 13, STACK2
  47.7  3.14   1.  4    3      1     1
SMX, SMY, SMZ, SLNG, SWID, SDEP $SM #14 TRAY 14 OF STACK2
2.33 1.96 1.55  4.    0.3  .015
  SMASS,SPOR,SLOSS,NFCL,IORNT,IDIREC,IFTYP $END TRAY 14, STACK2
   59.7  3.14   1.  4    3      1     1
SMX, SMY, SMZ, SLNG, SWID, SDEP $SM #15 TRAY 15 OF STACK2
2.33 1.96 1.35  4.    0.3  .015
  SMASS,SPOR,SLOSS,NFCL,IORNT,IDIREC,IFTYP $END TRAY 15, STACK2
   22.1  3.14   1.  4    3      1     1
SMX, SMY, SMZ, SLNG, SWID, SDEP $SM #16 TRAY 16 OF STACK2
2.33 1.96 1.15  4.    0.3  .015
  SMASS,SPOR,SLOSS,NFCL,IORNT,IDIREC,IFTYP $END TRAY 16, STACK2
   16.1  3.14   1.  4    3      1     1
SMX, SMY, SMZ, SLNG, SWID, SDEP $SM #17 TRAY 17 OF STACK2
2.33 1.96 0.95  4.    0.3  .015
  SMASS,SPOR,SLOSS,NFCL,IORNT,IDIREC,IFTYP $END TRAY 17, STACK2
   16.1  3.14   1.  4    3      1     1
SMX, SMY, SMZ, SLNG, SWID, SDEP $SM #18 TRAY 18 OF STACK2
2.33 1.96 0.75  4.    0.3  .015
  SMASS,SPOR,SLOSS,NFCL,IORNT,IDIREC,IFTYP $END TRAY 18, STACK2
   26.  3.14   1.  4    3      1     1
SMX, SMY, SMZ, SLNG, SWID, SDEP $SM #19 TRAY 19 OF STACK2
2.33 1.96 0.55  4.    0.3  .015
  SMASS,SPOR,SLOSS,NFCL,IORNT,IDIREC,IFTYP $END TRAY 19, STACK2
   26.  3.14   1.  4    3      1     1
SMX, SMY, SMZ, SLNG, SWID, SDEP $SM #20 CABLE STACK4
2.45 4.11 2.25  4.5   0.3  .015
  SMASS,SPOR,SLOSS,NFCL,IORNT,IDIREC,IFTYP $END  STACK4
   25.  3.14   1.  4    2      3     1
SMX, SMY, SMZ, SLNG, SWID, SDEP $SM #21 CABLE STACK5
3.3  4.39 2.25  4.5    0.3  .015
  SMASS,SPOR,SLOSS,NFCL,IORNT,IDIREC,IFTYP $END  STACK5
   44.3  3.14   1.  4    2      3     1
SMX, SMY, SMZ, SLNG, SWID, SDEP $SM #22 CABLE STACK6
4.15 4.61 2.25  4.5    0.3  .015
  SMASS,SPOR,SLOSS,NFCL,IORNT,IDIREC,IFTYP $END  STACK6
   22.4  3.14   1.  4    2      3     1
SMX, SMY, SMZ, SLNG, SWID, SDEP $SM #23 CEILING
 3.6 2.33 4.69 4.67  4.66  .105
  SMASS,SPOR,SLOSS,NFCL,IORNT,IDIREC,IFTYP $END CEILING
   1.     1.   1.    1    1      3     2
SMX, SMY, SMZ, SLNG, SWID, SDEP $SM #24 WALL 1
 0.  1.55 2.35 4.69  3.1  .4
  SMASS,SPOR,SLOSS,NFCL,IORNT,IDIREC,IFTYP $END WALL 1
```

**Figure 12 (Continued): E42.2 COMPBRN III Input Deck**

```
  1.     1.   1.    1    1      3     3
SMX, SMY, SMZ, SLNG, SWID, SDEP $SM #25 WALL 2 XZ, Y=4.66
2.33 4.66 2.35 4.69  4.66  .275
  SMASS,SPOR,SLOSS,NFCL,IORNT,IDIREC,IFTYP $END WALL 2
  1.     1.    1.    1    2      3     3
SMX, SMY, SMZ, SLNG, SWID, SDEP $SM #26 WALL 3, YZ, X=4.66
4.66  3.5  2.35 4.69 2.85  .275
  SMASS,SPOR,SLOSS,NFCL,IORNT,IDIREC,IFTYP $END WALL 3
   1.    1.    1.    1    1      3      3
SMX, SMY, SMZ, SLNG, SWID, SDEP $SM #27 WALL 4, XZ Y=2.33
6.09 3.06 2.35 4.67  2.85  .275
  SMASS,SPOR,SLOSS,NFCL,IORNT,IDIREC,IFTYP $END WALL 4
   1.    1.    1.    1    2      3     3
SMX, SMY, SMZ, SLNG, SWID, SDEP $SM #28 WALL 5, YZ X=7.2
7.2  1.63 2.35 4.69  2.65  .275
  SMASS,SPOR,SLOSS,NFCL,IORNT,IDIREC,IFTYP $END WALL 5
   1.    1.    1.    1    1      3     3
SMX, SMY, SMZ, SLNG, SWID, SDEP $SM #29 WALL 6, XZ Y=0
2.33  0. 2.35 4.69  4.66  .275
  SMASS,SPOR,SLOSS,NFCL,IORNT,IDIREC,IFTYP $END WALL 6
   1.    1.    1.    1    2      3     3
IPIL, JPIL, IPFUEL, PMASS
 5      2      1     .05
IFUEL,        DENS,              SPHT
1,40,20,2     1715.,2*130.,756. 1045.,2*1000.,2099.
 THK          HEAT               EFF
.092,3*0.1    1.7E7,2*1.,4.2E7  .9,2*0.,.9
FIGTP         FTDAM              FIGTS
723.,3*2000. 673.,3*2000.    723.,3*2000.
ERATV         ERATS0             ERATS1
.05,3*0.     .0022,2*0.,.061  .186E-6,2*0.,4.3E-7
GAMMA         FABSRP             REFL
4*.5          4*1.4              4*.1
RTEMP     FLCF     HROOM   CALTEM
290.       23.       10.     0.
IPOOL, ESIGN,  EPIGN,    EDAMG,    QCRITS,   QCRITP, QCRITD
  1     1.E12    1.E12     1.E12     1.E9     1.6E9   7.2E9
SEE:  IV=I,J,K,L
NSEE:  NV=I,J,K,L
 1,888,3,11
 2,888,4,11
 3,888,5,11
 4,888,6,11
 5,888,6,11
 1,888,14,19
 2,888,14,19
 3,888,14,19
 4,888,14,19
 5,888,14,19
 1,888,21,22
```

**Figure 12 (Continued): E42.2 COMPBRN III Input Deck**

```
 2,888,21,22
 3,888,21,22
 4,888,21,22
 5,888,21,22
12,888,14,19
13,888,14,19
12,888,6,11
13,888,6,11
12,888,21,22
13,888,21,22
20,888,6,11
20,888,14,19
20,888,21,22
23,888,6,11
23,888,14,19
23,888,21,22
24,888,6,11
24,888,14,19
24,888,21,22
25,888,6,11
25,888,14,19
25,888,21,22
26,888,6,11
26,888,14,19
26,888,21,22
27,888,6,11
27,888,14,19
27,888,21,22
28,888,6,11
28,888,14,19
28,888,21,22
29,888,6,11
29,888,14,19
29,888,21,22
 ROOM DATA: DCFIN,DCFOUT,DHGT,DWID,FC,FH,GABSRP,HCEIL,PLCF,VFV
            1.0   0.7    0.   0.   0. 1.  1.3    10.   0.  0.472
INITG DATA :  TG     DG      QEXT
FCTR
16*1.0
INCHCK   IOUTPT   MOUTPT
  2        11    1,2,3,4,6,8,11,12,13,14,15
MSMOUT   MSMOUT
  19      1,2,3,4,5,6,12,13,14,20,21,22,23,24,25,26,27,28,29
```

**Figure 12 (Continued): E42.2 COMPBRN III Input Deck**

the calculations could not be carried out for times greater than 9 minutes (Phase 1).

The measured mass loss rate was supplied to all participants before the calculations were performed. Some of the participants chose to directly use the supplied mass loss rate for their calculations. For our purposes, the supplied values were used to guide some of the parameter selections in COMPBRN III. The fire model then calculated a mass loss rate of its own.

The plots of the fire power output, the total energy released, and the mass loss rate are shown in Figures 13-15, respectively. Of these three quantities, only the mass loss rate was measured in the actual test. As seen in Figure 15, COMPBRN III significantly under-predicts the mass loss rate during the first 5 minutes of the test. The calculations indicate that there is very little flame spread during this time. The non-burning cables are pre-heating, but have not reached the ignition temperature. COMPBRN III does a reasonable job of predicting the cable mass loss rate during the 6 - 9 minute time frame, and slightly overpredicts the mass loss rate from the cable trays. The calculated and experimental results have the same slope during this period.

The hot gas layer temperature as a function of time is shown in Figure 16. The results indicate a steady rise in hot gas layer temperature between 4 and 9 minutes into the fire. This corresponds to the ignition and subsequent burning of cable trays 2, 3, and 4 during this time period. The COMPBRN III results greatly underpredict the temperatures measured with thermocouple CT5298 during the first 5 minutes of the test. This result is expected based on the large difference between the calculated and measured mass loss rates during this time period. However, it is interesting to note that COMPBRN calculates a HGL temperature of 405 C at the 9 minute mark, which agrees well with the measured value of 440 C.

In Table 3, the calculated time at which each cable tray ignites is shown (in minutes). For cable trays which have not ignited by the 9 minute mark, the surface temperature of the cable trays is shown (in degrees Kelvin) at 9 minutes. Note that since each tray was divided into 4 segments in the COMPBRN model, the time/temperature is given for each of the 4 segments. From this table, we can deduce the following sequence of cable tray ignition and fire growth. One quarter of tray 5 of rack I is the only cable tray that burns during the first 4 minutes of the fire. At 4 minutes, the quarter of trays 2, 3, and 4 of rack I that are directly above the burning quarter of tray 5 also ignite. At 6 minutes, the quarter of tray 1 of rack I that is directly above the burning quarter of tray 2 ignites. From 6 to 9 minutes, no new ignitions occur. However, at 9 minutes much of the remaining cable insulation ignites, or is very close to ignition. At 9 minutes, 2 quarters (out of the remaining 3 quarters) of trays 1-5 ignite, so that 75% of these trays are burning or have been burned. Additionally, 3 quarters of cable tray 20 of rack IV have ignited at the 9 minute mark, and all of the remaining cable insulation is seen to be within 50 C of the assumed ignition temperature.

As seen in Table 3, a radical change in the fire environment is predicted by COMPBRN III at the 9 minute mark. All of the combustible cable insulation is either burning or within 50 C of the ignition temperature. It appears that the fire room is very close to the flash-over point. Unfortunately, no longer times could be modeled due to the limitations of COMPBRN III (the test specification indicated that the doors would be opened at this time in the test).

The results shown in Table 3 are in very good agreement with regard to the observed timing of cable tray ignition in the tests, with the exception of the initial stages of the fire. The test results indicate that all of the trays directly above the initial burning tray ignited within 2 minutes of the first tray (based on thermocouple data), whereas the calculated results indicate 4 minutes (or more) is required to ignite any of these trays. This partly explains the large differences in calculated and measured cable tray mass loss rate during the early part of the test. This may also be a result of the relatively long time

step used in the COMPBRN calculations (1 minute).

The COMPBRN results also indicate that more than 50% of the combustible material in the fire room will be involved in the fire (burning) by the 9 minute mark. This is in very good agreement with observations made during the test which indicated that this occurred between 8 and 9 minutes following ignition.

While these results are in fairly good agreement with the test data, the COMPBRN III results were noted to be very sensitive to the choice of input parameters. The above results are a strong function of the PVC heat of combustion, ignition temperature, PVC thickness used, discretization of the cable trays, time step size, and combustion efficiency assumed. For reasonable ranges of these parameters, the results varied from no secondary ignition within 10 minutes following primary ignition, all the way to full involvement of all of the fuel within about 4 minutes following primary ignition. The particular set of results discussed above was selected as the most realistic because it was closest to the mass loss rate data provided prior to the calculations. While the above results are limited to the COMPBRN III model, many of the other fire models used by the other participants exhibited similar sensitivities to input parameters.

**Table 3: Cable Tray Ignition/Temperature**

| Rack # | I* | | | | | II* | | IV* |
|---|---|---|---|---|---|---|---|---|
| Cable Tray # | 1 | 2 | 3 | 4 | 5 | 12 | 13 | 20 |
| Segment 1 | 9 min | 9 min | 9 min | 9 min | 9 min | 718 K | 716 K | 707 K |
| Segment 2 | 6 min | 4 min | 4 min | 4 min | 0 min | 722 K | 715 K | 9 min |
| Segment 3 | 9 min | 9 min | 9 min | 9 min | 9 min | 696 K | 695 K | 9 min |
| Segment 4 | 705 K | 706 K | 701 K | 695 K | 688 K | 677 K | 677 K | 9 min |

* Numbers indicate the time at which the cable tray segment ignited, or the surface temperature of the cable tray at 9 minutes (if no ignition has occurred). An ignition temperature of 723 K was assumed for the calculations.

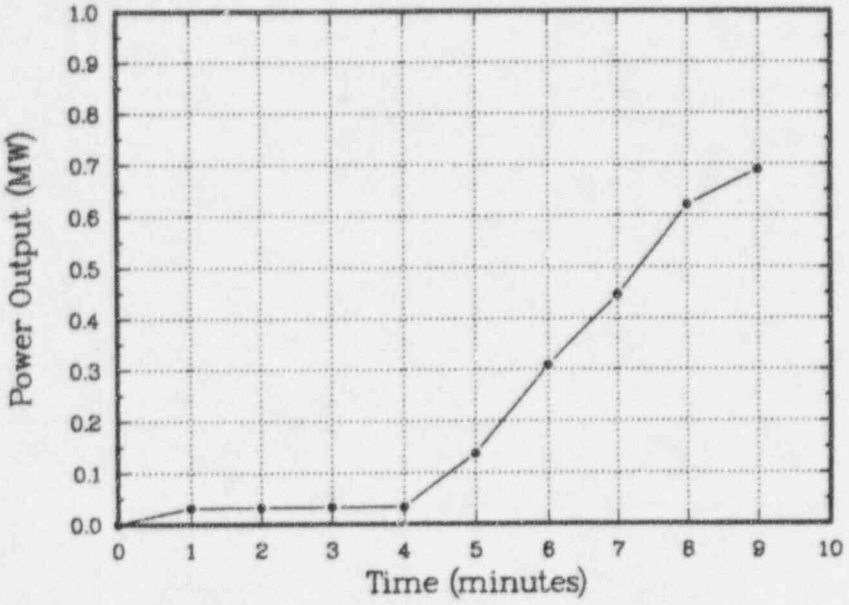


**Figure 13: COMPBRN E42.2 Fire Power Output**

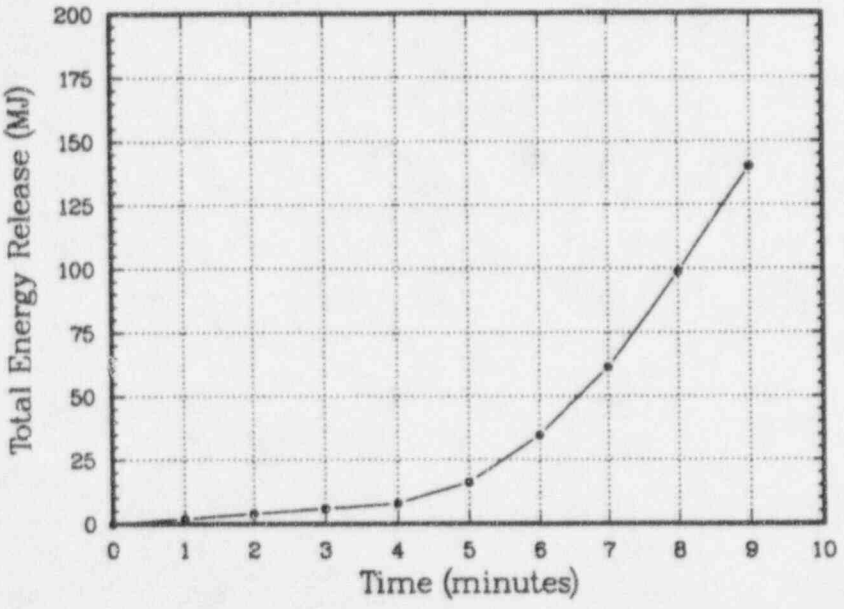


**Figure 14: COMPBRN E42.2 Fire Total Energy Output**

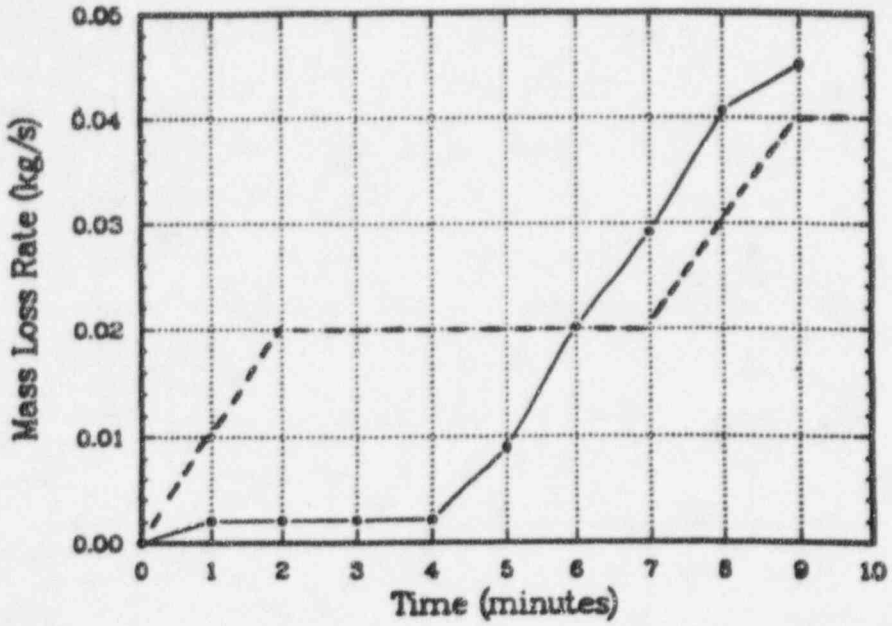


Figure 15: COMPBRN E42.2 Fuel Mass Loss Rate
(Solid = COMPBRN results, Dash = Measured)

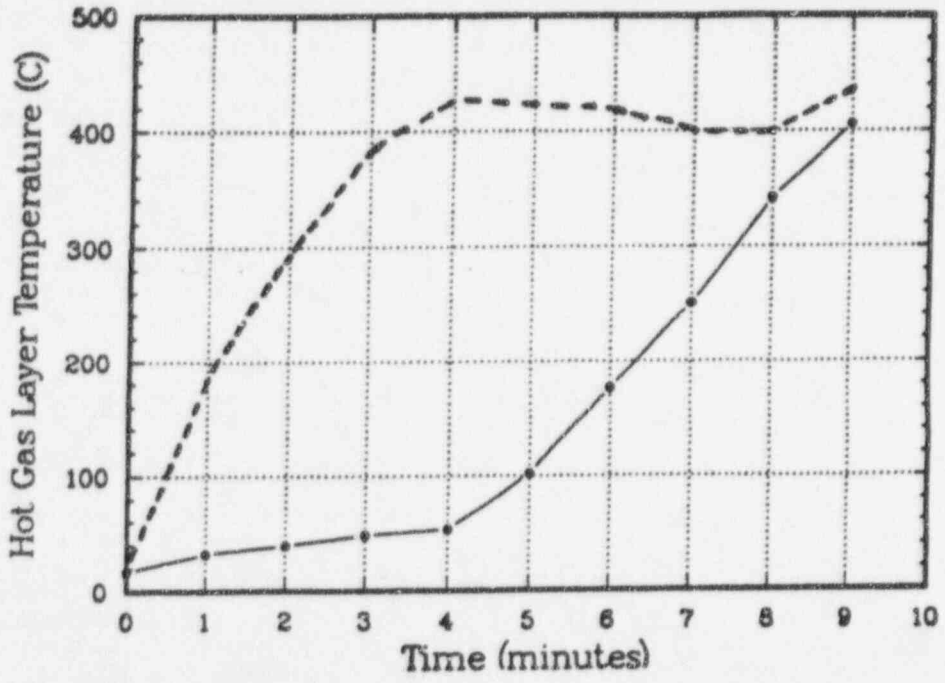


Figure 16: COMPBRN E42.2 Hot Gas Layer Temperatures
(Solid = COMPBRN results, Dash = Measured by CT5298)

# 4 Other HDR Fire Modeling Efforts

Because the HDR program has been international in scope, there have been many inter-related efforts by researchers in many countries. In this chapter, the participants for each set of calculations and their results will be discussed. Appendix A contains a brief description of some of the fire models that have been used by these researchers.

## 4.1 E41.7 Participants

A list of participants attending the E41.7 problem specification meetings is shown in Table 4. These meetings were held in May 1990 in Kahl, Germany, and were chaired by Mr. K. Müller of KfK

**Table 4: E41.7 Participants**

| Name | Institution/Country |
|---|---|
| K. Müller | KfK, Germany |
| M. Rowekamp | GRS, Germany |
| W. Kruger | SAA, Germany |
| K. Jungling | TUV, Germany |
| V. Nicolette | SNL, USA |
| K. Fischer | Battelle, Germany |
| R. Dobbernack | TUB, Germany |
| R. Huhtanen | VTT, Finland |
| O. Keski-Rahkonen | VTT, Finland |
| H. Jahn | GRS, Germany |
| B. Schwinges | GRS, Germany |
| A. Roche | CEA, France |
| R. Rzekiecki | CEN, France |
| R. Schmidt | Fichtner, Germany |
| R. Volk | HDR, Germany |
| U. Max | U.Kassel, Germany |

It is interesting to note that the majority of participants at this meeting indicated that they would use zone models for the modeling of test E41.7. The only exceptions to this were Sandia, VTT, and Battelle-Frankfurt, which indicated that they would use field models or hybrid models for the calculations (possibly in addition to any zone model calculations). The other participants were very skeptical that field modeling could be applied to such a complex problem, and were openly dubious of the possibility of succeeding. In fact, the geometric information that KfK distributed to all participants was not nearly as detailed or extensive as required for an accurate field model calculation of the whole containment. This necessitated getting the information from an extended plant walk-down or from plant layout drawings at each elevation.

There were also many lively discussions at this meeting between the people conducting the experiments and those trying to model the resulting fires. These discussions point to the need for experimentalists and fire modelers to work closely together, if progress is to be made in fire modeling. It is critical that the people conducting a fire experiment understand the sensitivity of fire model predictions to such factors as complex geometries, ventilation boundary conditions, and fuel properties. Likewise, it is critical that the people developing and validating fire models have a good understanding of the technical issues faced by the experimentalists in attempting to conduct a realistic test.

At times in the HDR discussions, there was obviously a wide gap between the perspectives of the experimentalists and those of the modeling people. The experimentalists were determined to conduct tests that would be as realistic as possible, complete with changing ventilation rates, doors opening, filters clogging, actual electrical

cables, etc. This goal is very praiseworthy, and as a result, a wealth of very unique experimental data was generated on realistic fire environments in a nuclear power plant containment.

Unfortunately, fire models are generally not well developed enough to handle these very real elements of a fire. (For example, some of the models require that the user must input the burning rate of the fuel as a known parameter.) As a consequence, some of the test scenarios were beyond the capabilities of any fire model that has been developed to date.

While the discussions concerning the HDR experiments and modeling efforts were sometimes heated, they were very educational. As a consequence of these discussions, the people involved in the HDR experiments as well as those involved in the modeling efforts gained a deeper appreciation for the problems faced by the other camp. Hopefully, this will result in a tighter integration of experimentalists and modeling people in fire modeling development and validation efforts (as well as in fire test efforts) in the future.

## 4.2 E41.7 Calculations by Other Participants

Only a brief summary of the E41.7 calculations by other participants will be given. Sandia was the only participant to apply a field model to this problem (in addition to a zone model). All of the other participants applied multi-room zone models or control volume models to test E41.7.

The level of agreement of the model results with the test measurements is a strong function of location in the containment. Within the fire room itself, the MRFC (see Appendix A) model (applied by Schneider and Lebeda of the Univ. of Wien, Austria) and the BRI2 (see Appendix A) model (applied by J. Rockett of Fire Analysis & Modeling, and O. Keski-Rahkonen and L. Heikkila of VTT, Finland) appeared to give the best agreement in the hot gas layer region. This can be seen in Figures 17a and 17b. In both figures, the dark line represents the measured thermocouple temperatures.

Note that these two models were the only two that were consistently within 250 C of the measured temperatures. This poor agreement was heavily influenced by the fact that the fire room was virtually a fireball, which most fire models are not designed to model. In general, the agreement became worse (and the disparity wider) as rooms other than the fire room were examined.

This level of agreement (and the wide disparity in modeling results) reflects on the state of the art in fire modeling, and why it is sometimes considered to be more of an art than a science. In meetings with the other participants, the large influence that modeling assumptions have on the model results was often the focus of the discussion. Again, it must be recognized that the results of a fire model are not only a function of the model itself, but are also a strong function of the experience and judgement of the one who applies the model.

## 4.3 E42.2 Participants

A list of participants attending the E42.2 problem specification meetings is shown in Table 5. These meetings were held in Karlsruhe, Germany, in May 1992, and were also chaired by Mr. K. Müller of KfK. Notice that this group of fire modeling participants is larger and broader than that for the E41.7 test. At these meetings, each participant was asked to indicate the fire models that they were planning to apply to the ISP. These fire models are listed in Table 6. A brief description of some of these fire models is given in Appendix A.

Of particular note is the fact that most of the E42.2 participants expressed great interest in field models. While only a few indicated that they might try to use field models for the E42.2 calculations, most participants openly discussed the development of (and need for) fire field models. Compared to opinions expressed at the E41.7 meeting 2 years previous, this represented quite a shift in international opinion within a very short time frame, and resulted (to a large

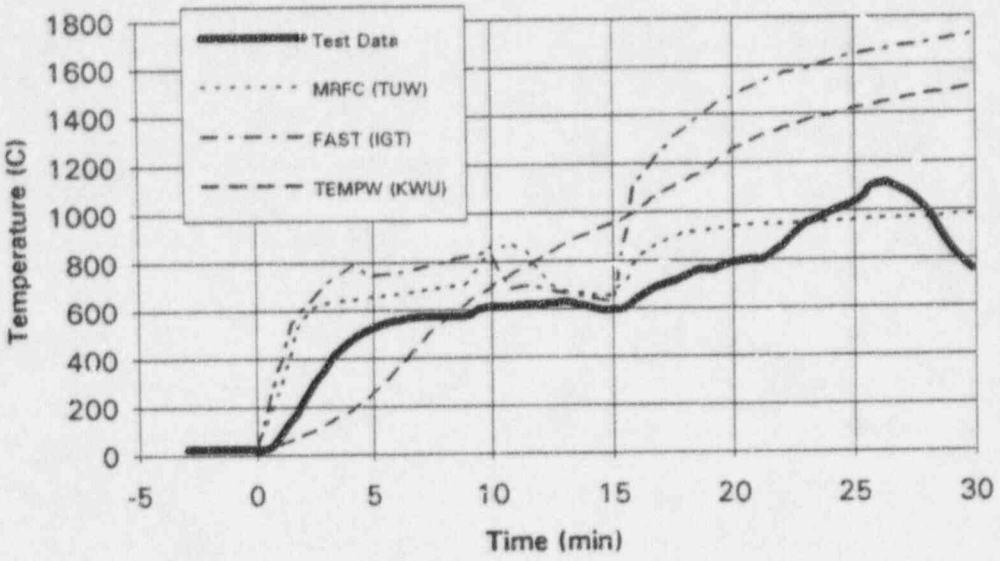


**Figure 17a: E41.7 Comparison of Models to Experiment**

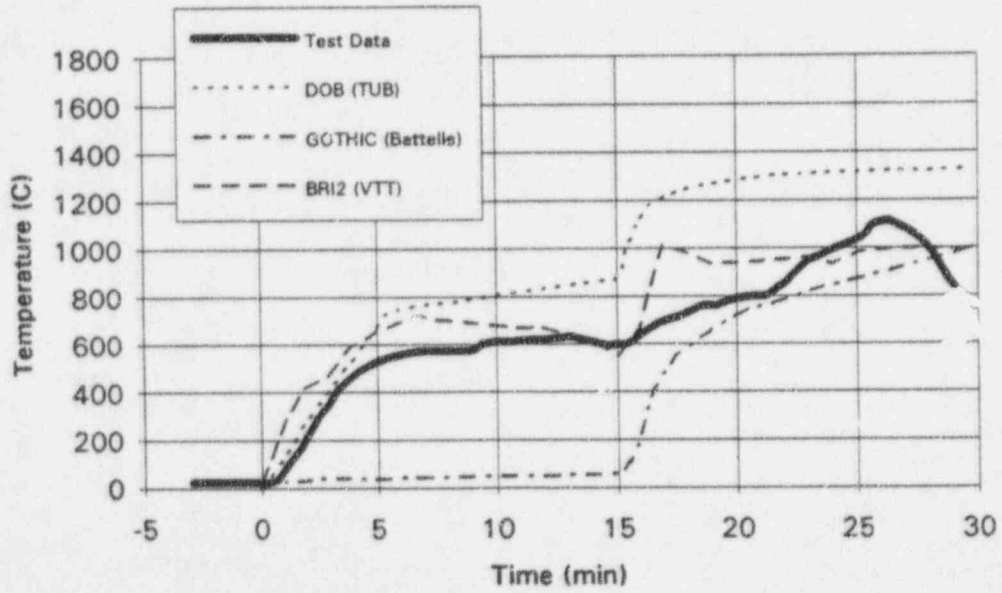


**Figure 17b: E41.7 Comparison of Models to Experiment**

extent) from the successful application of a field model to the King's Cross fire (Simcox, et al., 1988).

## 4.4 E42.2 Calculations by Other Participants

Only a brief summary of the E42.2 calculations by other participants will be given. More detailed information is available in the Proceedings of the 1993 Structural Mechanics in Reactor Technology (SMiRT) Conference, Post-Conference Seminar #6, in Heidelberg, Germany, August 1993 (KfK 1994). A final report from the European Commission is also available (Karwat, 1994).

Test E42.2 was an international standard problem, and the modeling results were coordinated and assembled by Professor Karwat of the University of Munich. As mentioned previously, all of these calculations were performed in a blind fashion, except that the measured cable mass burning rate (not the HRR) was given.

Of the approximately 25 organizations originally interested in participating in the ISP (see Table 5), only 8 (including Sandia) submitted calculations (indicated in Table 6). This was perhaps due in part to the complexity of modeling cable tray fires. It was also interesting to note that there were no field model calculations submitted by any of the participants. This reflects the fact that it is generally not cost-justifiable to apply CPU-intensive field models to fire scenarios in which the heat source (input to the field model) is poorly defined (as in a cable tray fire), since the heat source input drives the field model calculations.

Two general comments can be made concerning the comparisons of all of the participant's calculations to the E42.2 test data. First, in every case the calculated hot gas layer temperatures in the fire room lag far behind the measured temperatures (Figures 18a and b). This may result from the use of quiescent plume correlations in all of the models, when in fact, significant velocities can be generated in the surrounding air for fires in enclosed spaces. The use of quiescent plume correlations for such fires can result in significant underprediction of the air entrainment and fuel burning rates (Rockett, et al., 1992).

The second comment that can be made from the results is that a good model for cable pyrolysis and burning is not presently available. There was great disagreement between the burn rates predicted by the various models. This points to the fact that the modeling of solid material combustion (pyrolysis and burning) is perhaps the most immature aspect of fire modeling. All participants expressed the need for further research in this area in particular. Even knowing the mass loss rate of the cable trays, the HRR estimates varied greatly among the different models.

Of note in this regard, fire models generally require the user to input the heat of combustion of a material as a constant value. During discussions of the E42.2 results, Mr. Keski-Rahkonen of VTT pointed out that the heat of combustion for a real material is generally a function of time. One should not expect that the energy released (and the rate of release) for volatile components that are produced initially in a fire will be the same as that of the remaining charred material. Mr. Keski-Rahkonen was well-qualified to discuss this issue, as he had experimentally measured the heat of combustion for the cables used in test E42.2. His measurements indicate that the heat of combustion varied over the range of 10 - 37 MJ/kg, depending upon the time into the fire and the incident heat flux to the cables.

**Table 5: HDR E42.2 Calculation Participants (Originally Interested)**

| Name | Affiliation |
|---|---|
| V. Nicolette | Sandia National Labs., USA |
| H. Holzbauer | Battelle Institute, Frankfurt, Germany |
| O. Keski-Rahkonen | VTT, Finland |
| W. Gregory | Los Alamos Lab., USA |
| P. Büttner | Energiewerke Nord GmbH, Germany |
| C. Wheatley | AEA Technology, UK |
| A. Samman | Siemens KWU, Germany |
| W. Hensel | Siemens KWU, Germany |
| R. Rzekiecki | CEA, Cadarache France |
| U. Max | Univ. of Kassel, Germany |
| C. Lebeda | Tech. Univ. of Wien, Austria |
| Kaercher | EDF, Lyon France |
| Chabert | EDF, Paris France |
| Mosse | EDF, Lyon France |
| A. Ranelletti | ENEL, Italy |
| R. Dobbernach | Tech. Univ. Braunschweig, Germany |
| P. Stolze | Tech. Univ. München, Germany |
| M. Rowekamp | GRS, Koln Germany |
| A. Alemberti | Ansaldo, Italy |

**Table 6: Fire Models for ISP (Originally Planned)**

| Institution | Fire Model | Type* |
|---|---|---|
| GRS | CRDLOC | 3,4 |
| Sandia** | COMPBRN III | 1 |
| Battelle Frankfurt** | GOTHIC | 4 |
| VTT** | BRI2 | 2 |
| Los Alamos | FIRAC & FLOW3D | 1,3,5 |
| Energiewerke Nord** | FAST | 2 |
| AEA Technology | FLOW3D | 5 |
| Siemens - KWU** | TEMPW | 1,2,3 |
| CEA | FLAMME & LIQUINET | 1 |
| ENEL | COMPBRN III | 1 |
| EDF** | MAGIC | 2 |
| Tech. Univ. Wien** | MRFC | 2 |
| Ansaldo | COMPBRN III | 1 |
| Tech. Univ. Braunschweig** | DOB or FIGARO | 1,2 |

*Types of Models: 1) zone, 2) multi-room, 3) lumped, 4) lumped 3D, 5) field

**Indicates organization submitted final set of blind calculations as part of ISP.

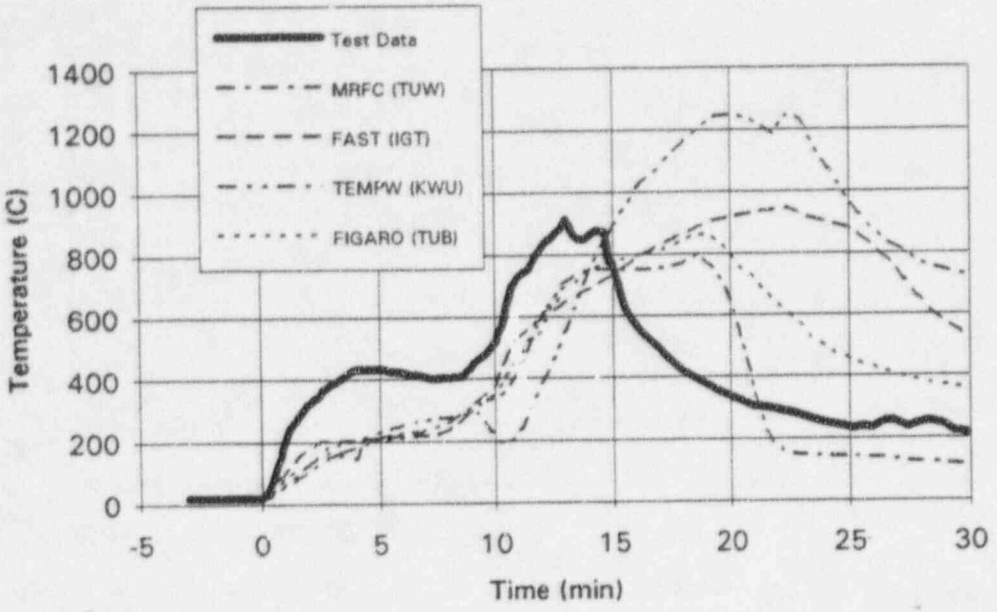


**Figure 18a: E42.2 Comparison of Models to Experiment (Hot gas layer temperatures from CT5298 in fire room)**

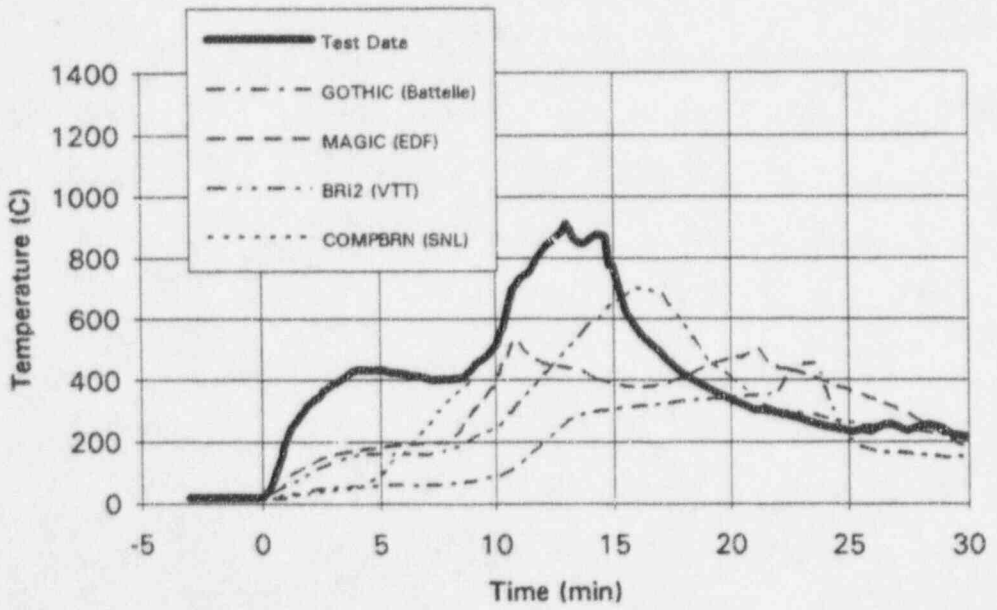


**Figure 18b: E42.2 Comparison of Models to Experiment (Hot gas layer temperatures from CT5298 in fire room)**

# 5 Summary

Many lessons have been learned regarding nuclear power plant fire modeling as part of this work. These lessons are not specific to the HDR containment and the tests conducted therein, but have a broader application to fire modeling in general.

## 5.1 E41.7 Lessons Learned

The E41.7 COMPBRN calculations could not be obtained beyond 4-7 minutes into the fire (depending on the input parameters) due to numerical instabilities in the COMPBRN code. The calculations were unstable due to the large radiative heat fluxes that are calculated. These results indicate that COMPBRN cannot model very large fires in small rooms (it was not developed with fires of this type in mind). The limitations of the model are also seen in that the opening of a door part way into the test cannot be modeled with the code.

The E41.7 Notre Dame Fire Model calculations demonstrate the capabilities of a fire field model. Good agreement is obtained for gas temperatures that are in the hot gas layer but outside of the fire plume. The limitations of the model are seen to be its lack of a combustion model to represent the flame volume, and the large CPU time required to operate it.

The lessons learned from the results of the other E41.7 participants can be summarized as follows. The level of agreement of the different model results with the test measurements is a strong function of location in the containment. Within the fire room itself, only two of the models were consistently within 250 C of the measured gas temperatures. This poor agreement was heavily influenced by the fact that the fire room was virtually a fireball, which most zone fire models are not designed to model. Zone fire models assume that the fire develops as a typical pool fire (or jet fire). In general, the agreement became worse (and the disparity wider) as rooms other than the fire room were examined. This is a consequence of inaccuracies in the room-to-room transport submodels.

In meetings with the other participants, the large influence that modeling assumptions have on the model results was often the focus of the discussion. Thus, it must also be recognized that the results of a fire model are not only a function of the model itself, but are also a strong function of the experience and judgement of the one who applies the model.

## 5.2 E42.2 Lessons Learned

The E42.2 COMPBRN results demonstrate the types of fires for which COMPBRN will yield reasonable results: small to medium sized fires (a pre-flashover compartment). Note that results were only obtained early in the fire, before the fire room door was opened. This also corresponded to the time when the fire was not yet a very large fire. The strengths of COMPBRN are seen to be its ability to model the transient ignition and burning of cable tray fires. Very few other fire models possess this feature.

Agreement of the COMPBRN III results with E42.2 experimental data is reasonable, but hot gas layer temperatures and cable tray mass loss rates are significantly underpredicted during the initial stages of the fire. The timing and sequence of cable tray ignition were well-predicted by COMPBRN, with the exception of the early stages of the fire. In particular, the time to involvement of 50% of the combustible material was in good agreement with the test observations. Unfortunately, the COMPBRN results were very sensitive to the user's choice of input parameters.

The lessons learned from the results of the other E42.2 participants can be summarized as follows. First, for every model applied to this test, the calculated hot gas layer temperatures lag far behind the measured temperatures.

This may result from the use of quiescent plume correlations in all of the models, when in fact, significant velocities can be generated in the surrounding air for fires in enclosed spaces. Second, it was obvious from the large disparity in model results that a good model for cable pyrolysis and burning is not presently available. This points to the fact that the modeling of solid material combustion (pyrolysis and burning) is perhaps the most immature aspect of fire modeling. Third, the heat of combustion for a real material is generally a function of time, and fire models are generally not set up to handle this.

## 5.3 General Observations from HDR Fire Modeling

Some general observations can be made regarding fire modeling of nuclear power plants based on the HDR fire modeling effort. These observations are based on the opinions and experiences of those who have participated in the HDR fire modeling efforts, and should be regarded as such.

Fire modeling continues to grow and develop in maturity. However, compared to most other areas of science, it is still relatively immature. Its development has been hindered by the complexity and tight coupling of the non-linear phenomena involved. In many respects, there is still somewhat of an art to making accurate fire modeling calculations. Experience with a particular fire model is essential to determine its weak areas and potential pitfalls. Unfortunately, many models require the input of parameters which are not well known, and to which the results are very sensitive.

Just a few years ago, fire modeling efforts were dominated by zone models and control volume models. With advances in computers and computational methods such as computational fluid dynamics (CFD), many of the fire modeling efforts world-wide are moving in the direction of field model development. These models are rapidly improving in their capabilities and ease of use. They have eliminated the need for some of the ill-defined input parameters which other models require (such as flow loss coefficients). The development of graphical user interfaces has greatly facilitated the necessary input of information and grid generation. It is not expected that fire field models will replace the other types of fire models, but rather will serve to complement the suite of fire analysis tools available for fire safety analyses.

Validation of fire models remains an important issue. The HDR comparisons have demonstrated that fire models perform poorly when used outside of the realm for which they were designed. This should be no surprise, since many of the models rely extensively on experimental correlations derived for a specific geometry and ventilation condition. Thus, validation of the models against more fire data representative of fires in nuclear power plants is needed. This is especially important for fire field models, which are relatively new, and consequently, have not been validated to the same extent as the other types of models.

Validation of fire models also raises the issue of the need for experimentalists and fire modelers to work closely together, if progress is to be made in fire modeling. It is critical that the people conducting a fire experiment understand the sensitivity of fire model predictions to such factors as complex geometries, ventilation boundary conditions, and fuel properties. Likewise, it is critical that the people developing and validating fire models have a good understanding of the technical issues faced by the experimentalists in attempting to conduct a realistic test. As a consequence of the HDR fire project, the people involved in the experiments as well as those involved in the modeling efforts gained a deeper appreciation for the problems faced by the other camp. Hopefully, this will result in a tighter integration of experimentalists and modeling people in fire modeling development and validation efforts in the future.

In conclusion, the HDR fire tests and modeling efforts have contributed a wealth of information regarding fires in

nuclear power plant containments, and the strengths and weaknesses of present day fire models for simulating these fires. Based on our experiences with the HDR fire modeling efforts, fire models can potentially contribute to improved fire safety of nuclear power plants, when they are used within their realm of applicability. Defining this realm of applicability, and the sensitivities inherent in today's fire models, is a task that remains to be completed.

# 6 References


Ho, V., N. Siu, G. Apostolakis, "COMPBRN III - A Computer Code for Modeling Compartment Fires," UCLA-ENG-8524, College of Engineering, University of California at Los Angeles, November (1985).

Karwat, H., "Prediction of Effects Caused by a Cable Fire Experiment within the HDR facility," European Commission, Nuclear Science and Technology Report EUR 15648, August (1994).

Karwat, H., K. Müller, and U. Max, "CEC Standard Problem: Prediction of Effects caused by a Cable Fire Experiment within the HDR Containment," Technische Universitat Munchen and Kernforschungszentrum Karlsruhe (KfK) Germany, revised July (1992).

KfK, "Proceedings of 3rd International Seminar on Fire Safety of Nuclear Power Plants," held in conjunction with 12th International Conference on Structural Mechanics in Reactor Technology, August 23-24, 1993, Heidelberg, Germany, Kernforschungszentrum Karlsruhe Work Report PHDR 40.070/94 (1994).

Lambright, J.A. and M.P. Bohn, "Analysis of Core Damage Frequency: Peach Bottom Unit II External Events," NUREG/CR-4550, Vol. 4, Part 4, January (1989a).

Lambright, J.A. and M.P. Bohn, "Analysis of Core Damage Frequency Due to External Events at the DOE N-Reactor" SAND89-1147, Sandia National Laboratories, Albuquerque, NM, March (1989b).

Liu, V.K., and K.T. Yang, UNDSAFE-II: A Computer Code for Buoyant Turbulent Flow in an Enclosure with Thermal Radiation, University of Notre Dame, Notre Dame, IN, TR-79002-78-3, July (1978).

Lambright, J.A., S.P. Nowlen, V.F. Nicolette, and M.P. Bohn, "Fire Risk Scoping Study: Investigation of Nuclear Power Plant Fire Risk, Including Previously Unaddressed Issues," NUREG/CR-5088, SAND88-0177, Sandia National Laboratories, Albuquerque, NM, January (1989).

Müller, K., and U. Max, "Input Data set for E41.7 Blind postcalculations of an Oil Fire in a Closed Subsystem with Ventilation System Connected," PHDR Report No. 40.036/91, Kernforschungszentrum Karlsruhe (KfK) Germany, December (1991).

Nicolette, V.F., and S.P. Nowlen, "Fire Models for Assessment of Nuclear Power Plant Fires," Nuclear Engineering and Design, Vol. 125, pp. 389-394 (1991).

Nicolette, V.F., S.P. Nowlen, and J.A. lambright, "Observations Concerning the COMPBRN III fire growth code," Proceedings of the International Topical Meeting on Probability, Reliability, and Safety Assessment: PSA '89, vol. 2, pp. 1279, Pittsburgh, April 2-7 (1989).

Nowlen, S.P., "A Summary of Nuclear Power Plant Fire Safety Research at Sandia National Laboratories, 1975-1987," NUREG/CR-5384, SAND89-1359, Sandia National Laboratories, Albuquerque, NM (1989).

Nowlen, S.P., "A Summary of the Fire Testing Program at the German HDR Test Facility," NUREG/CR-6173, SAND94-1795, Sandia National Laboratories, September 1995.

Rockett, J.A., O. Keski-Rahkonen, and L. Heikkila, HDR Reactor Containment Fire Modeling with BRI2, Technical Research Center of Finland (VTT), VTT publication 113 (1992).

SFPE Handbook of Fire Protection Engineering, First ed., Society of Fire Protection Engineers, Boston, MA (1988).

Simcox, S., N.S. Wilkes, and I.P. Jones, Fire at King's Cross Underground Station 18th November 1987: Numerical Solution of the Buoyant flow and Heat Transfer, AERE-G 4677 (1988).

# Appendix A: Brief Description of Fire Models Used by Other HDR Participants

## A.1 Introduction

During the course of this project, many different fire models were discussed with the other HDR participants. Some of these models may not be familiar to fire modelers in the U.S. and in other countries. A brief description of some of these models is included here for information purposes, and also as somewhat of a status report on what the rest of the nuclear power plant fire modeling community has recently been doing. It is in no way intended to be exhaustive in either scope or in detail.

The information herein was gathered over the course of several years in discussions with HDR fire modelers from around the world. In this regard, it may not be quite up to date. It is intentionally presented in a somewhat informal style to reflect this consideration.

## A.2 Zone Models

### FLAMME

The French have developed a zone model known as FLAMME. Two versions of the code presently exist. The first version has been validated for liquid pool fires. The second version handles multiple fire sources within a room and has not yet been validated. Either version can be connected to a ventilation model so that multiple rooms can be modeled. At the May 1992 meeting, discussions indicated that the French are now moving in the direction of the other European Community (EC) members in developing 2-dimensional and 3-dimensional fire field models for use in their fire risk assessments.

### DOB

Faculty at the University of Braunschweig have developed a zone model, named DOB. It was used as the basis for designing fire experiments in the HDR (in terms of heat release rates, maximum hot gas layer temperatures, fuel loading). This model is a multi-compartment model.

### MRFC

The University of Kassel has used several zone models for calculation of fires in the HDR. One of these models (internally developed) is called the Multi-Room Fire Model (MRFC). They have also applied the FAST code (developed at the National Institute of Standards and Technology (NIST)) to the HDR. They have mentioned that these models have great difficulties when the hot gas layer reaches the floor of the fire compartment.

## A.3 Hybrid (Control Volume) Models

### RALOC

GRS has used the RALOC code for both hydrogen distribution and fire calculations in the HDR. This control volume code does not have a combustion model in it. Their work has demonstrated that the model can be sensitive to the user's choice of nodalization (i.e., how the containment rooms are subdivided and represented as control volumes) and flow loss coefficients, and that, in some instances the user must know beforehand in which direction the flow from room to room will be, in order to properly construct a nodalization. They have had reasonable success in predicting HDR fire mass loss rates. The RALOC code was developed by the German government, and its availability outside Germany is not clear.

## CRDLOC

H. Jahn of the Technical University in Munich is the primary developer of the CRDLOC code (he also was largely responsible for the RALOC code). This code is similar to RALOC, but has a Chemical Reactions and Distributions (CRD) submodel for modeling pyrolysis and devolatilization rates. The code also models convection, radiation, evaporation, and condensation phenomena. The evaporation and pyrolysis models are not well verified. When applied to pool fires, they have seen some instabilities due to thermal feedback to the pool accelerating the evaporation rate which in turn enhances the thermal feedback.

## FIREIN (See FLOW3D in A.4)

## FATHOMS (GOTHIC)

Another model that somewhat fits this category is the FATHOMS (GOTHIC) model developed by NAI, in Richland, Washington. This model can be used as a zone, control volume, or field model (or any combination of the above). However, its field modeling capabilities are somewhat limited, so it has been included in the hybrid models section. Battelle Frankfurt has applied FATHOMS to the HDR fires.

This code has an interesting history (according to discussions with those who have followed it). The origins of this model are in the COBRA-NC code developed at Battelle Northwest with USNRC funding. The developers of COBRA-NC left Battelle and formed their own company (NAI) about 1988. They proceeded to modify and improve the model, and developed a new version known as FATHOMS. This code can be leased from NAI. In 1989, NAI received a contract from EPRI to improve FATHOMS. The new code is known as GOTHIC.

This code is available to U.S. utilities through EPRI. It is expected that it will be used to address equipment qualification questions (such as maximum local air temperatures near operating equipment) and to address details of licensing procedures (such as hydrogen recombiner locations). It could also be used for utility fire risk assessments. In fact, this model has been used by Westinghouse to address design issues for the AP600 plant.

The FATHOMS (GOTHIC) model is extremely versatile. This code can be used as a 1-, 2-, or 3-dimensional model, and in either a control volume or field model approach. It models the gas/vapor, droplets, and liquid pools with separate equations. It was originally developed as a two-phase flow code for reactor thermal hydraulics. One of the latest versions has the MAEROS aerosol model (developed by F. Gelbard, Sandia National Laboratories, for the CONTAIN code) in it. The code presently does not have a combustion model. The nice feature of the code is that regions of the containment can be modeled in a lumped fashion while others can be modeled with a field modeling approach as desired. This model also has a very easy to use preprocessor that greatly facilitates the input deck generation.

Users of the FATHOMS/GOTHIC model have stressed the importance of proper selection of flow loss coefficients for the geometry of interest. This is absolutely critical to the performance of any control volume model (see previous comments on the RALOC model). In application of FATHOMS/GOTHIC to the HDR fires, it has been possible to alter the direction of flow in the containment by slightly changing the relative values of the flow loss coefficients. This implies that truly 'blind' calculations with these types of models are potentially subject to considerable error.

The field modeling capabilities of FATHOMS/GOTHIC are limited. Only Cartesian coordinates can be modeled. The turbulence model is an algebraic Prandtl mixing length model. The code is somewhat inefficient in that it always solves the droplet and liquid conservation equations, even when there is none present. It is also limited to about 1,000 nodes, which may be too few to properly capture the physics of a fire environment.

## A.4 Field Models

### PHOENICS

VTT Finland has used the PHOENICS field model (a proprietary code licensed from CHAM) for the HDR calculations. Their work appeared to be a tremendously tedious task, as obtaining all of the necessary geometric information for the HDR containment was not straight forward. Their calculations indicate that 90% of the energy is deposited in the walls and equipment of the containment. They used the combustion model in COMPBRN to generate heat release information.

Finland has recently embarked on a joint program with Sweden and the UK to develop a non-proprietary fire field model. The UK participants include the Fire Research Station and Cranfield Technology. The model will have an unstructured grid to allow the user freedom to refine areas of the mesh of particular interest. Their goal is that within a few years time, they will have a model with the same capabilities as the JASMINE code. JASMINE is a proprietary fire field model (based on PHOENICS) that is marketed by D. Spalding's CHAM corporation in the UK.

### HMS

J. Travis (formerly of Los Alamos National Laboratories) has applied his 3-dimensional field model (HMS) to the HDR containment for hydrogen distribution calculations, but not for simulation of the fire tests. He personally developed all of the necessary geometric information for field model calculations for the HDR containment. The VTT field modeling effort as well as the Sandia/Notre Dame field modeling effort benefited from his work.

### FLOW3D (Los Alamos)

Los Alamos National Laboratories originally planned to apply the FLOW3D code developed at Los Alamos to the ISP. However, for unknown reasons, no calculations were submitted. They are also pursuing the development of a compartment fire model to couple with their ventilation system model (FIRAC). This compartment fire model will be a descendant of the FIREIN code, and is being developed in cooperation with Battelle, Northwest. The Los Alamos system model FIRAC is a very unique model, as it is capable of modeling the clogging of filters due to aerosols (such as soot).

### CFDS FLOW-3D (Harwell/AEA)

This proprietary code is different than the Los Alamos FLOW3D code mentioned above. It was developed at AEA Technology (formerly Harwell) in the UK. It is available commercially, and has been used with some success for modeling large-scale fires. The successful application of this code to the King's Cross subway fire gained much attention world-wide.

### KAMELEON Fire

The KAMELEON Fire field model was developed at SINTEF/NTH in Trondheim, Norway. This model has been successfully applied to large-scale open and enclosed fires. The majority of applications has been to offshore drilling platforms in the North Sea. Recently, the model has also been applied by Sandia National Laboratories (Albuquerque, NM) with very good success to large, open pool fires involving aviation fuel.

Sandia has entered into a collaborative agreement with SINTEF/NTH to advance the capabilities of the existing model. Development of this advanced model began during the past year.

# Appendix B: University of Notre Dame Field Model Calculations for HDR Test E41.7

The following report on the Notre Dame Field Model Calculations for HDR Test E41.7 is included as a stand-alone report. It has been published in Computational Mechanics, Vol. 14, No. 5, pp. 468-479, August 1994.

# FIELD MODEL SIMULATION OF FULL-SCALE FORCED-VENTILATION ROOM-FIRE TEST IN THE HDR FACILITY IN GERMANY

by

K. T. Yang and H. J . Huang
Department of Aerospace and Mechanical Engineering
University of Notre Dame
Notre Dame, IN 46556

and

V. F. Nicolette
Thermal and Fluid Engineering (Dept. 1513)
Sandia National Laboratories
Albuquerque, NM 87185

## ABSTRACT

A full-scale forced-ventilation room fire test is simulated numerically based on a fire field model. The fire room, located inside a decommissioned nuclear reactor at the Heiss Dampf Reaktor (HDR) facility in Germany, is characterized by a very complex 3-D geometry. The field model utilized in the simulations accommodates full compressibility, turbulence, wall losses, surface-to-surface and surface-to-flame radiation exchange, and the specific geometries associated not only with the fire room itself, but also with the elevated fuel bed and forced ventilation inlet and outlet. Good correspondence between the measured temperatures at different locations in the fire room and those from the simulations has been found for the first four minutes into the fire during which all fuel in the fuel pan is depleted. Some of the discrepancies in the temperature comparison are explained in terms of shortcomings in the field model.

## INTRODUCTION

In fire modeling, the unique advantages of field models and their use in predicting the spread of fire and smoke in rooms and compartments have long been recognized. These include their capability to predict detailed unsteady movements of both fire and smoke and to account for fluid and thermal interactions among different parts of the fire room. While significant shortcomings still exist for field models in general, especially in the formulation of turbulent

combustion submodels, field models have not been utilized to a great extent in recent years, primarily because their use was very computing intensive and access to high-power computing resources was, in general, rather limited. However, with increasing accessibility to supercomputers, mini-supercomputers, high-power workstations and high-speed desk-top personal computers, field modeling computations have since received increasing attention among fire modelers. This fact alone will undoubtedly spur more research and code development in making field models a timely, viable tool in our efforts to mitigate loss of lives and properties due to fire.

Increasingly, fire field models have been utilized to simulate real fire situations, at least in cases with limited objectives. For instance, the use of the Harwell-Flow 3D code to simulate the air flow in the King's Cross underground station fire in London in 1987 is a good example. Other instances can be found in discussions held at the 1990 Eurotherm Seminar on Fire Modeling (Jones, 1990). While existing field models can indeed be applied to real compartment fire situations and produce quantitative results, it is not well established that such results are sufficiently accurate for real world applications. Consequently, model validation by experimental data in realistic fires is extremely important before the field models can be used with confidence. Such experimental data, especially for full-scale room fires, are difficult and very expensive to obtain, but are critically needed to provide validation for fire models including the field models. Also, these data provide critical information on the deficiency of fire models to guide future development efforts.

In the last several years, an international cooperative effort has been under way to use the latest fire models (both zone and field models) to simulate the full-scale fire tests conducted in a decommissioned nuclear reactor at the Heiss Dampf Reaktor (HDR) facility in Germany in order to assess the viability of using such fire models for future fire-hazard mitigation in nuclear reactors. It is interesting to note that these are the only fire tests ever conducted inside an actual nuclear reactor containment building. The Sandia National Laboratories has been involved in this program as technical consultants to the United States Regulatory Commission (NRC), and has utilized both the COMPBRN III zone model for steady compartment fires developed at UCLA (Ho et al., 1985) and the field model UNDSAFE developed at the University of Notre Dame (Nies, 1986; Raycraft et al., 1990; Yang et al., 1992).

Two series of full-scale fire tests were conducted in the same designated fire room inside the HDR building for the purpose of providing data for comparison with model simulations. One series, designated as the E41.5 Test, deals with a naturally-ventilated fire (Mueller and Volk, 1990), while the second series, known as the 41.7 Test deals with a forced-ventilation fire (Mueller and Max, 1991). Results of the numerical simulation of the E41.5 Test based on the

Notre Dame field model have been given previously by Yang et al. (1992), and the purpose of this paper is to report results for the E41.7 Test with forced ventilation in the fire room.

## DESCRIPTION OF FORCED-VENTILATION FULL-SCALE FIRE TEST

Details of the geometry of the containment building including the fire room and materials and the liquid fuel, can be found in the two reports by Mueller and Volk (1990) and Mueller and Max (1991). Briefly, the containment building is in the form of a vertical pressure vessel, about 60 m in height and 20 m in diameter, and the bottom of the building is about 11 m below grade. The fire room floor is located 4.5 m above ground and is shown in Figure 1. The main fire room has a height of 5 m and that of the entry room, which contains two double doors at the right wall, is about 3 m. The ventilation exhaust, located above the entry room on the right wall of the main fire room can also be seen in the Figure 1. The combined room has a total volume of about 100 $m^3$, and a floor or ceiling area of about 23 $m^2$. The side and rear curved walls are made up of largely 10 cm thick and 15 cm thick of Ytong, respectively, ($\tilde{\rho}$ = 340 kg/$m^3$, $\tilde{c}_p$ = 0.95 kJ/kgK, $\tilde{k}$ ~0.19 w/mK); the floor is covered by a 25 cm thick Ytong layer; and the ceiling is covered with insulation made up of 3 cm of Promatec ($\tilde{\rho}$ = 250 kg/$m^3$, $\tilde{c}_p$ = 0.84 kJ/gK, $\tilde{k}$ ~ 0.13 w/mK) and 2.5 cm of Alsiflex ($\tilde{\rho}$ = 130 kg/$m^3$, $\tilde{c}_p$ = 1.0 kJ/kgK, $\tilde{k}$ ~ 0.1 w/mk). Also, most of the walls and floor are also covered with 2 cm of Alsiflex mats.

The oil fuel pan, equipped with fuel loss weighing scale is elevated 0.61 m from the floor to accommodate a 0.3 m in diameter ventilation inlet underneath. The fuel oil is SOL-T made by Shell Company which produces only dry soot which is not greasy. It has a density of 0.756 kg/$m^3$ at 20°C, a flash point at 54°C, and a heating value of 42,500 kJ/kg.

In the test, the oil in the fuel pan was depleted at the end of 4 minutes into the fire, during which the two doors were closed and the forced ventilation was maintained at 0.85 $m^3$/s. The forced ventilation had been turned on before the fire was ignited. Ignition was achieved using alcohol and electric discharges. Extensive measurements of gas and flame temperatures, various gas concentrations, mass rates of flow, pressures, and doorway velocities were made. For the numerical simulations in the present study, which covers the first four minutes of the fire, simulated temperatures at various locations in the fire room and the entry area are compared to those from the test. These results will be interpreted and discussed on the basis of shortcomings in the field model as well as the local details of the unsteady temperature field.

## THE FIRE FIELD MODEL

As pointed out previously, the fire field model utilized in the present study has been under continuous development at the University of Notre Dame in recent years. Early efforts were concentrated on two-dimensional room fire problems accounting for strong buoyancy, full

compressibility, turbulence, one-dimensional (ceiling to flow) radiation exchange, simple rectangular geometry, but not including effects of combustion and wall losses. Under the code name of UNDSAFE (University of Notre Dame Smoke and Fire in Enclosures), the field model was successfully applied to a variety of room and external fire situations (Yang et al., 1984; Yang and Lloyd, 1985; Satoh et al., 1983; Kou et al., 1986). More recently, this field model has been extended to three-dimensional compartments including wall losses and pressurization in closed compartments (Nies, 1986), complex geometries (Raycraft et al., 1990), internal ventilation in closed compartments (Houck, 1988), effects of sprinklers (Chow and Fong, 1993), and a simulation of full-scale fire tests (Delaney, 1992, Yang et al., 1992).

Despite the versatility of the application of this field model, it is still not complete and validation, especially for large fires, has been insufficient to ascertain its general validity. This is essentially the case for all existing field models. For the Notre Dame field model, still lacking is a combination of a viable turbulent combustion model for complex fuels and the incorporation of multi-dimensional radiative transfer for participating media based on reasonable models for gas and soot radiation spectral propoerties. For the latter, basic information is essentially available, even though its implementation into a fire field model is still complex. However, the lack of detailed knowledge on combustion kinetics for complex but realistic fuels will impede the development of complete fire field models for some time to come.

In the present study, the same fire field model as that used recently by Yang et al. (1992) is utilized with the exception that the model has been modified to incorporate the elevated fuel pan and the forced ventilation in and out of the fire room. This model is now briefly described as follows.

In the present formulation, no combustion model is used, and the heat release rate is taken to be prescribed as volumetric heat sources, and the flame region is also postulated. It is of interest to note that even in the tests, the heat release rate was not measured, but must be determined through the fuel loss data, the heat value of the fuel, and some assumed combustion efficiency. Another deficiency of the model is that gas and soot radiation is neglected, but the surface-surface and surface-flame radiation exchanges are accounted for in the model. It, however, should be noted that the net effect of participating medium is to produce a more uniform temperature field and therefore the model tends to overpredict the heat losses through the wall and ceiling regions where temperatures are high. As it will be shown later, within the first short four minutes into the fire, the heat losses through the ceiling and walls are only a small portion of the heat from the fire, and consequently the effect of participating medium is not expected to be significant. Under these conditions, the species equations need not be considered, and the dimensionless governing field equations for turbulent buoyant compressible flow (Yang et al., 1992) can be written in tensor forms as:

$$\rho_{,t} + (\rho u_i)_{,i} = 0 \tag{1}$$

$$(\rho u_i)_{,t} + (\rho u_i u_j)_{,j} = -p_{,i} - \rho G + (\sigma_{ij})_{,j} \tag{2}$$

$$(\rho c_{pm} T)_{,t} + (\rho u_i c_{pm} T)_{,i} = (kT_{,i})_{,i} + Q_c \tag{3}$$

where the dimensionless shear stress tensor $\sigma_{ij}$ and mean specific heat $c_{pm}$

$$\sigma_{ij} = \mu\left(u_{i,j} + u_{j,i} - \frac{2}{3}\delta_{ij}u_{k,k}\right) \tag{4}$$

$$c_{pm} = \frac{1}{T-1}\int_1^T c_p dT \tag{5}$$

where $\delta_{ij}$ is the Kronecker delta function. It is noted here that both viscous dissipation and pressure work can be neglected in the fire phenomena. The above dimensionless quantities are normalized as follows: The coordinates $\tilde{x}_i$ with the height of the fire room H; the time variable $\tilde{t}$ with $H/u_R$ where $u_R$ is a constant reference velocity; all velocity components $\tilde{u}_i$ with $u_R$; absolute temperature $\tilde{T}$ with $T_R$ where $T_R$ is again a reference temperature normally taken to be the air inlet temperature; the pressure difference $(\tilde{p} - \tilde{p}_e)$, where $(\tilde{p}_e)$ is the hydrostatic equilibrium pressure, with $\rho_R/u_R^2$ where $\rho_R$ is a constant reference air density based on $\tilde{\rho}$ and $T_R$; the gravitational acceleration $G = (0,0,g)$, with $u_R^2/H$; and the thermophysical properties $\tilde{\rho}$ (density), $\tilde{c}_p$ (specific heat), $\tilde{\mu}$ (viscosity) and $\tilde{k}$ (thermal conductivity), with, respectively, $\rho_R$, $c_{pR}$, $\rho_R u_R H$, and $\rho_R c_{pR} u_R H$ where $c_{pR}$ is a constant reference specific heat evaluated at $T_R$. All $\tilde{u}_i$ and $\tilde{T}$ are Reynolds averaged quantities, and $\tilde{\mu}$ and $\tilde{k}$ consist of both laminar and turbulent quantities. In addition, $Q_c$ is a dimensionless volumetric heat source, prescribed inside the flame zone and zero outside the flame zone. Also, for convenience, the origin of the coordinate system is fixed at the left front corner of the fire room. Thus, the i-coordinate is in the direction from the fire room to the entry room; the j-coordinate is in the direction of the depth, from the front to the rear; and the k-coordinate is from the floor to the ceiling (see Figure 1).

Since during the first four minutes of the fire the two doorways are closed, the combined room is all closed except the inlet and outlet of the forced ventilation, and the boundary conditions are relatively simple to write. All velocity components vanish at any solid surface. At the ventilation inlet, the normal air velocity at $T_R$ is distributed uniformly over the inlet area so that the flow rate is that of the prescribed ventilation rate. At the outlet, all velocity components and temperature have zero gradients normal to the outlet area. The temperature boundary condition at the walls, ceiling and floor is in accordance with a heat balance and is coupled to the conduction through the solid thicknesses. The heat balance here involves surface radiation fluxes from the rest of the surfaces including those of the flame, the convection fluxes from the fluid flow, and conduction fluxes into the solid. Details of this heat balance will be described later in the wall-loss submodel.

The formulation of the fire field model is not complete until several submodels are incorporated. Compressibility is inherent in the governing differential equations and density is computed from the perfect gas law, with pressure nearly constant throughout the rooms due to ample ventilation. Strong buoyancy is accounted for in Equation (2) without involving the Boussinesq approximation. Other submodels for wall losses, turbulence, radiation and combustion are described in the following.

Heat transfer through the walls, ceiling and floor is taken to be that of one-dimensional unsteady conduction through the solid material. The boundary conditions are that at the inner surface the arriving heat flux is that due to a combination of radiation and convective heat fluxes, while at the exterior surface of the walls and ceiling, a convection boundary condition utilizing prescribed constant coefficient of heat transfer h and ambient temperature $T_R$. The floor, in view of its thickness of 25 cm, is taken to be insulated at the bottom surface. In the previous natural ventilation tests E41.5 (Yang et al., 1992), the test lasted over 18 minutes into the fire and the heat loss through the walls and ceiling was considerable. In the current forced-ventilation test E41.7, numerical simulation only covers four minutes into the fire during which most of the heat was absorbed by the solid. Consequently, losses to the ambient were very small and hence a reasonable coefficient of heat transfer h is all that is needed.

While several field models such as, for instance, Harwell-FLOW 3D (Simcox et al., 1988) and KAMELEON (Holen et al., 1990) utilize the standard k-ε model of turbulence, the Notre Dame field model has always advocated a much simpler mixing length type of algebraic turbulence model which accounts for stratification effects and has sufficient accuracy for the fire phenomena, as validated by experiments (Yang and Lloyd, 1985; Raycraft et al., 1990). Such an algebraic model is retained in the current simulation study and is given by the following:

$$\frac{\mu}{\mu_R} = 1 + \frac{\left(\frac{l}{H}\right)^2 \sqrt{\left(\frac{\partial u_i}{\partial x_j}\right)\left(1-\delta_{ij}\right)}}{2 + \frac{Ri}{Pr_t}} \tag{6}$$

where

$$\frac{\ell}{H} = K\left\{\frac{\sqrt{u_i u_i}}{\sqrt{\sum_{ij}\left(\frac{\partial u_i}{\partial x_i}\right)^2}} + \frac{\sqrt{\sum_{ij}\left(\frac{\partial u_i}{\partial x_j}\right)^2}}{\sqrt{\sum_{ij}\left(\frac{\partial^2 u_i}{\partial x_i \partial x_j}\right)^2}}\right\} \tag{7}$$

$$Ri = \frac{H}{u_R^2} \frac{\left(\frac{\partial T}{\partial n}\right)\vec{n}\cdot\vec{g}}{\sum_i\left[\left(\frac{\partial u_i}{\partial n}\right)\vec{n}\cdot\vec{g}\right]^2} \tag{8}$$

where $Ri$ is the gradient Richardson number, $\ell$ is a mixing length, and $\vec{n}$ is a unit vector in the direction opposite to gravity. The quantity $Pr_t$ is a turbulent Prandtl number, which is also used to provide a model for the effective thermal conductivity $k$ (molecular plus turbulent):

$$\frac{k}{k_R} = \left(1 - \frac{Pr}{Pr_t}\right) + \frac{Pr}{Pr_t}\frac{\mu}{\mu_R} \tag{9}$$

where $Pr$ is the molecular Prandtl number, which is also taken as a function of temperature $\bar{T}$. In this algebraic model, $Pr_t$ is assigned a numerical value of unity, for simplicity. Equation (6) clearly shows the stratification effect as represented through the use of the Richardson number. It should be mentioned here that the k-ε model of turbulence does produce a more accurate estimate of the strain rates in the turbulent flow which could be useful in relating turbulence to the combustion process (Candel et al., 1990).

As indicated previously, the hot gas in the rooms is taken to be transparent and only surface to surface radiation exchange is included in the present field model. Consequently, the radiation flux only comes into play in the thermal boundary conditions at the walls, ceiling and floor. Furthermore, the flame surfaces are taken to be opaque and are treated the same as any other solid surface. Each surface, which, for convenience, coincides with the computational cell,

is taken to be gray and diffuse, and the radiation flux there is calculated by the standard radiosity method (Siegel and Howell, 1992) in terms of the surface emissivity and view factors. All view factors are determined once for all, taking into account shading due to obstructions along the line of sight. Partial blockages are accommodated by modifying the surface areas involved. In general, nonzero view factors are calculated by using the view factor definition, treating each surface as a sufficiently small area. This formulation is not accurate for two surfaces in close proximity, in which case the exact view factors based on finite areas are utilized (Howell, 1982). Even though this specific field model does not consider a participating medium, it can be included without any fundamental difficulty, despite the fact that this would create much additional complexity in the radiative transfer calculations (Yang, 1986). For instance, such a scheme based on P-N approximations and exponential wide-band models for participating gases, together with a combustion model, is now being incorporated into a computer code for dealing with compartment fire problems (Londino, 1993).

From a fundamental point of view, a turbulent combustion model is needed in a complete fire field model and, together with appropriate turbulence and gas radiation models, will provide information about fuel and combustion product species concentration distributions, flame zones, and time-dependent heat release rates and their spatial variations in the fire. Since a combustion model is not utilized in the current field model, information must be provided on the flame size and shape, and the volumetric heat release rate and distribution. This simplification is another reason that the effect of participating medium is not considered here because it does not have any meaning without a combustion model. In the present numerical simulation, the following provisions are made. The overall heat release rate used in the simulations does not come from the experimental data, since at the outset of the entire study, it was understood that for all simulations based on our model as well as on other fire models, no experimental data were allowed, so that an objective assessment on the merits and failings of the various fire models can eventually be made. In the present simulation, the heat release rate is given by that determined by the fire zone model COMPBRN III developed at UCLA (Ho et al., 1985) under quasi-steady conditions as well as with an estimated combustion efficiency of 70%. Details of this formulation can be found in the reference by Nicolette and Yang (1993). This numerical data will be described later. In addition, the flame or fire plume envelope is taken, for convenience, the same as that of the fuel pan, and extends from the fuel pan all the way to the ceiling. The volumetric heat source within this flame envelope is taken to be uniformly distributed. This assumption is obviously incorrect, since normally for a large fire, the maximum heat release rate occurs at about one third of the height from the fuel pan. However, as the simulation results will show, they indeed underpredict the temperatures in the plume region above the fuel pan. On the

other hand, since the total heat release is preserved in the simulation, temperatures away from the fuel pan and in the hot gas layer at the ceiling agree much better with those in the test.

The numerical algorithm in the Notre Dame field model is based on a finite-volume finite-difference staggered-cell formulation (Raycraft et al., 1990, McCarthy, 1991), which is a direct extension of the 2-D formulation in our earlier room fire studies (Yang et al., 1984, Yang and Lloyd, 1985) with several improvements. One improvement is that in the local pressure correction algorithm to satisfy flow continuity, the temperature and density fields are recalculated in each iteration. A second improvement is that the convective terms in the governing equations (2) and (3) are discretized on the basis of the QUICK scheme (Leonard, 1983) to minimize numerical diffusion effects. Also, a global pressure correction routine is included to accommodate possible global pressure build-up due to insufficient ventilation (Nicolette et al., 1985). Also, as mentioned previously, the numerical algorithm incorporates the heat loss calculations at any solid boundary. The radiation fluxes arriving at the boundary cells are updated once every several time steps to reduce computation time and the view factors are calculated only once and are stored in the form of a lookup table for subsequent radiative flux calculations.

The numerical algorithm as applied to the HDR combined fire room and entry room has been numerically validated in the earlier E41.5 natural-ventilation fire test simulation (Yang et al., 1992) in terms of heat balances and mass flow balances, and hence it will not be repeated here.

## SIMULATION RESULTS AND COMPARISON WITH TEST DATA

In the numerical simulation utilizing the Notre Dame fire field model, the geometry of the combined fire and entry rooms is simplified somewhat to eliminate the curvature in the rear wall, and is shown in Figure 2. A uniform cell grid is adopted, and each cell has a side of $\Delta = 273$ mm. Altogether there are 12,768 calculation cells. The cells are designated by indices I, J, K as also shown in Figure 1. To improve the calculation resolution, both the ventilation inlet and outlet have 4 adjacent cells, and are thus larger than they are in reality. The coefficient of heat transfer on the exterior surfaces of the walls and ceiling is taken to be 85 $w/m^2K$, corresponding to that of a mixed convection condition. As pointed out previously, the exact value of this coefficient is not critical because the simulation only covers the first four minutes of the fire. The emissivity of all solid surfaces is taken to be a constant of 0.9 and that of the flame surfaces, 1.0. The heat release rates, in accordance with the COMPBRN III simulation (Nicolette and Yang, 1993), are closely given by

$$Q = 1.9625\,\bar{t} \qquad 0 \le \bar{t} \le 2.0$$

$$= 1.2615\,\bar{t} + 1.402 \qquad 2.0 \le \bar{t} \le 4.0 \tag{10}$$

where $Q$ is in MW and $\bar{t}$ is in minutes from ignition. The average power of the fire in the four minutes is 3.6 MW. Also, the simulation started with forced ventilation only and the fire commenced only after the flow field was already established.

The entire simulation was run on an IBM RISC 6000 computer. The time steps ranged from 0.05 to 0.001 second as called for by numerical stability requirements and the total CPU time for the four-minute simulation was about 50 real hours.

Much data can be extracted from the results of the simulation. However, limited space only allows showing a limited data set. In the following, the general temperature field behaviors at six different sections through the rooms are first shown and discussed physically. Temperature data at certain specific locations are then compared with the test data and also discussed in terms of the adequacy of the field model.

Figure 3 shows the isotherms and the isometrics of the temperature fields at section I=9 for the two time instants $\bar{t}$ = 2 min and $\bar{t}$ = 4 min. This section goes from the front to the back at close to the center of the fuel pan. The fire plume region can be seen in the isometrics plot. Other than this plume region, the temperature field is already stratified to a large extent even at $\bar{t}$ = 2 min. This feature persists at $\bar{t}$ = 4 min, even though the hot gas already is penetrating into the floor region. The packed isotherms, signifying steep temperature gradients, generally indicate locations of walls and ceiling where heat losses occur. The isotherms are spread out close to the floor even at $\bar{t}$ = 4 min because of the relatively low temperature there. The void on the right of the figures is outside the computational domain due to the curved wall at the rear of the fire room (see Figure 1). Figure 4 refers to another front-back section, now at I = 25, which is located in the entry room. The top and right side of the isotherms are again locations outside the computational domain. Figure 4 displays just a hot gas coming in at the ceiling and cool air leaving near the floor, and the temperature field is very much stratified. This is true at both time instants, except that more heat loss exists at the ceiling at $\bar{t}$ = 4 min due to much higher temperatures in the ceiling layer.

The same type of information is shown in Figure 5 for the left-right vertical section at J = 9 just beyond the center of the fuel pan. For both time instants, the fire plume regions can be clearly discerned. The much thicker ceiling hot gas layer can also be seen at $\bar{t}$ = 4 min, with temperatures exceeding 600°C there. Another left-right vertical section at J = 14 (Figure 6) is located just beyond the back wall of the entry room and also close to the forced-ventilation

outlet. In the right lower corner region, the hot gas has reached almost to the floor, even at $\tilde{t}$ = 2 min, where there is essentially little flow. The effect of the ventilation outlet can also be seen on the right upper wall at both time instants.

The section K=9 is a horizontal section located about midheight of the fire room. The slanted zig-zagged isotherms shown in Figure 7 are those on the curved rear wall, which is approximated in the simulations by a straight line, and the zig-zags are plotting artifacts. The fire plume, the returning hot wall jet, and the ventilation outlet effects can all be seen in both plots. It is also seen that, except for the two peak temperature regions, the temperatures are essentially uniform throughout, another indication of strong stratification. Figure 8 is at K = 18 for a similar horizontal section very close to the ceiling, and therefore is definitely in the ceiling layer. The temperatures are even more uniform except for the wall loss effects, giving credence to the ceiling layer having a uniform temperature This behavior is essentially the same for both time instants, except for the different temperature levels.

It may be of interest to note that according to the numerical simulations, heat loss throughout the boundary surface amounts to only about 7% of the total heat release rate. Before the simulation results are compared to the test data in terms of temperatures at specific locations, it is pertinent to mention two minor uncertainties. One is the uncertainty regarding the exact instant $\tilde{t}$ = 0. In the test, ignition is accomplished by burning alcohol by electric ignition first, which is then in contact with the fuel to initiate its combustion. Even though this ignition period is relatively short, it does take a finite time, especially in terms of sensor responses. This point should be kept in mind in interpreting the comparisons. In addition, simulated temperatures at the computational cell centers may not be at the exact locations of the thermocouples. However, the differences in the locations are never over 1/2 the cell size, which is 273 mm. Slight variations can be expected in regions of large temperature gradients.

Comparison of the temperature data at thermocouple CT 5246 is shown in Figure 9. This thermocouple is located above the doorway in the right upper corner of the entry room when viewed from outside this room. The simulation underpredicts the temperatures there, even though the time-dependent trend is still reasonable. A likely reason for this discrepancy is that while the two doors are closed, there is always infiltration at the doorways due to the slight pressurization caused by the forced ventilation system. This would tend to bring more hot gas into the entry room at the ceiling. Incidentally, the unevenness of the simulated temperature curve is due to the fact that only simulated temperatures at 0.5 min intervals are used in the plotting and straight lines are used to connect adjacent data points.

Figures 10 and 11 show the comparisons of temperature data at thermocouples CT 5203 and CT 5204, respectively, which are located right above the fuel pan in the fire plume. Thermocouple CT 5203 is at close to midheight, while CT 5204 is in the hot ceiling layer close

to the ceiling. For CT 5203, the simulation grossly underpredicts the test data. The obvious reason is that in the simulation a uniform volumetric heat release rate is assumed, while in reality this thermocouple is likely to fall right in the maximum heat release rate zone above the region of fuel gasification. The very fact that the simulation predicts the temperatures at CT 5204 well is an indication that the ceiling layer temperature is much less sensitive to the heat release rate nonuniformity, but only depends on the total heat that is released. The dip in the temperature at CT 5204 prior to $\bar{t} = 4$ min is likely due to enhanced heat loss through the ceiling.

Thermocouples CT 5290, CT 5293 and CT 5294 are located on a vertical line in the corner of the fire room next to the entry room opening. The thermocouple CT 5290 is close to the floor, CT 5294 is located next to the ceiling, and CT 5293 is only a short distance below CT 5294. For CT 5290, as shown in Figure 12, temperatures are very low for obvious reasons, and the test data show very slight temperature rises in the 3-4 min period. A likely reason for this is the infiltration of cool air through the doors close to the floor. The higher temperature rise in the simulated results is due to the hot gas descending into the floor region. The comparisons at thermocouples CT 5293 and CT 5294 are shown in Figures 13 and 14, respectively. Good agreements can be seen, especially at CT 5294. This is really somewhat surprising in view of all the uncertainties in the submodels of the field model.

## CONCLUDING REMARKS

This paper describes a fire field model which is utilized to simulate a full-scale forced-ventilation fire test in a fire room with an adjoining entry room located in a decommissioned nuclear reactor containment building in Germany. The simulation results show that during the first four minutes of the fire the hot gas has already penetrated into the floor region. Other than the fire plume region and regions that are immediately affected by the ventilation inlet and outlet, the temperature fields are essentially stably stratified into layered structures. The numerical simulations, which are completely independent from the test data, predict temperature behaviors reasonably well over the four-min simulation period. Serious discrepancies only occur in the region directly above the fuel pan because of the unrealistic assumption on the spatial distribution of the heat release rates used in the simulations.

While this numerical simulation study can be considered as reasonably successful and the results do capture much of the physics contained in the full-scale fire test, further refinements of the field model are clearly needed. The lack of a turbulent combustion model and the neglect of gas and soot radiation represent serious shortcomings that must be overcome before the field model can be considered as complete. The prospect of developing a generic turbulent combustion model is still not very encouraging primarily because of the lack of data on combustion kinetics for common liquid and solid fuels. In the meanwhile, the approach adopted

in the present study, namely, the joining of a field model and a zone model, may represent a viable alternative. Such a combined tool, which is now available, may have sufficient accuracy to play a valuable role in many fire mitigation efforts, as demonstrated in the present study.

## ACKNOWLEDGMENT

The support of NRC Grant FIN L1330 is gratefully acknowledged. The authors are also grateful for the support and help of the University of Notre Dame Computer Center.

## NOMENCLATURE

| | |
|---|---|
| $c_p$ | Dimensionless specific heat |
| G | Dimensionless generalized gravitation vector |
| g | Dimensionless gravity |
| $\tilde{g}$ | Gravitational vector |
| H | Height of fire room, m |
| h | Coefficient of heat transfer, $W/m^2K$ |
| I,J,K | Coordinate indices |
| K | Constant in turbulence model, K = 0.4 |
| k | Turbulent kinetic energy, $m^2/s^2$ |
| k | Dimensionless effective thermal conductivity |
| $\ell$ | Mixing length in turbulence model, m |
| $\tilde{n}$ | Unit vector in direction opposite of gravity |
| Pr | Molecular Prandtl number |
| $Pr_t$ | Turbulent Prandtl number |
| pi | Dimensionless pressure difference |
| Q | Heat release rate, MW |
| $Q_C$ | Dimensionless Volumetric heat source |
| Ri | Gradient Richardson number |
| T | Dimensionless temperature |
| $u_i$ | Dimensionless velocity components |
| $x_i$ | Dimensionless coordinates |
| $\Delta$ | Spatial step size, mm |
| $\varepsilon$ | Dissipation rate of turbulent kinetic energy, $m^2/s^3$ |
| $\mu$ | Dimensionless effective viscosity |
| $\rho$ | Dimensionless density |
| $\sigma_{ij}$ | Dimensionless shear stress tensor |

## SUPERSCRIPT

| | |
|---|---|
| * | Dimensional quantities |

## SUBSCRIPTS

| | |
|---|---|
| e | Equilibrium conditions |
| ,i | Derivatives with respect to $x_i$ |
| m | Mean conditions |
| R | Reference conditions |

## REFERENCES


Candel, S., Veynante, D., Lacas, F., Maistret, E., Darabiha, N., and Poinsot, T., 1990, Flamelet Description of Turbulent Combustion, Proceedings of the 9th International Heat Transfer Conference, Vol. 1, Hemisphere Publishing Co., New York, pp. 113-128.

Chow, W.K. and Fong, N.K., 1993, Application of Field Modeling Technique to Simulate Interaction of Sprinkler and Fire-Induced Smoke Layer, Combustion Science and Technology, Vol. 89, pp. 101-151.

Delaney, M.A., 1992, Numerical Field Model Simulation of Full Scale Fire Tests in a Closed and an Open Compartment, M.S. Thesis, Naval Postgraduate School, Monterey, CA.

Ho, V., Siu, N. and Apostolakis, G., 1985, COMPBRN III-A Computer Code for Modeling Compartment Fires, Report UCLA-ENG-8524, College of Engineering, University of California at Los Angeles.

Holen, J., Brostrom, M. and Magnussen, B.F., 1990, Finite Difference Calculation of Pool Fires, Twenty Third Symposium (International) on Combustion, The Combustion Institute, pp. 1677-1683.

Houck, R.R., 1988, Numerical Field Model Simulation of Full-Scale Fire Tests in a Closed Spherical/Cylindrical Vessel with Internal Ventilation, M.S. Thesis, Naval Postgraduate School, Monterey, CA.

Howell, J.R., 1982, A Catalog of Radiation Configuration Factors, McGraw-Hill Book Co., New York.

Jones, I.P., 1990, Fire Modelling, Eurothrm Seminar No. 13, Abstract of Papers, Harwell Laboratory, England.

Kou, H.S., Yang, K.T., and Lloyd, J.R., 1986, Turbulent Buoyant Flow and Pressure Variations around an Aircraft Fuselage in a Cross Wind Near the Ground, Fire Safety Science in Proc. First International Symposium, pp. 173-184.

Leonard, B.P., 1983, A Convectively Stable, Third-Order Accurate Finite Difference Method for Steady Two-Dimensional Flow and Heat Transfer, Numerical Properties and Methodologies in Heat Transfer, ed. T.M. Shih, Hemisphere Publishing Corp., Washington, D.C. pp. 211-226.

Londino, J., 1993, Turbulent Buoyant Flow in an Open Compartment with Participating Medium and Combustion, Ph.D. dissertation research in progress, Department of Aerospace and Mechanical Engineering, University of Notre Dame.

McCarthy, T.G., 1991, Numerical Field Model Simulation of Full Scale Fire Tests in a Closed Spherical/Cylindrical Vessel Using Advanced Computer Graphics Technique, M.S. Thesis, Naval Postgraduate School, Monterey, CA.

Mueller, K., and Max, U., 1991, Input Data Set for E41.7 Blind Postcalculations of an Oil Fire in a Closed System, Kernforschungszentrum Karlsruhe GmbH.

Mueller, K. and Volk, R., 1990, Characteristics of an Oil Fire in a Closed Subsystem with the Ventilation System Connected and Variable Degrees of Door Opening, Design Basis Report, Kernforschungszentrum Karlsruhe GmbH.

Nicolette, V.F., Yang, K.T., and Lloyd, J.R., 1985, Transient Cooling by Natural Convection in a Two-Dimensional Square Enclosure, International Journal of Heat and Mass Transfer, Vol. 28, No. 9, pp. 1721-1732.

Nicolette, V.F. and Yang, K.T., 1993, Modeling of HDR Oil and Cable Fire Tests, paper presented at the Conference on Structural Mechanics in Reactor Technology (SMIRT 93), Fire Safety Seminar, Heidelberg, Germany, August 24-28, 1993.

Nies, G.F., 1986, Numerical Field Model Simulation of Full Scale Tests in a Closed Vessel, M.S. and M.E. Thesis, Naval Postgraduate School, Monterey, CA.

Raycraft, J., Kelleher, M.D., Yang, H.Q., and Yang, K.T., 1990, Fire Spread in a Three-Dimensional Pressure Vessel with Radiation Exchange and Wall Heat Losses, Mathematical and Computer Modelling, Vol. 14, pp. 795-800.

Satoh, K., Lloyd, J.R., Yang, K.T., and Kanury, A.M., 1983, A Numerical Finite-Difference Study of the Oscillating Behavior of Vertically Vented Compartments, in Numerical Properties and Methodologies in Heat Transfer, Ed. T.M. Shih, Hemisphere Publishing Corp., Washington, D.C., pp. 517-528.

Siegel, R. and Howell, J.R., 1992, Thermal Radiation Heat Transfer, 3rd Ed., Hemisphere Publishing Co., Washington, D.C.

Simcox, S., Wilkes, N.S., and Jones, I.P., Computer Simulation of the Flows of Hot Gases from the Fire at King's Cross Underground Station, AERE-G4782, 1988.

Yang, K.T., 1986, Numerical Modeling of Natural Convection-Radiation Interactions in Enclosures, Keynote Address, in Proceedings of the 8th International Heat Transfer Conference, Vol. 1, Hemisphere Publishing Co., Washington, D.C., pp. 131-140.

Yang, K.T. and Lloyd, J.R., 1985, Turbulent Buoyant Flow in a Vented Simple and Complex Enclosure, in Natural Convection-Fundamentals and Applications, Eds. S. Kakac, W. Aung and R. Viskanta, Hemisphere Publishing Co., Washington, D.C., pp. 303-329.

Yang, K.T., Lloyd, J.R., Kanury. A.M., and Satoh, K., 1984, Modeling of Turbulent Buoyant Flows in Aircraft Cabins, Combustion Science and Technology, Vol. 39, pp. 107-118.

Yang, K.T., Xia, Q., and Nicolette, V.F., 1992, Simulation of Strong Turbulent Buoyant Flow in a Vented Complex Enclosure, Computational Mechanics '92, Eds. S.N. Alluri, G. Yagawa, P. Tong, and R. Jones, Technology Publications, Atlanta, Ga.,, p. 235. Also to appear in Computational Mechanics, an International Journal, 1994.

LIST OF FIGURES FOR APPENDIX B


Figure 1 HDR Fire Room Geometry

Figure 2 Computational Domain

Figure 3 Calculated Temperature Fields at I=9 and $\bar{t}$=2 and 4 minutes

Figure 4 Calculated Temperature Fields at I=25 and $\bar{t}$ = 2 and 4 minutes

Figure 5 Calculated Temperature Fields at J=9 and $\bar{t}$=2 and 4 minutes

Figure 6 Calculated Temperature Fields at J=14 and $\bar{t}$=2 and 4 minutes

Figure 7 Calculated Temperature Fields at K=9 and $\bar{t}$=2 and 4 minutes

Figure 8 Calculated Temperature Fields at K=18 and $\bar{t}$=2 and 4 minutes

Figure 9 Comparison of Temperature Data at Location of Thermocouple CT 5246

Figure 10 Comparison of Temperature Data at Location of Thermocouple CT 5203

Figure 11 Comparison of Temperature Data at Location of Thermocouple CT 5204

Figure 12 Comparison of Temperature Data at Location of Thermocouple CT 5290

Figure 13 Comparison of Temperature Data at Location of Thermocouple CT 5293

Figure 14 Comparison of Temperature Data at Location of Thermocouple CT 5294

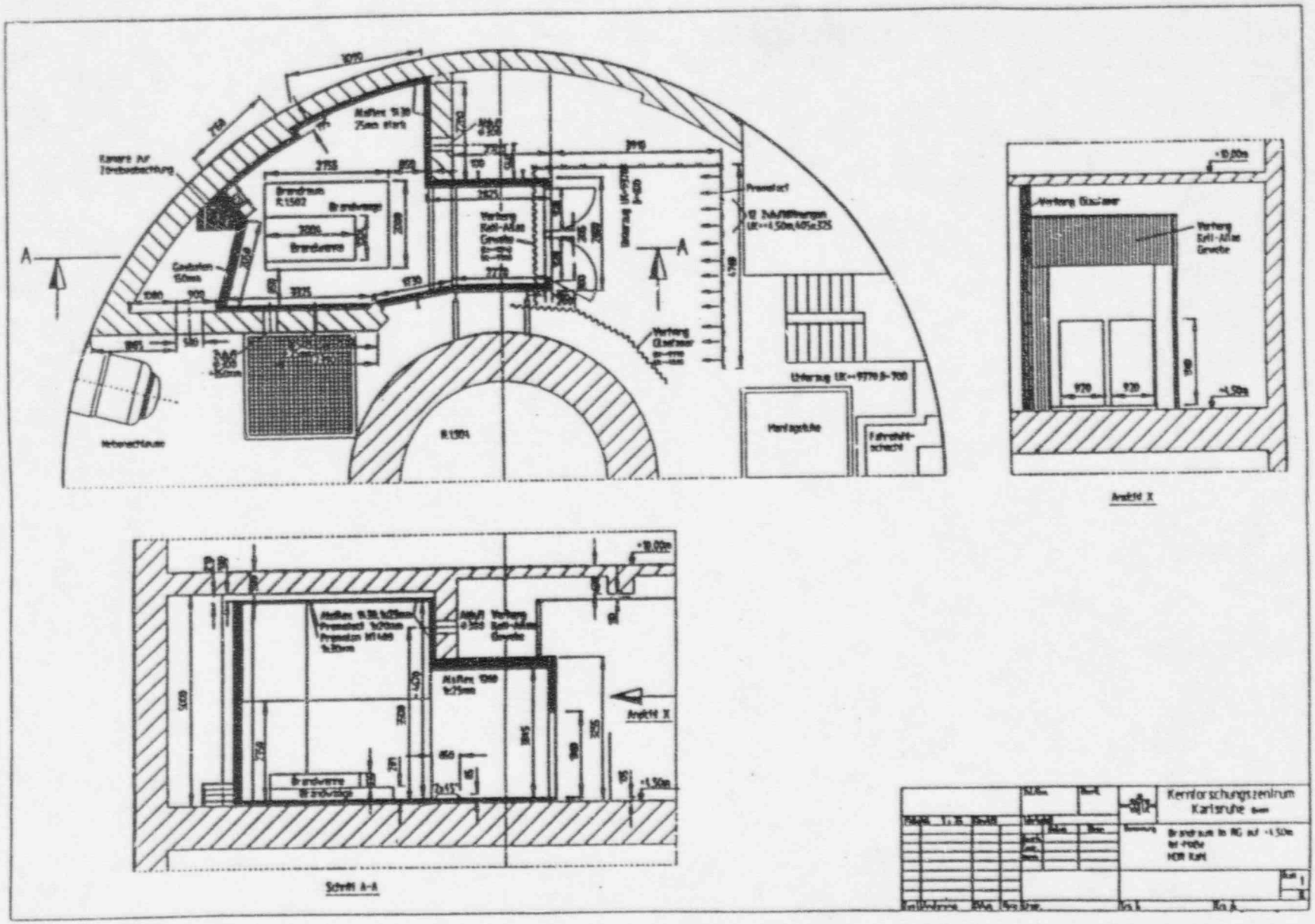


Figure B-1 HDR Fire Room Geometry

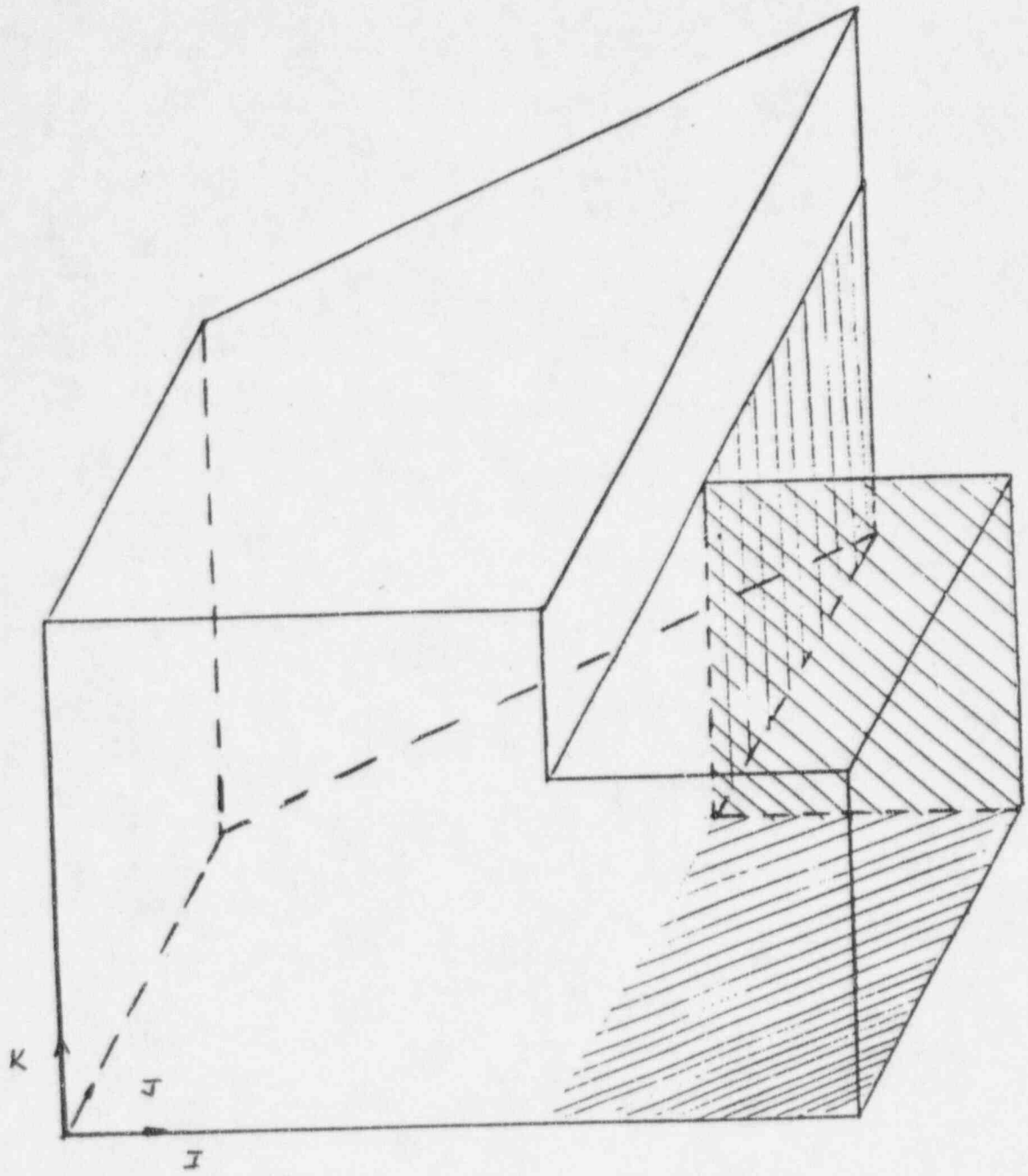


Figure B-2 Computational Domain

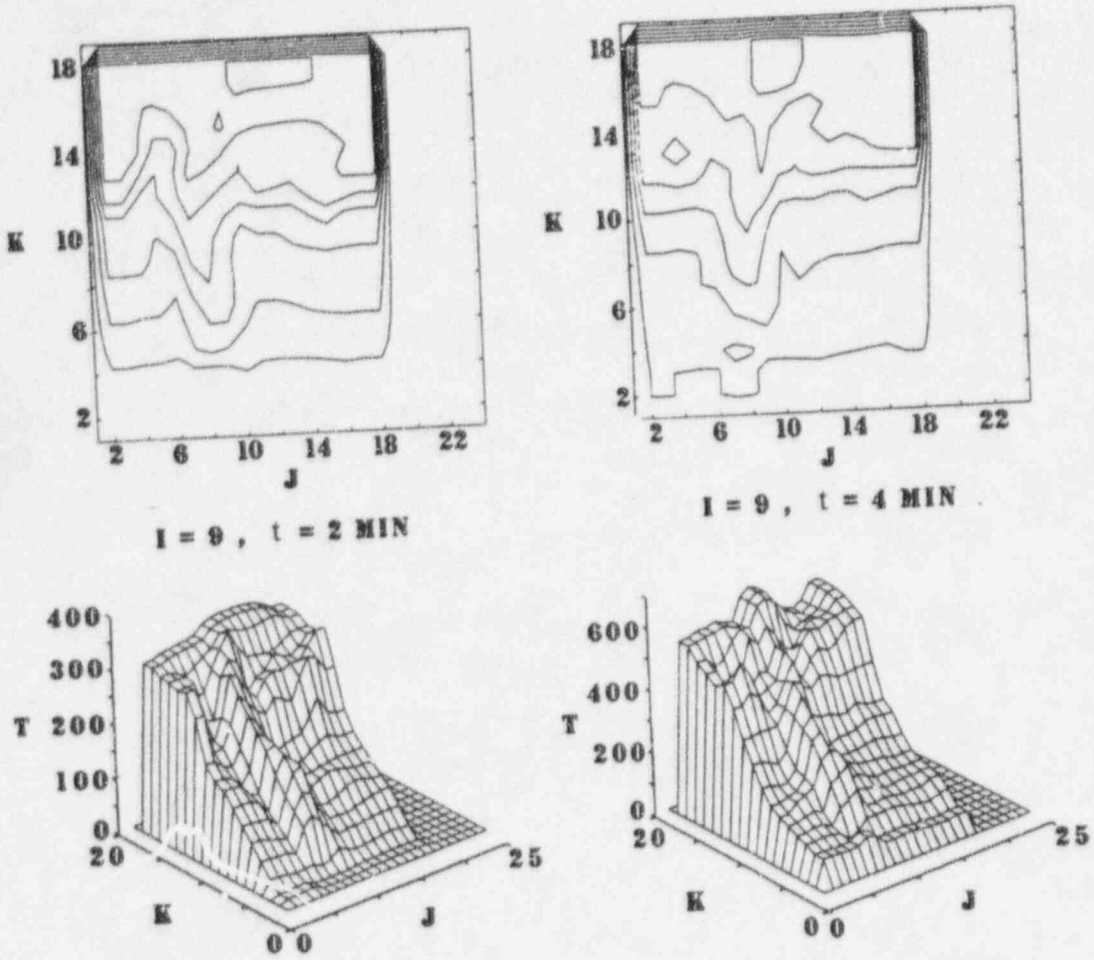


Figure B-3

Calculated Temperature Fields at I=9 and t=2 and 4 minutes

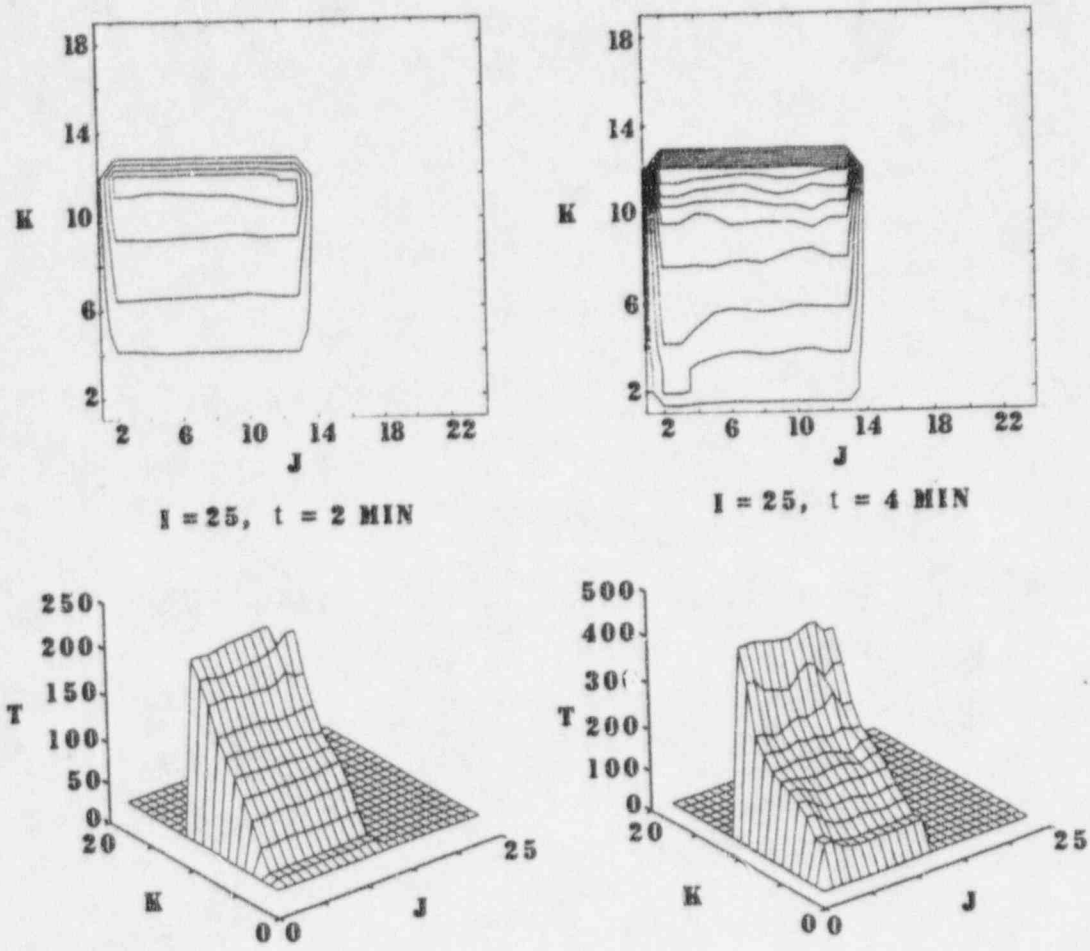


Figure B-4

Calculated Temperature Fields at I=25 and $\bar{t}$ = 2 and 4 minutes

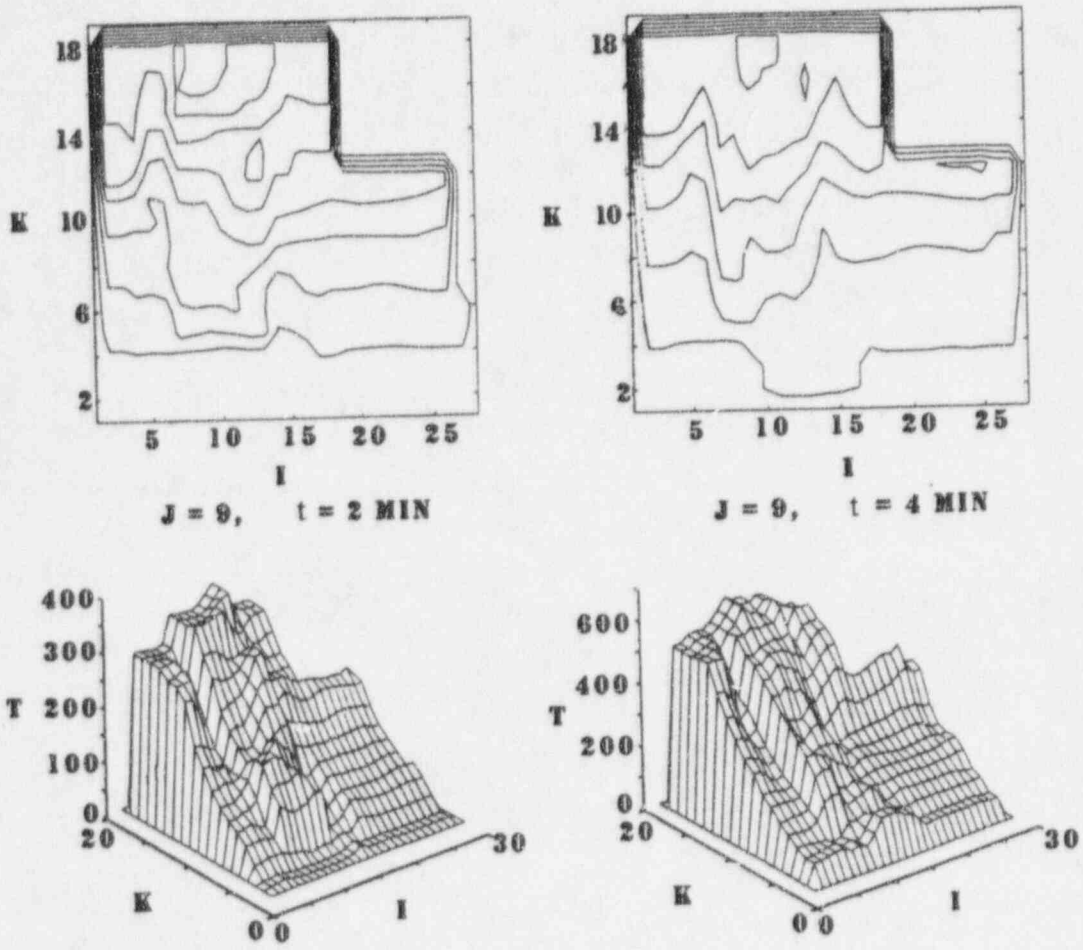


Figure B-5

Calculated Temperature Fields at J=9 and t=2 and 4 minutes

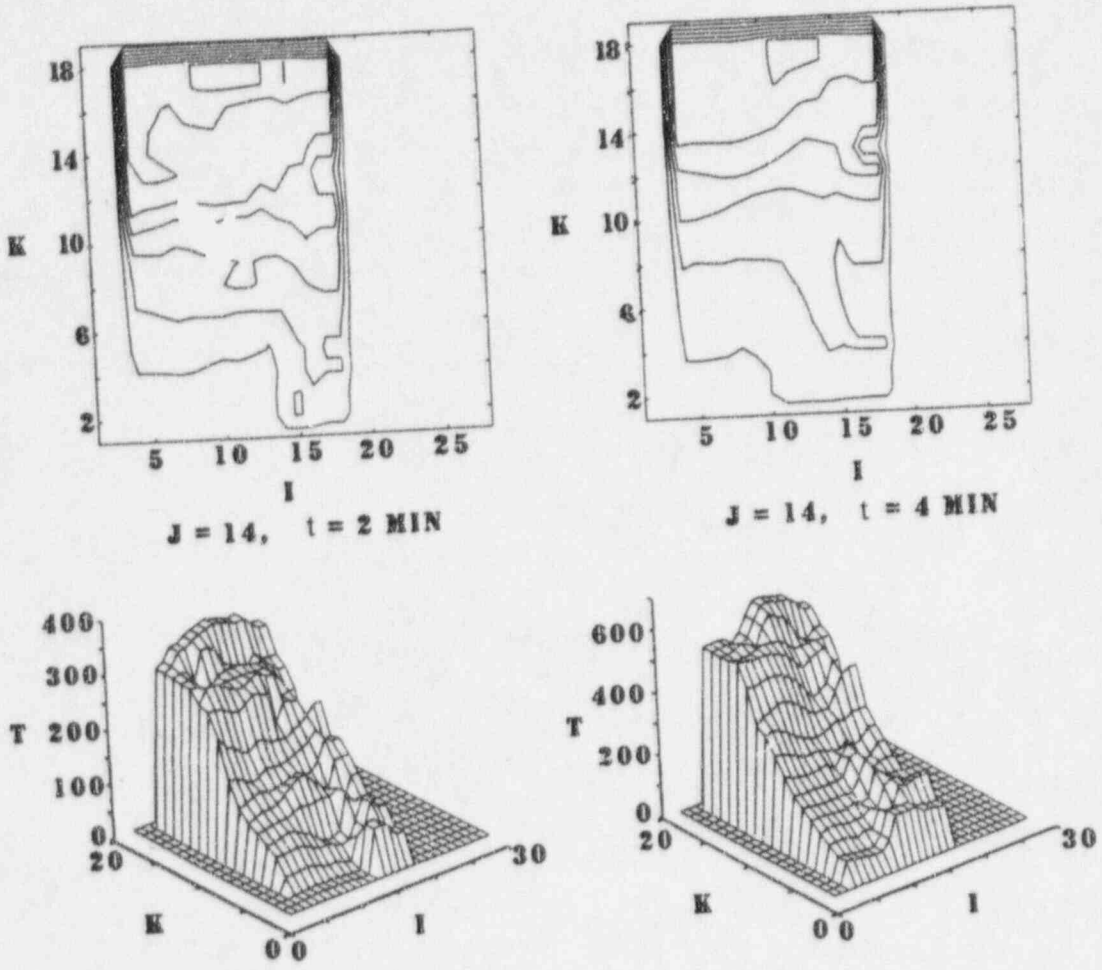


Figure B-6

Calculated Temperature Fields at J=14 and t=2 and 4 minutes

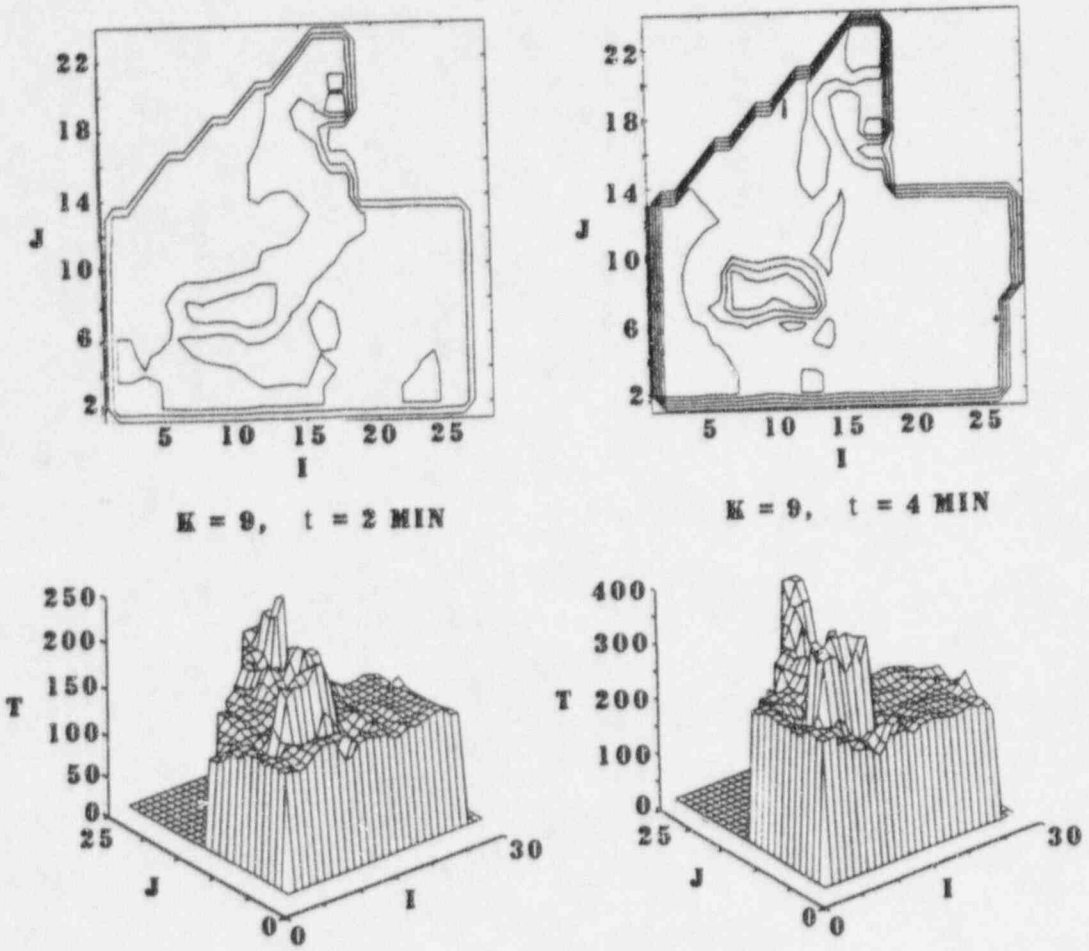


Figure B-7

Calculated Temperature Fields at K=9 and t=2 and 4 minutes

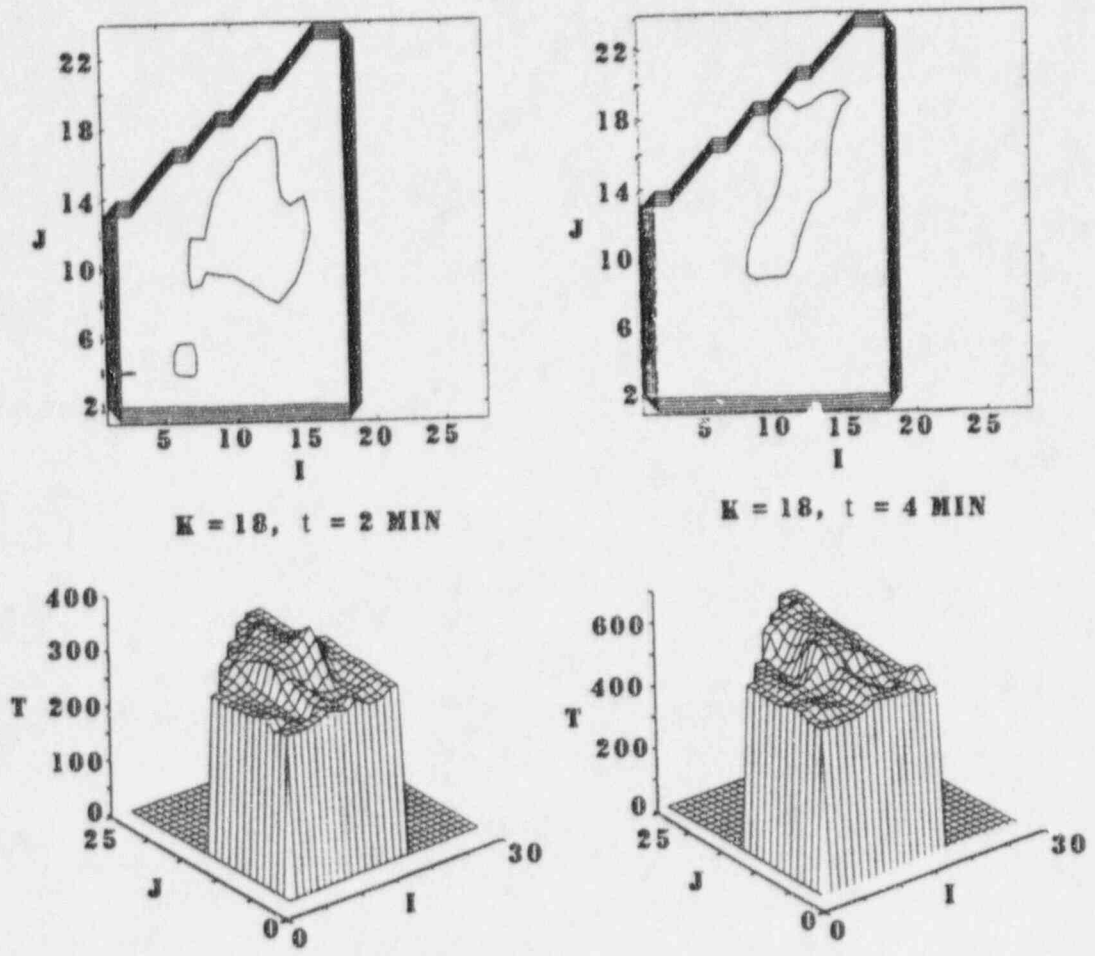


Figure B-8

Calculated Temperature Fields at K=18 and t=2 and 4 minutes

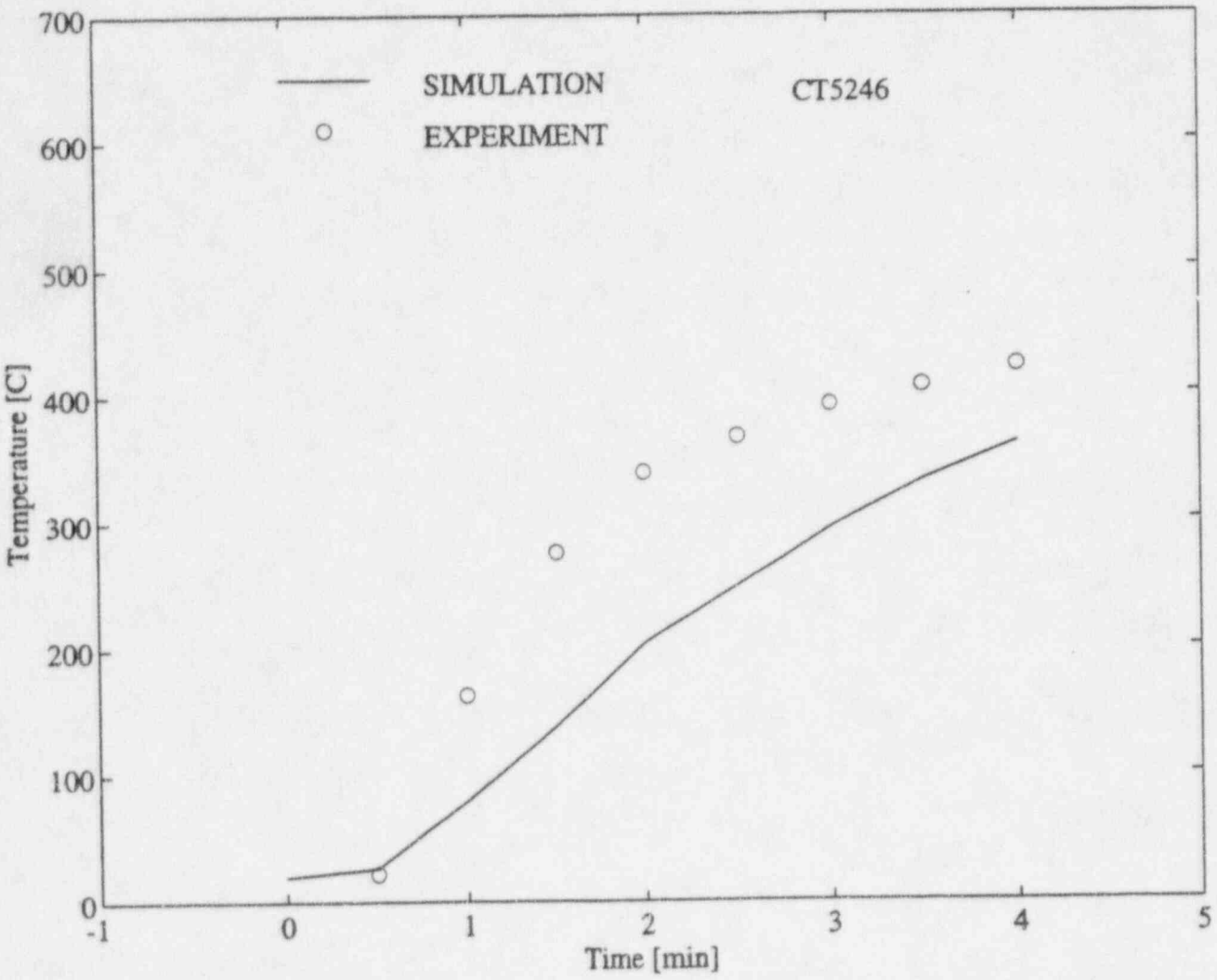


Figure B-9

Comparison of Temperature Data at Location of Thermocouple CT 5246

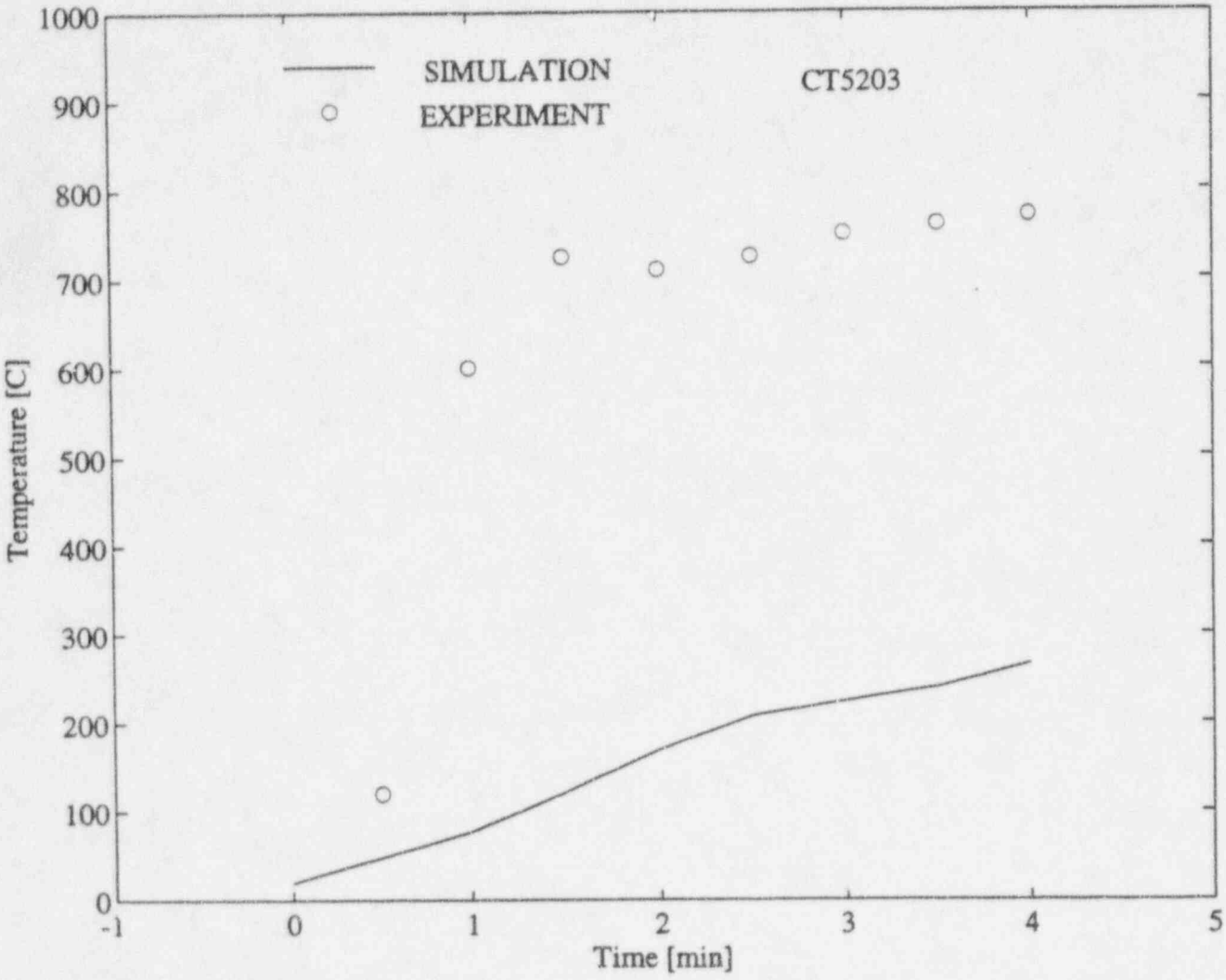


Figure B-10

Comparison of Temperature Data at Location of Thermocouple CT 5203

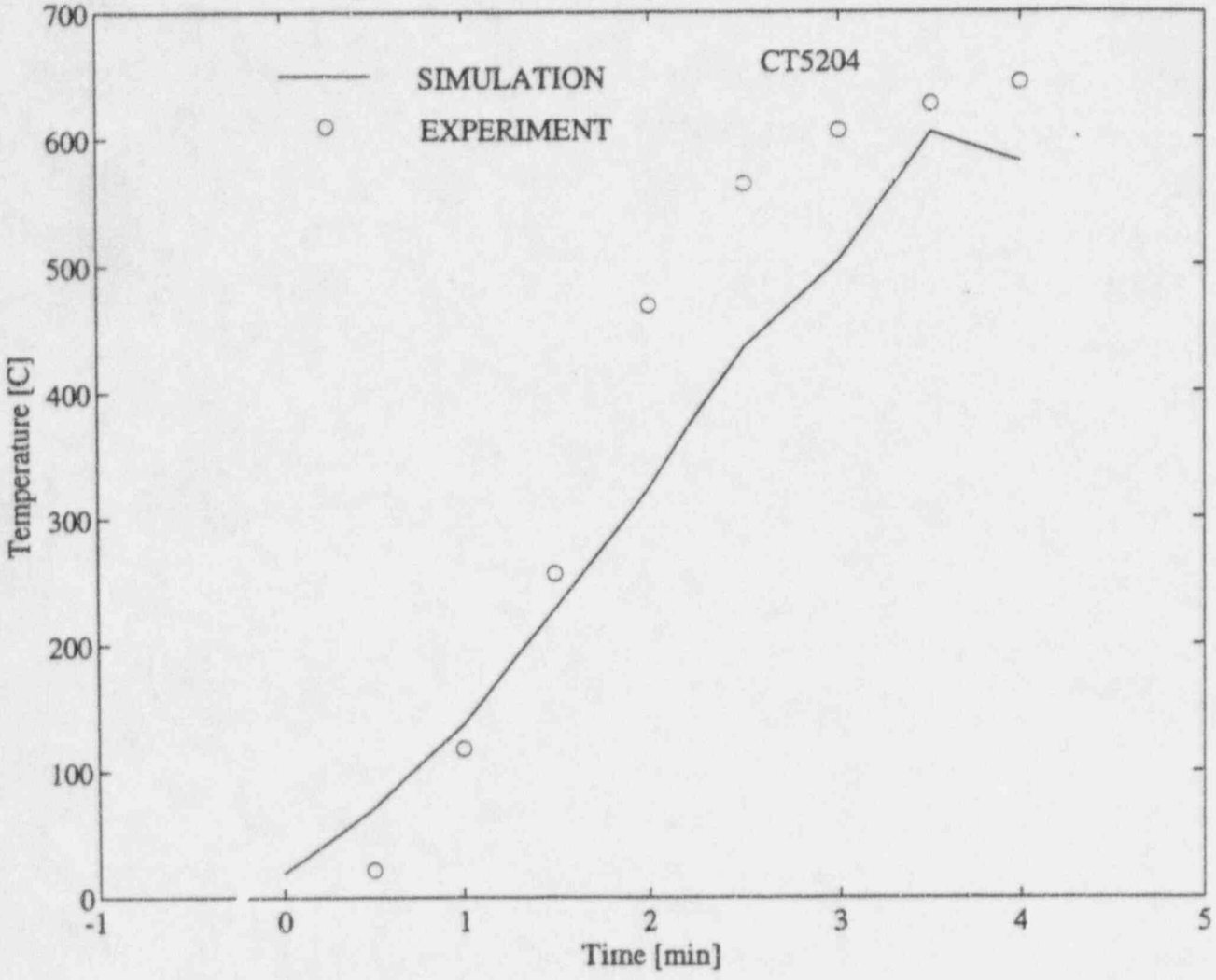


Figure B-11

Comparison of Temperature Data at Location of Thermocouple CT 5204

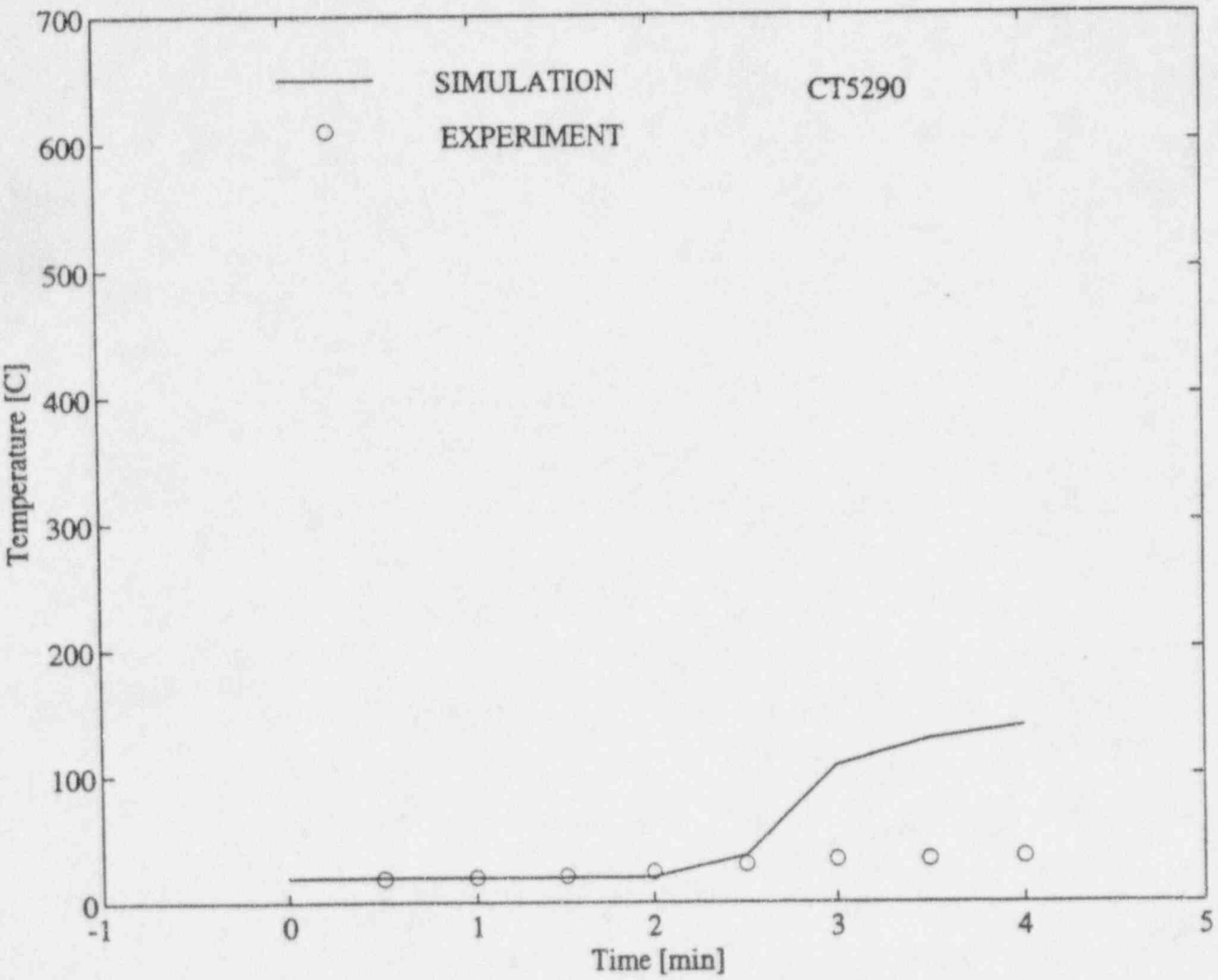


Figure B-12

Comparison of Temperature Data at Location of Thermocouple CT 5290

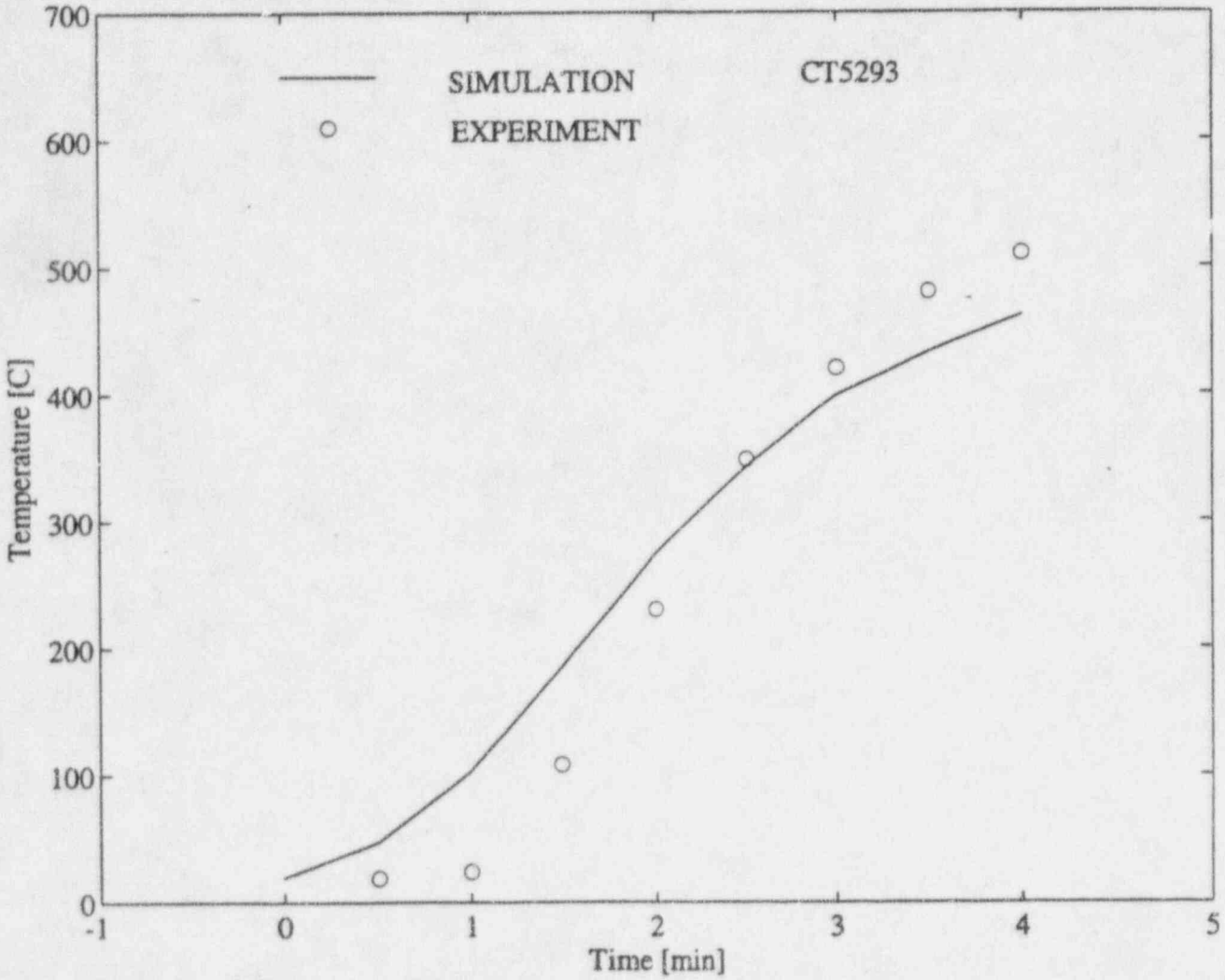


Figure B-13

Comparison of Temperature Data at Location of Thermocouple CT 5293

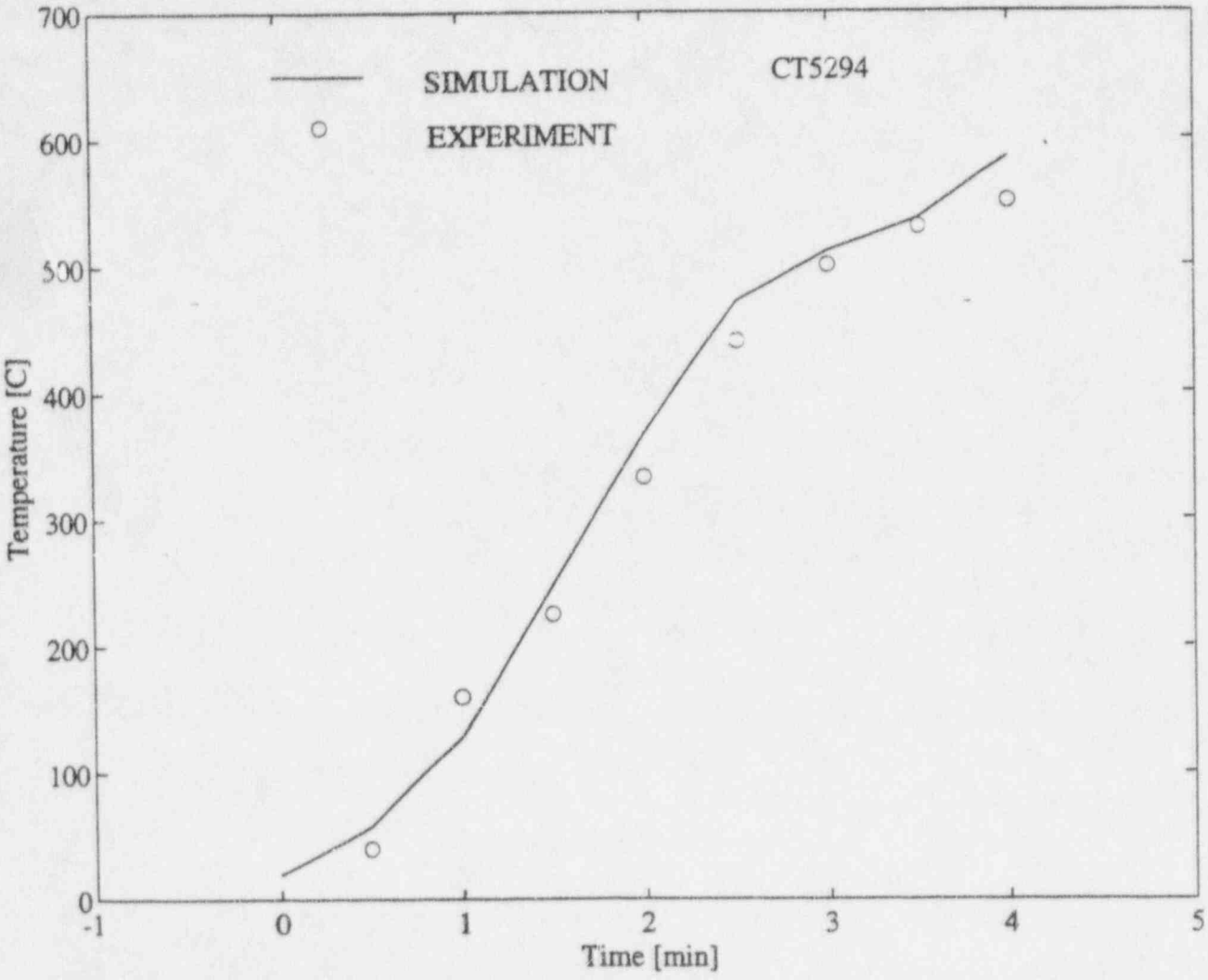


Figure B-14

Comparison of Temperature Data at Location of Thermocouple CT 5294

# Appendix C: University of Notre Dame Field Model Calculations for HDR Test E41.5

The following report on the Notre Dame Field Model Calculations for HDR Test E41.5 is included as a stand-alone report. It has been published in Heat Transfer in Fire and Combustion Systems, ASME HTD vol. 272, eds. W.W. Yuen and K.S. Ball, pp. 13-20, 1994.

# SIMULATION OF STRONG TURBULENT BUOYANT FLOW IN A VENTED COMPLEX ENCLOSURE

K. T. Yang* and Q. Xia
Department of Aerospace and Mechanical Engineering
University of Notre Dame
Notre Dame, IN 46556, USA

and

V. F. Nicolette
Thermal and Fluid Engineering
Sandia National Laboratories
Albuquerque, NM 87185, USA

## ABSTRACT

A three-dimensional field model for turbulent flow in an arbitrary compartment, taking into account strong buoyancy, full compressibility, turbulence, surface-surface radiation exchange, and wall heat losses is utilized to simulate a full-scale fire test in a fire room with open doorways located in a decommissioned nuclear reactor containment vessel in Germany. Results show that reasonable agreement in the numerical and test data in the unsteady temperature field at three locations inside the fire room was obtained, even though the numerical simulation underestimated the doorway instantaneous exit velocities by as much as 40%. The discrepancies are discussed in terms of both test uncertainties and adequacy of the physical submodels utilized in the field model.

*Corresponding Author

## 1. INTRODUCTION

It is now generally recognized that despite the great complexity of the real fire phenomenon it is still critical that their quantitative descriptions should be developed for the purpose to help to mitigate the losses of lives and properties. Such descriptions basically can be obtained by means of fire models which are the mathematical models for the physical and chemical processes involved in the spread of fire in a space as functions of the ignition source, space geometry, and materials content. Once validated by test data, such fire models, for instance, can be utilized to significantly reduce the need for full scale fire tests which are extremely expensive and requires a great deal of effort to study the consequences of various fire scenarios for fire hazard mitigation, and also in post-fire investigations.

Fire models can be classified in terms of zone models and field models with relative advantages and disadvantages which are now well recognized. Despite such advantages for the field models as the capability to provide seamless details of the velocity, temperature, and species concentration fields and interaction effects among various regions in the fire spread space such as stratification and thermal radiation, these field models and their development have not received the proper attention they rightly deserve in the past, The primary reasons are that they are very computing intensive and access to high-power computing resources was rather limited, and also that there were uncertainties in modeling such phenomena as turbulent combustion and thermal radiation. However, with increasing accessibility to supercomputers, mini-supercomputers, and high power workstations and personal computers, field models are increasingly being used to deal with the simulation of real fire scenarios. For instance, the use of the Harwell-Flow 3D code, a field model, to simulate the air flow in the King's Cross underground station fire in London in 1987 (Simcox, Wilkes, and Jones, 1988) is a good example, and several others have also been discussed at the 1990 Eurotherm Seminar on Fire Modeling (Jones, 1990). Despite such increased attention to the application of field models, there is still a great deal of uncertainty as to the generality of such models and the achievable accuracy of applying such models to real fire situations. This uncertainty is the result of the difficulty in modeling turbulent combustion of real fuels in fires and thermal radiation effects of participating media, as well as of the general lack of pertinent test data base, especially for full-scale fire tests. Such test data are indeed critically needed to provide a means for validating the field models and also to provide fundamental information on the deficiency of the models so that they can be properly improved in time.

In the past several years, an international cooperative effort has been established to assess the viabililty of the latest fire models, both zone and field models, on the basis of full-scale fire tests carried out in a decommissioned nuclear reactor containment building at the Heiss Dampf

Reaktor (HDR) facility in Germany. The objectives of this assessment is to determine the current state of development of fire models with the view toward their eventual use in the mitigation of fire hazards in nuclear reactors. It is noted that these are the only tests ever conducted inside an actual nuclear reactor containment building. The University of Notre Dame UNDSAFE three-dimensional fire model (Nies, 1986; Raycraft, Kelleher, Yang, and Yang, 1990) was one of the field models chosen for the assessment. Two series of full-scale fire tests were conducted in the same designated fire room inside the HDR building for the purpose of model validation. One series, designated as the E41.5 Test, deals with a naturally-ventilated fire (Mueller and Volk, 1990), while the second series known as the E41.7 Test deals with a forced-ventilation fire (Mueller and Max, 1991). The purpose of this paper is to show some of the numerical simulation results for the E41.5 Test as compared to the test data, while results of similar comparisons for the E41.7 Test are given in a separate paper (Yang, Huang, and Nicolette, 1994). It should be noted that these comparisons provide an excellent opportunity to assess the accuracies of the current available fire models as well as to point out critical shortcomings of such fire models.

## 2. DESCRIPTION OF NATURALLY-VENTILATED FULL-SCALE FIRE TEST

Details of the geometries of the HDR containment building and the fire room, and descriptions of the materials of the fire-room walls, ceiling, and floor and the fuel oil characteristics can be found in the report of Mueller and Volk, (1990). Briefly, the containment building is in the shape of a vertical pressure vessel, about 60m in height and 20m in diameter, and the bottom of the building is about 11m below grade. A schematic of this building is shown in Figure 1. The fire room floor is located at the 4.5m level above ground, and the fire room is shown in Figure 2. The main fire room has a height of 5m and that of the doorway area is about 3m. The fuel pan is located on the floor in the main fire room, as can also be seen in Figure 2. The combined room has a total volume of about $100m^3$, and the total floor or ceiling area is about $23m^2$. All side walls are made up of largely 10cm and 15cm thick Ytong, while the floor consists of 25cm thick Ytong. The ceiling is covered with insulations made up of 3cm Promalane and 2.5cm of Alsiflex. Most of the walls and floor are also covered with 2cm of Alsiflex mats. All thermophysical properties such as density, specific heat and thermal conductivity of these materials are known and tabulated in the reports by Mueller and Volk (1990) and Mueller and Max (1991). The fuel oil is SOL-T made by the Shell Company and produces only non-greasy dry soot. It has a density of $0.756\ kg/m^3$ at 20°C, and a heating value of 42,500 kJ/kg. The side fire room is equipped with two fire protection doors with variable openings and controlled remotely.

In the E41.5 Test with natural ventilation (buoyancy induced flow only with the doors open), the major portion of the test lasts 18 minutes, during which the burn rate of the fuel oil was measured, along with extensive measurements of gas and flame temperatures, temperatures at selected locations, gas concentrations, pressures, and doorway velocities. Some of these measured data will later be used to compare with simulation results from the field model, which will also be discussed on the basis of the shortcomings in the field model. It is pertinent to mention here that the heat release rate of the fire was not measured, but must be inferred from the fuel-loss data. This unavoidable deficiency in the measurements, as will be discussed later, does impact on the simulation results.

## 3. THE FIELD MODEL

The field model utilized in the present study, under the code name of UNDSAFE (University of Notre Dame Smoke and Fire in Enclosures), has been under continuous development in recent years. Early efforts were concentrated on two-dimensional room fire problems and could account for strong buoyancy, full compressibility, simple rectangular room geometry, one-dimensional ceiling-floor radiation exchange, but not including effects of turbulent combustion and wall losses. The model was applied to a variety of room and external fire scenarios with some reasonable validation by experimental data (Satoh, Lloyd, Yang, and Kanury, 1983; Yang, Lloyd, Kanury, and Satoh, 1984; Yang and Lloyd, 1985; Kou, Yang and Lloyd, 1986). More recently, this field model has been extended to three-dimensional enclosures including wall losses, pressurization and surface-surface radiation exchange (Nies, 1986), complex geometries (Raycraft, Kelleher, Yang and Yang, 1990), internal ventilation (Houck, 1988), and effects of sprinklers (Chow and Fong, 1993). Limited experimental validation has also been given by Raycraft, Kelleher, Yang, and Yang (1990) and by Delaney (1992). However, despite the versatility of this field model, as noted above, it is still not complete and in addition lacks sufficient validation to ascertain its general validity, as is the case for all existing field models. The glaring shortcoming in the present model resides with the lack of a viable turbulent combustion model, and a lesser shortcoming in accounting for the effects of species concentration in multidimensional radiative transfer. The former is particularly difficult because of the general lack of combustion kinetics for real complex fuels such as that employed in the HDR fire test. In essence, this difficulty is inherent in all field models.

Since no combustion model is used in the present field model, the heat release rate must necessarily be prescribed. As the combustion process takes place in the region above the fuel pan, the prescribed heat release rate is utilized as volumetric heat sources with a postulated flame region. As will be mentioned later, the flame surface is taken to be black, and surface-surface and surface-flame radiation exchanges are accounted for in the field model. Due to the neglect

of combustion and gas radiation, the species equations need not be considered, and the dimensionless governing field equations for turbulent buoyant compressible flow can be written in dimensionless tensor forms as (Nies, 1986; Raycraft, Kelleher, Yang, and Yang, 1990):

$$\rho_{,t} + (\rho u_i)_{,i} = 0 \tag{1}$$

$$(\rho u_i)_{,t} + (\rho u_i u_j)_{,j} = -p_{,i} - \rho G + (\sigma_{ij})_{,j} \tag{2}$$

$$(\rho c_{pm} T)_{,t} + (\rho u_i c_{pm} T)_{,i} = (kT_{,i})_{,i} \tag{3}$$

where the dimensionless shear stress tensor $\sigma_{ij}$ and mean specific heat $c_{pm}$ are given by

$$\sigma_{ij} = \mu\left(u_{i,j} + u_{j,i} - \frac{2}{3}\delta_{ij}u_{k,k}\right) \tag{4}$$

$$c_{pm} = \frac{1}{T-1}\int_1^T c_p dT \tag{5}$$

where $\delta_{ij}$ is the Kronecker delta function. It is noted here that both viscous dissipation and pressure work can be neglected in the fire phenomena. The above dimensionless quantities are normalized as follows: The coordinates $\tilde{x}_i$ with the height of the fire room H; the time variable $\tilde{t}$ with $H/u_R$ where $u_R$ is a constant reference velocity; all velocity components $\tilde{u}_i$ with $u_R$; absolute temperature $\tilde{T}$ with $T_R$ where $T_R$ is again a reference temperature normally taken to be the air inlet temperature; the pressure difference $(\tilde{p} - \tilde{p}_e)$, where $\tilde{p}_e$ is the hydrostatic equilibrium pressure, with $\rho_R/u_R^2$ where $\rho_R$ is a constant reference air density based on $\tilde{p}$ and $T_R$; the gravitational acceleration $G = (0,0,g)$ with $u_R^2/H$; and the thermophysical properties $\tilde{\rho}$ (density), $\tilde{c}_p$ (specific heat), $\tilde{\mu}$ (viscosity) and $\tilde{k}$ (thermal conductivity with, respectively, $\rho_R$, $c_{pR}$, $\rho_R u_R H$, and $\rho_R c_{pR} u_R H$ where $c_{pR}$ is a constant reference specific heat evaluated at $T_R$. All $\tilde{u}_i$ and $\tilde{T}$ are Reynolds averaged quantities, and $\mu$ and $k$ consist of both laminar and turbulent quantities. Also, for convenience, the origin of the coordinate system is fixed at the left front corner of the fire room. Thus, the i-coordinate is in the direction from the fire room to the entry room; the j-coordinate is in the direction of the

depth, from the front to the rear; and the k-coordinate is from the floor to the ceiling (see Figure 1).

The boundary conditions can be easily written. All velocity components vanish on a solid surface. At the doorway, the boundary conditions are written as follows: (Yang, 1987): where the velocity normal to the doorways, which were open during the E41.5 Test, is outward from the fire room, all velocity components and temperature have zero gradients at the doorway. For doorway locations where the normal velocity is directed inward, the temperature is that of the ambient temperature $T_R$ and all velocity components again have zero normal gradients. These conditions obviously allow for both in- and out-flows at the doorways. Except that for the doorways, the temperature boundary conditions at the walls, ceiling and flow are in accordance with a heat balance and coupled to the conduction through the thicknesses and convection at the outer surfaces. The heat balance involves surface radiation fluxes from all the other surfaces including those of the flame, except those that are shaded, the convection fluxes from the flow, and conduction fluxes into the solid.

The formulation of the field model is not complete without several submodels for compressibility, buoyancy, wall losses, turbulence, radiation and combustion. These are now described. Compressibility is already accounted for in the governing differential equations, and density is determined in accordance with the perfect gas law. It is noted here that due to the open doorway with ample ventilation, the pressure is nearly constant throughout the fire room. Strong buoyancy is accommodated in Equation (2) without invoking the Boussinesq approximation. Heat Transfer through the walls and ceiling is taken to be that of unsteady one-dimensional conduction through the thicknesses, coupled with convection at the exterior surfaces with a prescribed surface coefficient of heat transfer. The floor, in view of its large thickness, is treated as insulated.

In addition to affecting the flow field in general, turbulence plays two other roles in the fire phenomena. One is that turbulence stretches the flames, thus promoting the combustion process, and the other is that it provides a mixing mechanism for the gas species and soots, thus affecting the species and soot concentration distributions which in turn affect the radiation heat exchange from these radiation participating media. While these latter effects can be rather significant, especially in large fires such as the one considered here, they cannot be properly modeled without a turbulent combustion model, as is the case in the present field model. Consequently, the turbulence model utilized here does not need to be complex, but only requires simple descriptions relative to production and dissipation of turbulence. This is in fact another justification for simple turbulence models. While several field models such as, for instance, Harwell-Flow 3D (Simcox, Wilkes, and Jones, 1988) and KAMELEON (Holen, Brostrom, and Magnussen, 1990) have utilized the standard $k$-$\varepsilon$ model of turbulence, the Notre Dame field

model has, on the other hand, always advocated that a much simpler mixing-length type of algebraic model, which accounts for stratification effects, is of sufficient accuracy for the fire phenomena, as validated by experiments (Yang and Lloyd, 1985; Raycraft, Kelleher, Yang and Yang, 1990). Such an algebraic model is retained in the current simulation study, and is given as follows:

$$\frac{\mu}{\mu_R} = 1 + \frac{\left(\frac{l}{H}\right)^2 \sqrt{\sum_j \left(\frac{\partial u_i}{\partial x_j}\right)\left(1-\delta_{ij}\right)}}{2 + \frac{Ri}{\mathrm{Pr}_t}} \tag{6}$$

where

$$\frac{l}{H} = K\left\{\frac{\sqrt{u_i u_i}}{\sqrt{\sum_{ij}\left(\frac{\partial u_i}{\partial x_i}\right)^2}} + \frac{\sqrt{\sum_{ij}\left(\frac{\partial u_i}{\partial x_j}\right)^2}}{\sqrt{\sum_{ij}\left(\frac{\partial^2 u_i}{\partial x_i \partial x_j}\right)^2}}\right\} \tag{7}$$

$$Ri = \frac{H}{u_R^2} \frac{\left(\frac{\partial T}{\partial n}\right)\tilde{n}\cdot\tilde{g}}{\sum_i \left[\left(\frac{\partial u_i}{\partial n}\right)\tilde{n}\cdot\tilde{g}\right]^2} \tag{8}$$

where Ri is the gradient Richardson number, l is a mixing length, and $\tilde{n}$ is a unit vector in the direction opposite to gravity. The quantity $\mathrm{Pr}_t$ is a turbulent Prandtl number, which is also used to provide a model for the effective thermal conductivity k (molecular plus turbulent):

$$\frac{k}{\mu_R} = \frac{1}{\mathrm{Pr}} + \frac{1}{\mathrm{Pr}_t}\left(\frac{\mu}{\mu_R} - 1\right) \tag{9}$$

where Pr is the molecular Prandtl number, also taken as a function of temperature $\tilde{T}$. In this algebraic model, $\mathrm{Pr}_t$ is assigned a numerical value of unity, for simplicity. Equation (6) clearly shows the stratification effect as represented through the use of the Richardson number. It

should be mentioned here that the k-ε model of turbulence does produce a more accurate estimate of the strain rates in the turbulent flow which could be useful in relating turbulence to the combustion process (Candel, Veynante, Lacas, Maistret, Darabiha, and Poinsot, 1990).

As indicated previously, the hot gas in the rooms is taken to be transparent and only surface to surface radiation exchange is included in the present field model. Consequently, the radiation flux only comes into play in the thermal boundary conditions at the walls, ceiling and floor. Furthermore, the flame surfaces are taken to be opaque and are treated the same as any other solid surface. Each surface, which, for convenience, coincides with the computational call, is taken to be gray and diffuse, and the radiation flux there is calculated by the standard radiosity method (Siegal and Howell, 1992) in terms of the surface emissivity and view factors. The view factors are determined once for all, taking into account shading due to obstructions along the line of sight. Partial blockages are accommodated by modifying the surface areas involved. In general, nonzero view factors are calculated by using the view factor definition, treating each surface as a sufficiently small area. This determination is not accurate for two surfaces in close proximity, in which case the exact view factors based on finite areas are utilized (Howell, 1982). Even though this specific field model does not consider a participating medium, it can be included without any fundamental difficulty, despite the fact that this would create much additional complexity in the radiative transfer calculations (Yang, 1986).

From a fundamental point of view, a turbulent combustion model is needed in a complete fire field model, and together with appropriate turbulence and gas radiation models, will provide information about fuel and combustion product species concentration distributions, flame zones, and time-dependent heat release rates and their spatial variations in the fire. Since, as already mentioned previously, a combustion model is not utilized in the current field model, information must be provided on the flame size and shape, and the volumetric heat release rate and its distribution. This is another reason that the effect of participating medium is not considered here because it does not have any meaning without a combustion model. In the present numerical simulation, the following provisions are made. The flame or fire plume envelope is taken, for convenience, the same as that of the fuel pan, and extends from the pan all the way to the ceiling. These are obviously not correct strictly. The fire envelope does not have a constant cross section vertically because of the entrainment, while the assumption of fire plume extending to the ceiling is probably reasonable in view of the fact that a very large fire is being considered over a period of about 18 minutes into the fire and the door openings do provide a strong ventilation. The overall heat release rate in the fire, without a turbulent combustion model, is very difficult to estimate, even from the fuel loss rate data from the test because of the lack of combustion efficiency information. On the other hand, the heat release rate data were not measured in the test. As a result, the application of the present field model dictates the use of a calibration

scheme based on the test data to determine the heat release rate, and as will be described later, a single calibration point is utilized in the present simulation study. As it turns out, as will also be shown, this scheme is responsible for at least a part of the disagreement between the simulation results and the test data. In addition, in the present study, the heat release rate is also taken to be distributed uniformly over the volume enclosed within the flame envelope. This assumption is also incorrect for obvious reasons. Normally for a large fire, the maximum heat release rate occurs at about one third of the height from the fuel pan because of fuel gasification effects. On the other hand, since the total heat release is preserved in the simulation, temperatures in the hot ceiling layer should not be overly affected by this assumption of uniform spatial distribution of the heat release rates.

The numerical algorithm in the Notre Dame field model is based on a finite-volume finite-difference staggered-cell formulation (Raycraft, Kelleher, Yang and Yang, 1990; McCarthy, 1991), which is a direct extension of the 2-D formulation in our earlier room fire studies (Yang, Lloyd, Kanury, and Satoh, 1984; Yang and Lloyd, 1985) with several improvements. One is that in the local pressure correction algorithm to satisfy flow continuity, the temperature and density fields are recalculated in each iteration. A second improvement is that the convective terms in the governing equations (2) and (3) are discretized on the basis of the QUICK scheme (Leonard, 1983) to minimize numerical diffusion effects. Also, a global pressure correction routine is included to accommodate possible global pressure build-up due to insufficient ventilation (Nicolette, Yang, and Lloyd, 1985). In addition, as mentioned previously, the numerical algorithm incorporates the heat loss calculations at any solid boundary. The radiation fluxes arriving at the boundary cells are updated once every several time steps to conserve calculations and the view factors are calculated only once and are stored in the form of a table lookup for subsequent radiation flux calculations.

## 4. NUMERICAL VALIDATION STUDIES

Before the field model described above was applied to simulate the E41.5 Test in the present study, two sets of numerical validations were carried out to assure that the computer code based on the field model is self-consistent and does lead to plausible results. Both numerical validation exercises deal with the E41.5 Test fire-room geometry, but with different arbitrarily chosen heat release rates. The geometry of the fire room was simplified somewhat to eliminate the curvature in the rear wall, as shown by the computational domain given in Figure 3. A uniform cell grid was adopted, and each cell had a side of 273 mm. Altogether there were 12,768 calculation cells which are designated in indices I, J, K, as also shown in Figure 3. This cell structure is the same as that later used in the E41.5 Test simulations. The coefficient of heat transfer on the exterior surfaces of the walls and ceiling was taken to be 85 $w/m^2K$,

corresponding to that of a mixed convection condition. This value was also the same as that utilized in the full simulation of the test data. All computations in the present study were carried out on an IBM mainframe computer and an IBM RISC 6000 computer.

In the first numerical validation, a ramped heat release rate was utilized. A linear heat release rate was first prescribed from ignition to a level of 250 KW at 60 seconds into the fire, and was then maintained at that level until a little over 260 seconds, which represented the end of this validation study. The purpose of this exercise was to determine the suitability of chosen time steps for numerical stability considerations, to check both heat and mass balances at the doorways, and also to see if steady-state conditions were achievable. For these reasons the calculation of radiation fluxes was not included in the calculations in this first exercise. The calculations showed that numerical stability was achieved with an initial time step of 0.005 sec until $\bar{t}$ = 115 sec and then a second time step of 0.002 sec until the end of the calculations. The time step change was done automatically in the code at time instants where the numerical residual mass exceeded prescribed tolerances. The numerical results are shown in Figures 4. The solid curve in Figure 4(b) is evidently the ramped heat release rate described previously, and represents the rate of energy gained by the fire room. During this hypothetical fire, the doorways remained in the opened position, and hot gases would leave the upper part of the doorways, while cool air would in turn come into the fire room in the lower part of the same doorways. This scenario is typical of compartment fires with only one doorway (or one window) in ventilated fires. In general, it is expected that the total mass-flow rate of the incoming cool air would essentially follow that of the outgoing hot gases. This is shown in Figure 4(a), where the solid line represents the mass flow rate of cool air, while the dashed line is that of the outgoing hot gases. The dotted curve close to the zero mass-flow rate level represents the residual masses in the calculated results as time proceeds, giving an indication of the degree of inaccuracies involved. The heavily dotted region close to $\bar{t}$ = 115 sec was due to the transients as the time step was changed. The residual mass level could very well be reduced in the early times if the initial time step was chosen to be smaller, and it is also seen that the time step utilized beyond $\bar{t}$ = 115 sec was completely satisfactory. Also, it is interesting to note that even when the residual mass error is taken into account, the in-flow mass flow rate was somewhat higher than that of the outflow at early times into the fire. The primary reason for this is that the density of the hot gases is lower and there is a slight pressurization in the fire room. Also, there is a strong indication that a steady-state condition was achieved beyond t = 100 sec. This can also be discerned in Figure 4(b) for the heat rates, where the dashed curve gives the total instantaneous heat rate that leaves the fire room, i.e., the sum total of heat exiting through the doorway and wall losses. It is clearly seen that this heat balance is essentially maintained throughout the hypothetical fire. It is also worthy to note the large-scale oscillations in the responses to the fire

load. These oscillations have also been observed in both the observed and numerically simulated data in another full-scale fire test carried out at the Naval Research Laboratory (Raycraft, Kelleher, Yang, and Yang, 1990), and are believed to be due to flow separations and other large flow instabilities occurring in the fire room.

The second numerical validation study included every feature in the final E41.5 Test simulation except that the heat release rate is based on 25% of that corresponding to the experimental fuel-loss data and the heating value of the fuel. Physically, this represents a combustion efficiency of 25%, which is obviously too low. The purpose of this exercise was to carry out a simulation run which includes every part of the computer code based on the field model described previously including radiation, but at a lower level of heat release rate (a maximum of about 2 MW) to insure that numerical instability was not a problem, so that the entire simulation up to 18 min from the commencement of the fire, similar to the E41.5 Test, could be completed expeditiously. The results again in terms of the mass in-flow and out-flow rates and the corresponding heat rate are shown in Figures 5. It is noted here that all curves shown are time averaged to facilitate discussion of general trends. The mass out-flow rates, as shown by the dashed curve in Figure 5(a), also include the residual mass, and the very slight differences in the two curves represent numerical errors. The numerical errors in the heat rates in Figure 5(b) are also very slight, as evidenced by the heat rate due to the residual mass shown as the dotted curve. These errors are not included in any of the two curves above. It is seen here that at the earlier times, the heat rate that leaves the fire room, which includes the wall losses, lags behind that provided by the fire. This obviously is responsible for the increase of temperatures inside the fire room. At a later time, the trend is reversed and the overall temperature rise becomes more subdued.

From the above two numerical experiments, it can be concluded that the computer code based on the field model is capable of producing numerically accurate results, and any shortcomings in the result must be attributed to deficiencies in the formulation of the field model in terms of the many submodels used.

## 5. NUMERICAL SIMULATION OF THE E41.5 TEST

As mentioned previously, in the E41.5 Test the fuel burn rate was measured by a weighing scale located under the fuel pan. This data can be converted into the theoretical heat release rates by introducing the heating value of the fuel oil which is 42,500 kJ/kg, and these theoretical values are shown in Figure 6. The actual heat release rates are necessarily much lower due to incomplete combustion, and unfortunately the combustion efficiencies are not known, but must be somehow estimated. In the present study, the combustion efficiency was estimated by a single calibration based on temperatures and velocities in the hot-gas layer at the

doorways; the resulting efficiency was then taken as constant and utilized throughout the entire fire duration of 18 min. At the outset, it was realized that such a calibration scheme was full of hazards, largely due to the choice of the calibration data point. Even though it was basically possible to utilize several data points for calibration purposes, the overwhelming extent of the needed computing resources would have been impractical. Several sets of computations at combustion efficiencies of 50%, 55%, 60% and 100% were carried out up to 4 min, and the resulting ceiling hot-gas temperatures at a thermocouple location designated as 5216 at the 4 min instant and the hot-gas exit velocities at the doorway close to the ceiling at the 2 min instant were compared with the corresponding test data in the E41.5 Test. The thermocouple 5216 is located close to the ceiling in the small entry room right next to the main fire room. These comparisons are shown in Table 1. It is clearly seen that the best comparisons of the temperature and velocity occur at a combustion efficiency of 60%, which was somewhat lower than expected. This value of efficiency was then used in the simulations throughout the fire period of 18 min. It should be noted that this combustion efficiency, even if it is correct, is not the true value, but a value representing the combined effects of incomplete combustion, gas and soot radiation effects, and other effects which are not accounted for in the field model.

In the full numerical simulations, the initial time step was again taken to be 0.005 sec, which was changed to 0.002 sec at about 1.2 min into the fire. It was reduced again to 0.0005 sec at about 70 min time instant, which was then maintained until the end of computations at 28 min. This time step schedule followed closely the heat release rates as shown in Figure 6, as expected. In the E41.5 Test, several temperatures at specific locations in the fire room were measured, along with the exit velocities at the doorway. Comparisons of the measured temperatures and the numerically simulated temperatures at three thermocouple locations 5216, 5236 and 5230, and that of the exit velocities below the location 5236 are shown respectively in Figures 7 and 8. The location 5216 is at the 7.4m level above grade and close to the ceiling in the smaller entry room, but right next to the main fire room. This is a critical location, since all the hot gases from the fire would exit the fire room by this location. The location 5236 is at the same level as that of 5216, but right above the middle of the two doorways, and this is the same location where single calibration on the temperatures were made. Location 5230 is vertically below the location 5236, but at 0.35m above the floor in the cool-air stream coming in from outside the fire room. The velocity comparisons in Figure 8 are made in the hot-gas layer at a location below 5236 in the doorway, and this is the same velocity that was used in the calibration for the combustion efficiency.

With the single calibration on the combustion efficiency at the 3 min and 4 min time instants (see Table 1) in the temperatures at the 5236 location, it is seen from Figure 7 that the numerical simulations at all three thermocouple locations based on time-averaged temperature,

the solid lines, compare reasonably well with the test data up to a time instant of 8 min. Beyond that time, the computed hot gas layer temperatures are considerably higher than that from the measurements, even though the general trends in this time period are still similar. This comparison is obviously affected by the combustion efficiency calibration utilized in this study. However, the very fact that the test data show only moderate variations in the temperatures in this period may very well be caused by gas and soot radiation effects which are not accounted for in the field model. As it is generally known, such effects will tend to smear out the temperature field. Also, it is realized that in the early time period into the fire, the gas and soot radiation effects are not as critical because of the lower temperatures involved. As for the temperature at thermocouple location 5230, the field model underpredicts the test results again in the latter part of the fire phenomenon. This is surely the effect of gas and soot radiation. Incidentally, in such a large fire over a prolonged period of time, the losses through the wall and ceiling are quite significant, up to 30% according to the simulation results. Consequently, the choice of a single exterior wall coefficient of heat transfer in the present study may also have influenced the comparisons shown in Figure 7.

Figure 8 shows the comparison of exit velocities in the hot ceiling layer at the doorway. The solid curve represents the time-averaged velocities of the numerical simulations, while the open circles give the corresponding test data. At the outset, it should be realized that measuring velocities in an intense fire environment is difficult, and that in the E41.5 Test, there was a degree of uncertainty as to how close the probe was placed close to the wall. Nevertheless, while the simulation provides the correct trend, it overpredicted the exit velocities by a significant margin, and this overprediction signals deficiencies in the field model. However, since in buoyancy-driven flows the velocities are very sensitive to the varying temperature field, it is not surprising to see this overprediction in view of the fact that the temperatures are also overpredicted (Figure 7).

From the above comparisons it can be concluded that while the field model utilized in the present study does provide reasonably good trends in the temperature and velocity fields, its inability in modeling the combustion efficiency or the heat release rates in full-scale fires represents a significant shortcoming in its application to deal with such large fires. In this regard, it is pertinent to mention that a subsequent numerical simulation study dealing with a full-scale forced-ventilation fire in the same HDR facility fire room (E41.7 Test) has been completed recently (Yang, Huang, and Nicolette, 1994), in which the heat release rates were determined by the application of a zone model. Consequently, the results were completely independent of the test data. Very good agreement between the simulation data and the test data was found. Consequently, it can be said that at this stage of the development of the field model, a

combination of the field model and a zone model, which is used to provide a good estimate of the heat release rates, is a viable means to study real-world full-scale fires at the present time.

## 6. CONCLUDING REMARKS

In the present numerical study a three-dimensional field model is described to simulate a full-scale fire test carried out in a decommissioned nuclear reactor containment building. The fire room has a very complex geometry and the fire was fully naturally ventilated with open doorways. The field model is not complete in that it lacks a turbulent combustion submodel and also does not account for gas and soot radiation. Because of this deficiency, the combustion efficiency was estimated by a single calibration based on the experimental data on the temperature and velocity at specific locations and time instants. The field model with the fire-room geometry was numerically tested in terms of prescribed heat release rates with heat and mass flow balances before it was used to simulate the full-scale fire test. Results of the comparisons of temperatures at three specific thermocouple locations and velocities at the exiting hot ceiling layer at the doorway showed that the simulation results were good up to about 8 min into the fire, but overestimated both temperatures and velocities thereafter until the end of the fire at 18 min. Part of the discrepancy between the results in the latter time period is attributed to the fact that the field model did not account for gas and soot radiation.

The lack of a turbulent combustion submodel was considered a significant shortcoming of the field model utilized in the present study, and it is suggested that this shortcoming could be for the short term remedied by incorporating a zone model to provide the needed heat release rate data to the field model.

## 7. ACKNOWLEDGMENT

The support of NRC Grant FIN L130 is gratefully acknowledged. The authors are also grateful for help of technical personnel of the University of Notre Dame Computer Center.

## 8. NOMENCLATURE

| | |
|---|---|
| $c_p$ | Dimensionless specific heat |
| G | Dimensionless generalized gravitation vector |
| g | Dimensionless gravity |
| $\tilde{g}$ | Gravitational vector |

| | |
|---|---|
| H | Height of fire room, m |
| I,J,K | Coodinate indices |
| K | Constant in turbulence mode, K = 0.4 |
| k | Turbulent kinetic energy, $m^2/s^2$ |
| k | Dimensionless effective thermal conductivity |
| l | Mixing length in turbulence model, m |
| $\bar{n}$ | Unit vector in direction opposite of gravity |
| Pr | Molecular Prandtl number |
| $Pr_t$ | Turbulent Prandtl number |
| $p_i$ | Dimensionless pressure difference |
| Ri | Gradient Richardson number |
| T | Dimensionless temperature |
| t | Dimensionless time |
| $u_i$ | Dimensionless velocity components |
| $x_i$ | Dimensionless coordinates |
| $\varepsilon$ | Dissipation rate of turbulent kinetic energy, $m^2/s^3$ |
| $\mu$ | Dimensionless effective viscosity |
| $\rho$ | Dimensionless density |

$\sigma_{ij}$ Dimensionless shear stress tensor

**SUPERSCRIPT**

Dimensional quantities

**SUBSCRIPTS**

e Equilibrium conditions

,i Derivatives with respect to $x_i$

m Mean conditions

R Reference conditions

**REFERENCES**

Candel, S., Veynante, D., Lacas, F., Maistret, E., Darabiha, N., and Poinsot, T. (1990): Flamelet Description of Turbulent Combustion, Proceedings of the 9th International Heat Transfer Conference, Vol. 1, Hemisphere Publishing Co., New York, pp. 113-128.

Chow, W.K. and Fong, N.K. (1993): Application of Field Modeling Technique to Simulate Interaction of Sprinkler and Fire-Induced Smoke Layer, Combustion Science and Technology, Vol. 89, pp. 101-151.

Delaney, M.A. (1992): Numerical Field Model Simulation of Full Scale Fire Tests in a Closed and an Open Compartment, M.S. Thesis, Naval Postgraduate School, Monterey, CA.

Holen, J., Brostrom, M. and Magnussen, B.F. (1990): Finite Difference Calculation of Pool Fires, Third Symposium (International) on Combustion, The Combustion Institute, pp. 1677-1683.

Houck, R.R. (1988): Numerical Field Model Simulation of Full-Scale Fire Tests in a Closed Spherical/Cylindrical Vessel with Internal Ventilation, M.S. Thesis, Naval Postgraduate School, Montery, CA.

Howell, J.R. (1982): A Catalog of Radiation Configuration Factors, McGraw-Hill Book Co., New York.

Jones, I.P. (1990): Fire Modelling, Eurothrm Seminar No. 13, Abstract of Papers, Harwell Laboratory, England.

Kou, H.S., Yang, K.T., and Lloyd, J.R. (1986): Turbulent Buoyant Flow and Pressure Variations around an Aircraft Fuselage in a Cross Wind Near the Ground, Fire Safety Science in Proc. First International Symposium, pp. 173-184.

Leonard, S.P. (1983): A Convectively Stable, Third-Order Accurate Finite Difference Method for Steady Two-Dimensional Flow and Heat Transfer, Numerical Properties and Methodologies in Heat Transfer, ed. T.M. Shih, Hemisphere Publishing Corp., Washington, D.C. pp. 211-226.

McCarthy, T.G. (1991): Numerical Field Model Simulation of Full Scale Fire Tests in a Closed Spherical/Cylindrical Vessel Using Advanced Computer Graphics Technique, M.S. Thesis, Naval Postgraduate School, Monterey, CA.

Mueller, K., and Max, U. (1991): Input Data Set for E41.7 Blind Postcalculations of an Oil Fire in a Closed System, Kernforschungszentrum Karlsruhe GmbH.

Mueller, K. and Volk, R. (1990): Characteristics of an Oil Fire in a Closed Subsystem with the Ventilation System Connected and Variable Degrees of Door Opening, Design Basis Report, Kernforschungszentrum Karlsruhe GmbH.

Nicolette, V.F., Yang, K.T., and Lloyd, J.R. (1985): Transient Cooling by Natural Convection in a Two-Dimensional Square Enclosure, International Journal of Heat and Mass Transfer, Vol. 28, No. 9, pp. 1721-1732.

Nies, G.F. (1986): Numerical Field Model Simulation of Full Scale Tests in a Closed Vessel, M.S. and M.E. Thesis, Naval Postgraduate School, Monterey, CA.

Raycraft, J., Kelleher, M.D., Yang, H.Q., and Yang, K.T. (1990): Fire Spread in a Three-Dimensional Pressure Vessel with Radiation Exchange and Wall Heat Losses, Mathematical and Computer Modelling, Vol. 14, pp. 795-800.

Satoh, K., Lloyd, J.R., Yang, K.T., and Kanury, A.M. (1983): A Numerical Finite-Difference Study of the Oscillating Behavior of Vertically Vented Compartments, in Numerical Properties and Methodologies in Heat Transfer, Ed. T.M. Shih, Hemisphere Publishing Corp., Washington, D.C., pp. 517-528.

Siegel, R. and Howell, J.R. (1992): Thermal Radiation Heat Transfer, 3rd Ed., Hemisphere Publishing Co., Washington, D.C.

Simcox, S., Wilkes, N.S., and Jones, I.P. (1988): Computer Simulation of the Flows of Hot Gases from the Fire at King's Cross Underground Station, AERE-G4782.

Yang, K.T. (1986): Numerical Modeling of Natural Convection-Radiation Interactions in Enclosures, Keynote Address, in Proceedings of the 8th International Heat Transfer Conference, Vol. 1, Hemisphere Publishing Co., Washington, D.C., pp. 131-140.

Yang, K.T. (1987): Natural Convection in Enclosures, Chapter 13 in Handbook of Single-Phase Convective Heat Transfer, Wiley-Interscience Publishers, New York, pp. 13-1 to 13-51.

Yang, K.T., Huang, H.J., and Nicolette, V.F. (1994): Field Model Simulation of Full-Scale Forced-Ventilation Room-Fire Test in the HDR Facility in Germany, paper submitted for presentation at the 1994 AIAA/ASME Thermophysics and Heat Transfer Conference, Colorado Springs, CO.

Yang, K.T. and Lloyd, J.R. (1985): Turbulent Buoyant Flow in a Vented Simple and Complex Enclosure, in Natural Convection-Fundamentals and Applications, Eds. S. Kakac, W. Aung and R. Viskanta, Hemisphere Publishing Co., Washington, D.C., pp. 303-329.

Yang, K.T., Lloyd, J.R., Kanury, A.M., and Satoh, K. (1984): Modeling of Turbulent Buoyant Flows in Aircraft Cabins, Combustion Science and Technology, Vol. 39, pp. 107-118.

Table 1. Single Calibration for Estimating Combustion Efficiency

| Combustion Efficiency (%) | Hot Gas Temperature at Exit (T) | | Hot Gas Exit Velocity at 2 min (m/s) |
|---|---|---|---|
| | 3 min | 4 min | |
| 50 | 2.4 | 2.9 | 3.25 |
| 55 | 3.7 | 4.2 | 3.74 |
| 60 | 3.9 | 4.4 | 4.02 |
| 100 | --- | --- | 12.04 |
| E41.5 Test | 3.8 | 4.2 | 3.96 |

LIST OF FIGURES FOR APPENDIX C


| | |
|---|---|
| Figure 1 | HDR Reactor Containment Building |
| Figure 2 | Geometry of Fire Room |
| Figure 3 | Computational Domain |
| Figure 4 | Ramped Heat Input, 250 kw<br>(a) Mass Balance (b) Heat Balance |
| Figure 5 | Heat Release Rate at 25% Combustion Engineering<br>(a) Mass Balance (b) Heat Balance |
| Figure 6 | E41.5 Test Heat Release Rates (100% Combustion Efficiency) |
| Figure 7 | Comparison of Temperatures (Simulation Temperatures Time Averaged) |
| Figure 8 | Comparison of Hot Gas Exit Velocity (Simulation Velocities Time Averaged) |

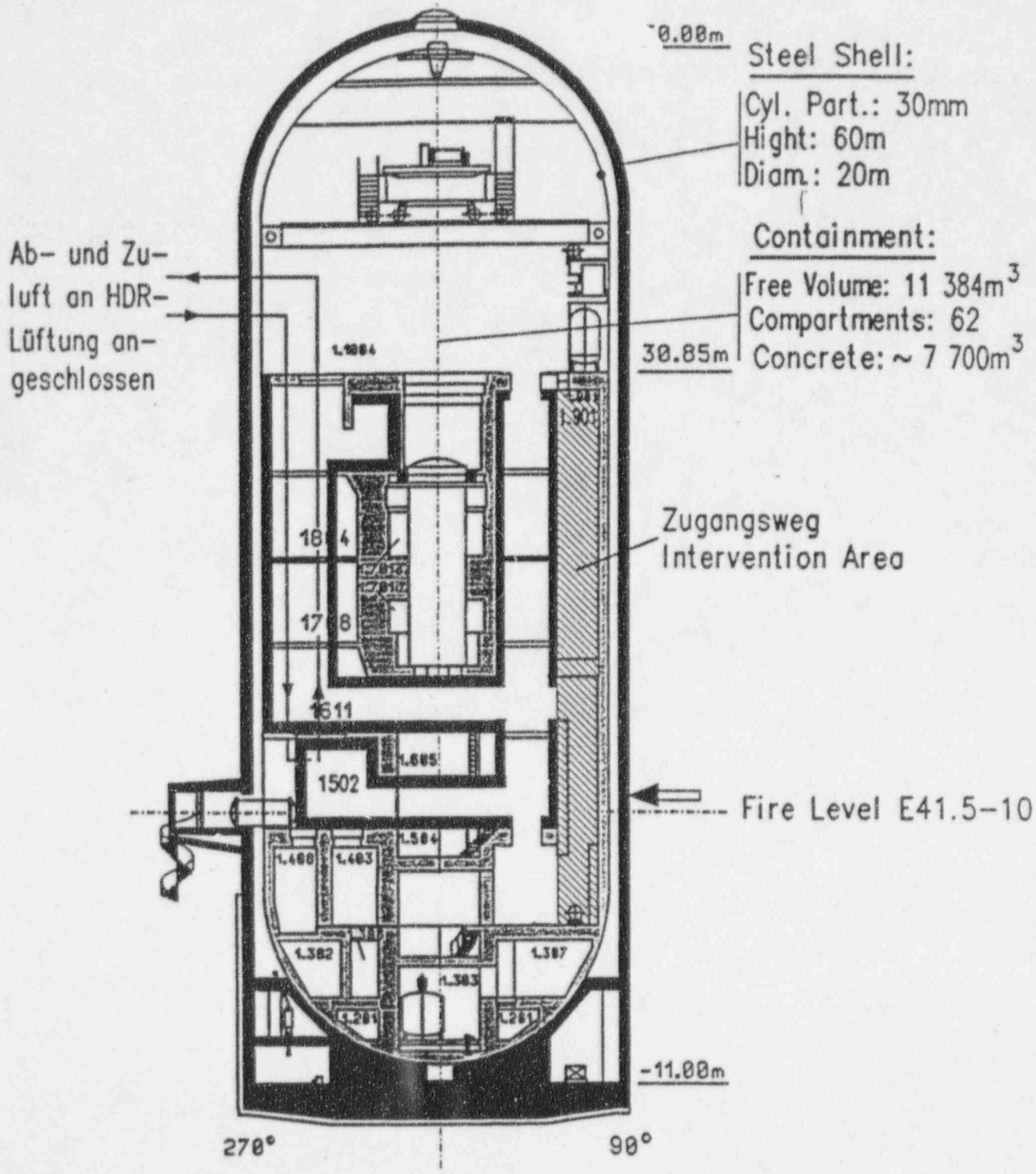


Figure C-1

HDR Reactor Containment Building

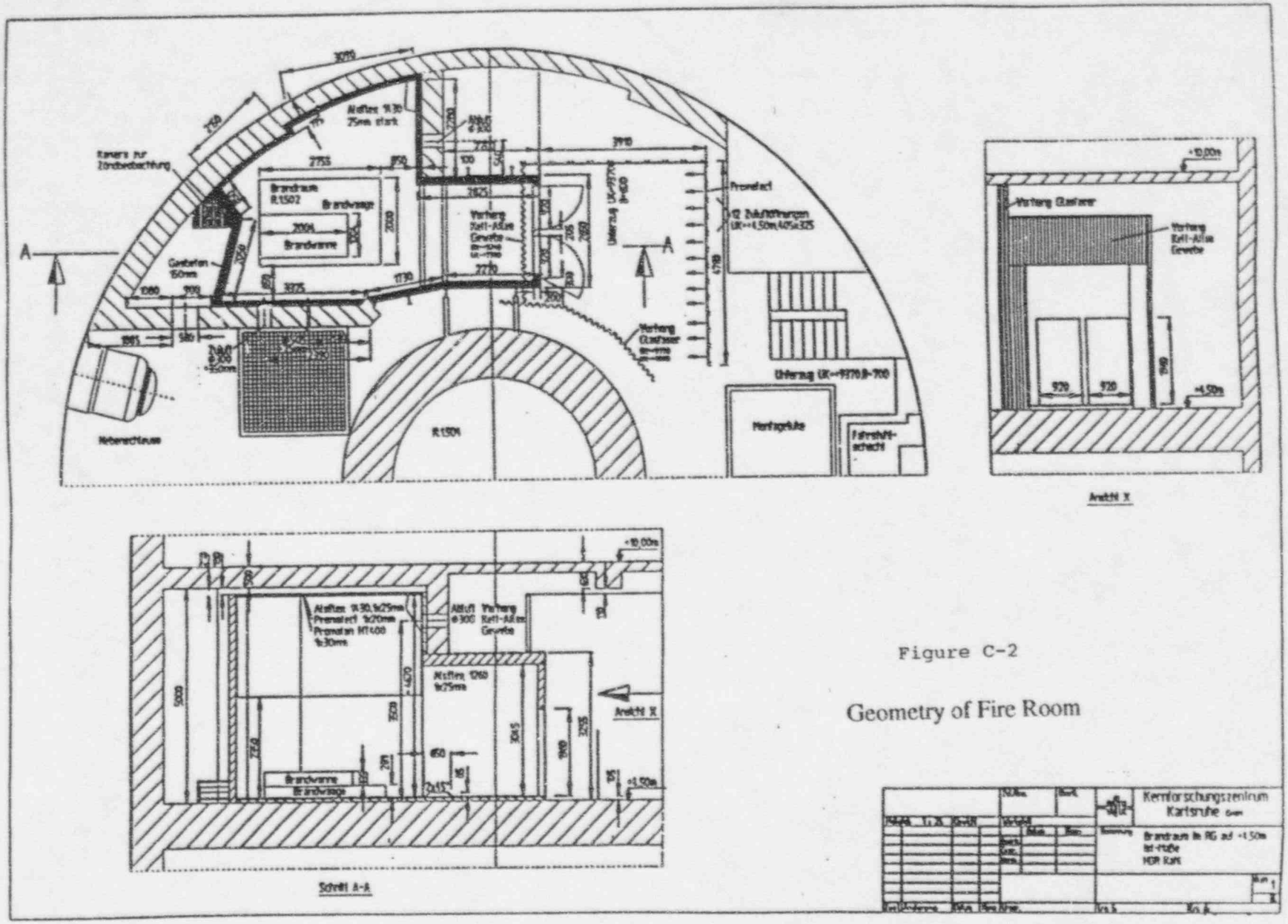


Figure C-2

Geometry of Fire Room

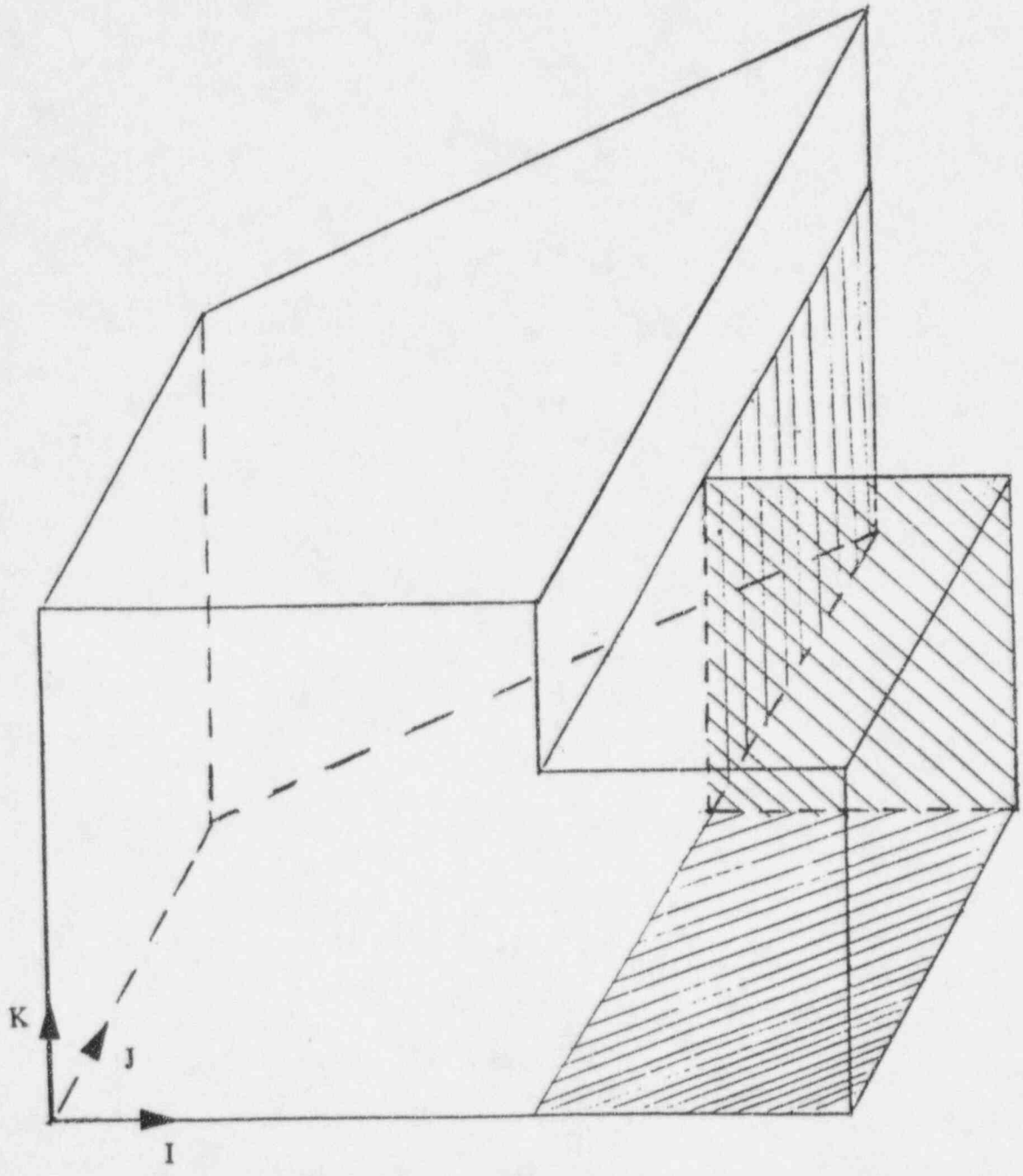


Figure C-3

Computational Domain

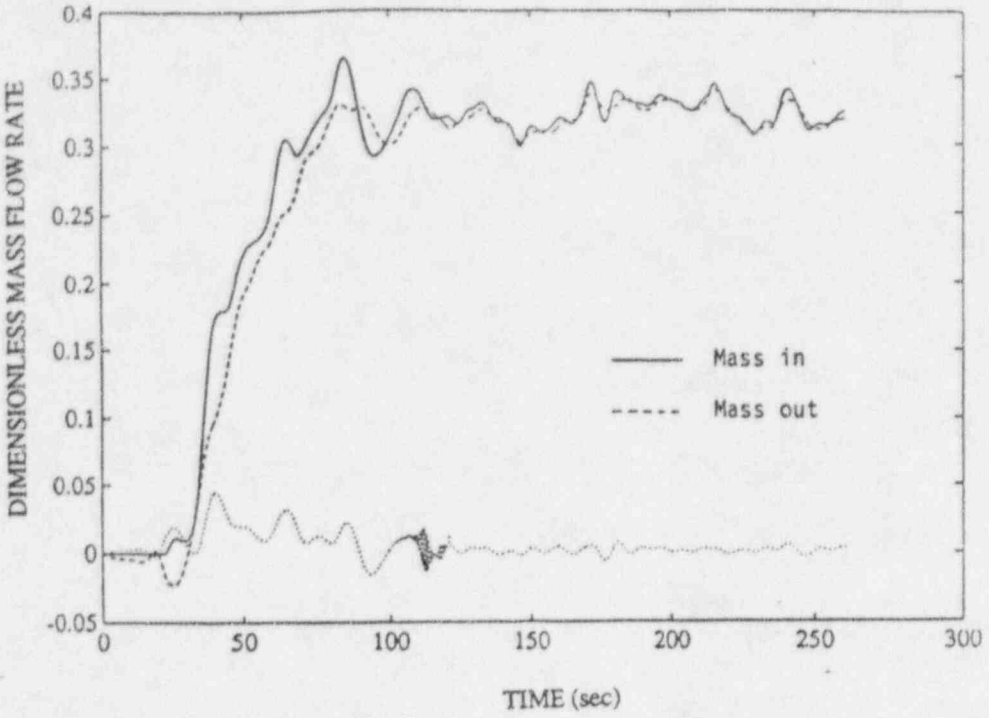


(a)

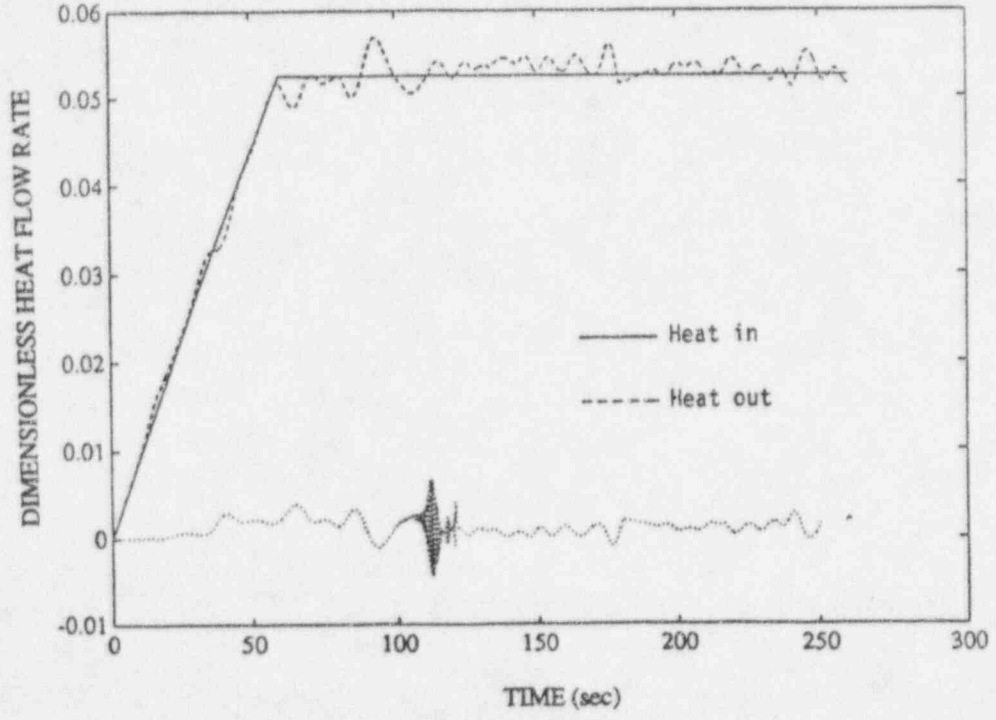


(b)

Figure C-4

Ramped Heat Input, 250 kw (a) Mass Balance (b) Heat Balance

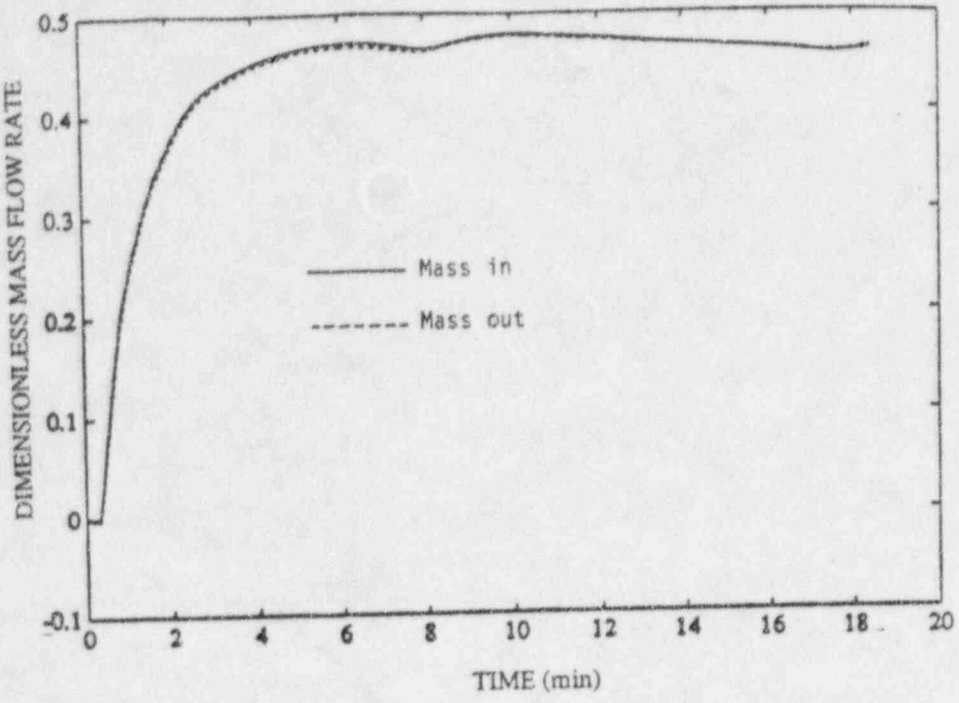


(a) Mass Balance

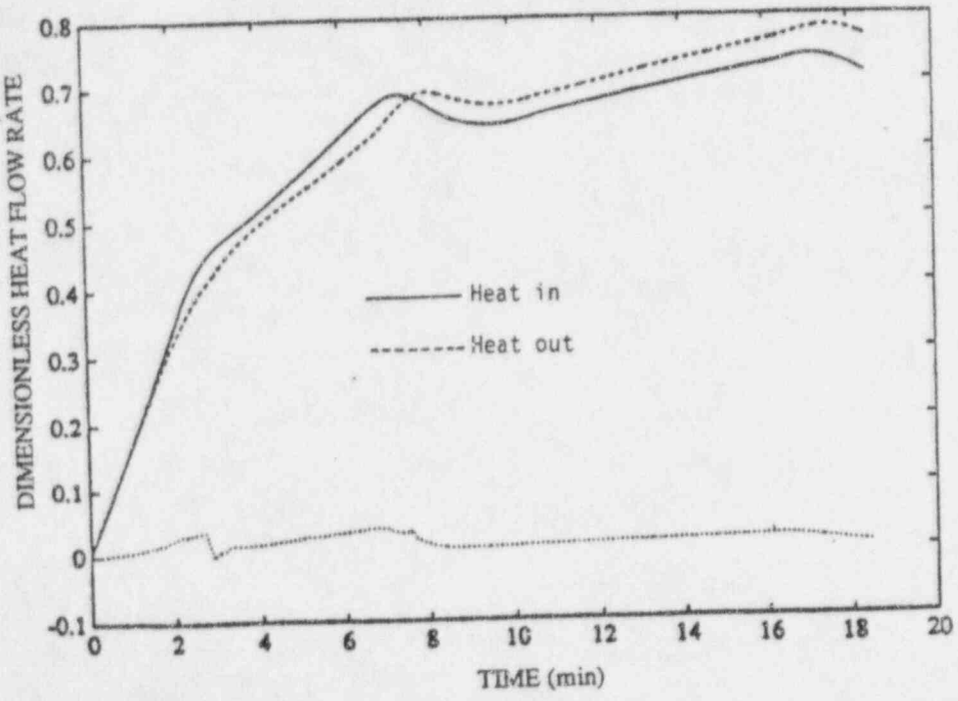


(b) Heat Balance

Figure C-5

Heat Release Rate at 25% Combustion Engineering

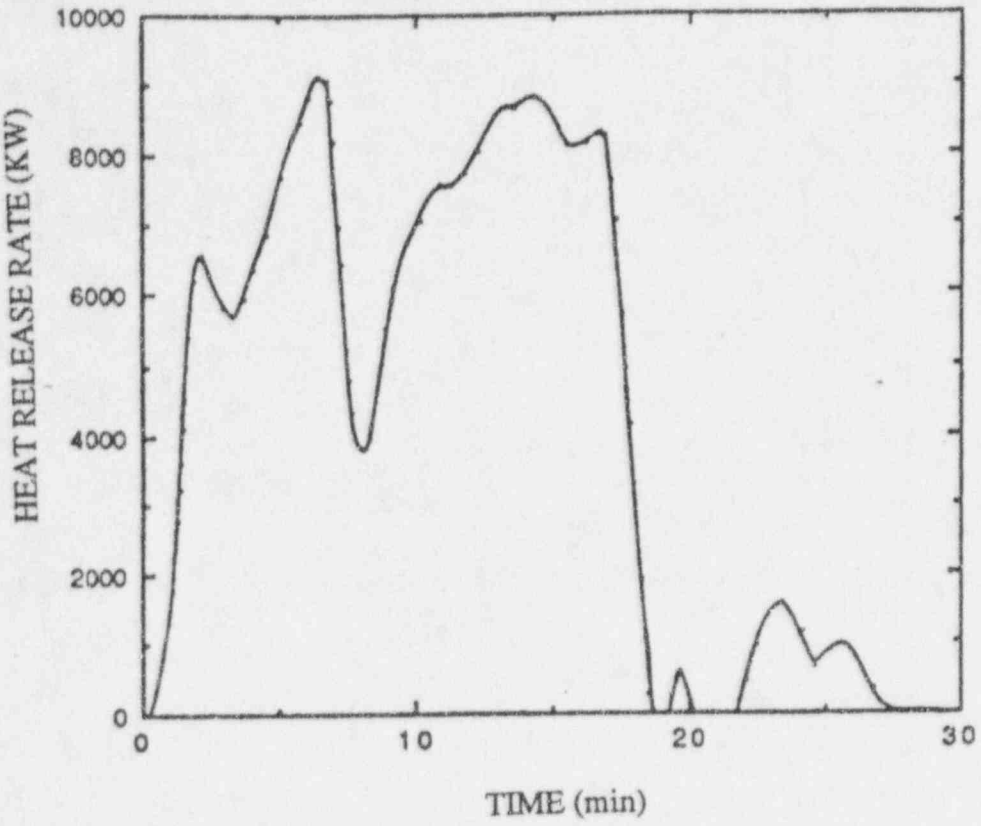


Figure C-6

E41.5 Test Heat Release Rates (100% Combustion Efficiency)

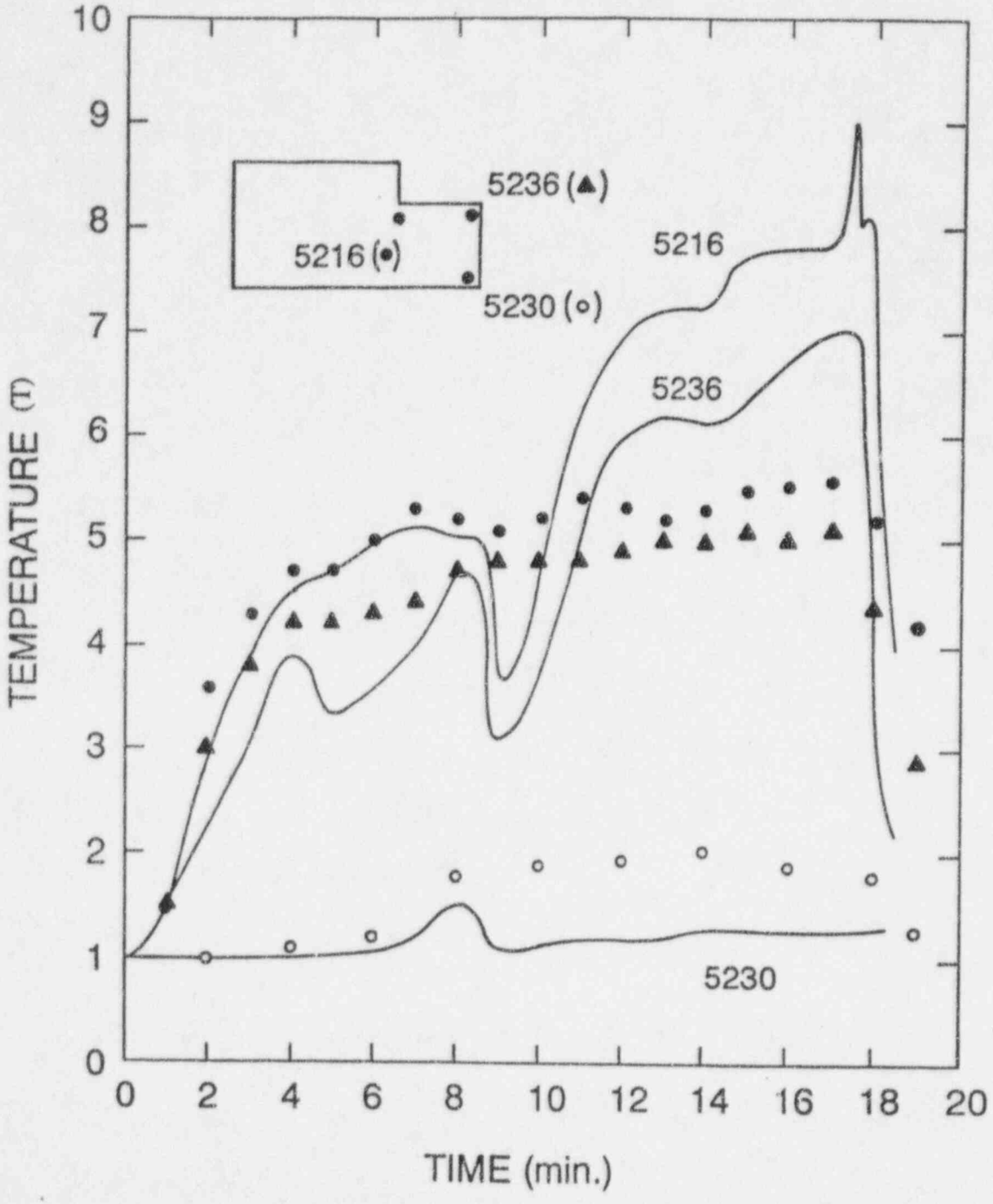


Figure C-7

Comparison of Temperatures (Simulation Temperatures Time Averaged)

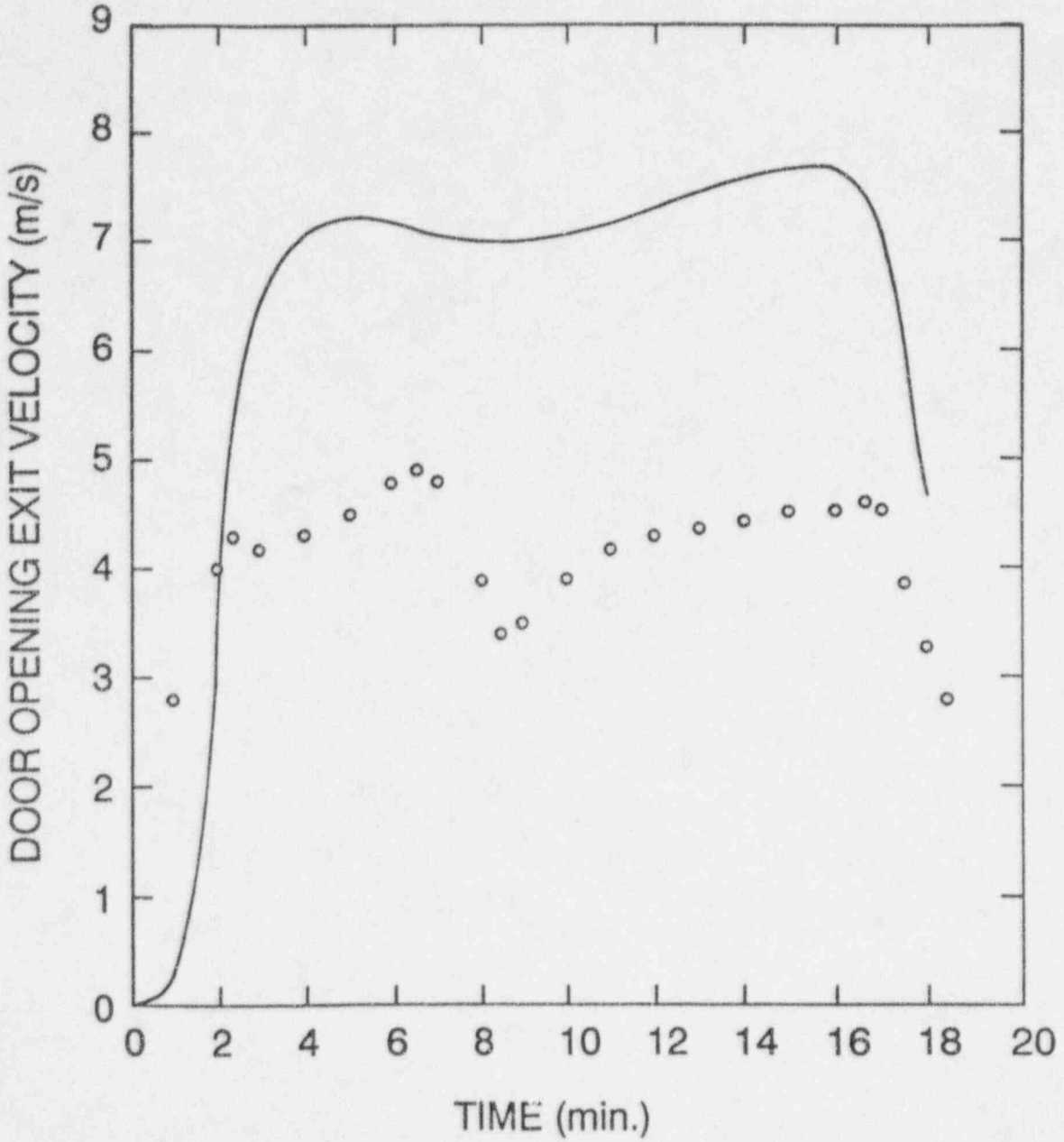


Figure C-8

Comparison of Hot Gas Exit Velocity (Simulation Velocities Time Averaged)

**DISTRIBUTION:**

U. S. Nuclear Regulatory Commission
Attn: **William Gleaves** (10)
Office of Nuclear Regulatory Research
Washington, DC 20555

U. S. Department of Energy
Attn: Andrew J. Pryor
Albuquerque Operations Office
PO Box 5400
Albuquerque, NM 87115

Professor K.T. Yang
Dept. of Mechanical Engineering
University of Notre Dame
Notre Dame, IN 46556

Electric Power Research Institute
Attn: Bob Kassawara
Nuclear Power Division
3412 Hillview Ave.
Palo Alto, CA 94303

National Institute of Standards and Technolgy
Attn: Walter Jones
Building 224, Room A249
Gaithersburg, MD 20899

T. Eklund
Fire Safety Research Branch
ACD-250, Bldg. 204
Atlantic City Int'l Airport, NJ 08405

Pravin Gandhi
Underwriter's Laboratory
333 Pfingsten Road
Northbrook, IL 60062

George Apostolakis
Dept. of Mechanical Engineering
Univ. of Calif. at Los Angeles
Los Angeles, CA 90024

Factory Mutual Research Corp.
Attn: Soonil Nam
1151 Boston-Providence Turnpike
PO Box 9102
Norwood, MA 02062

Doug Beller
Azure Dragon Enterprises, Inc.
22 George Hill Rd.
Grafton, MA 01519

Professor J. R. Barnett
Worcester Polytechnic Institute
Fire Protection Engineering
100 Institute Road
Worcester, MA 01609-2280

Professor Matt Kelleher
Chairman, Mechanical Eng. Dept.
Naval PostGraduate School
Monterrey, CA 93943

Fire Science and Technology, Inc.
Attn: Vyto Babrauskas
10900 Bethesda Church Rd.
Damascus, MD 20872

Professor A.F. Ghoniem
Mechanical Engineering Dept.
Massachusetts Institute of Technology
Room 3-342
77 Massachusetts Avenue
Cambridge, MA 02139

FireTech
Attn: Thomas Capaul
Brian Meacham
P.O. Box 199
CH-8706 FELDMEILEN, SWITZERLAND

Gesellschaft fur Anlagen und Reaktorsicherheit (GRS),mbH
Attn: H. Liemersdorf
M. Rowekamp
T. Riekert
B. Schwinges
Operational Behaviour Division
Schwertnergasse 1
50667 COLOGNE, FEDERAL REPUBLIC OF GERMANY

Gesellschaft fur Anlagen und Reaktorsicherheit (GRS),mbH
Attn: Hermann Jahn
Bereich Systemanalyse
Forschungsgelande
85748 GARCHING b. MUNCHEN
FEDERAL REPUBLIC OF GERMANY

Battelle-Institut e.V.
Attn: Karsten Fischer
Lothar Wolf
Am Romerhof 35
D-6000 Frankfurt am Main 90
FRANKFURT, FEDERAL REPUBLIC OF GERMANY

Distribution (Continued):

CEA IPSN/DRS/SEA
Attn: Roger Rzekiecki
Chef du Groupe Physique des Feux
DRS/SEA CEN CADARACHE
13108 Saint-Paul-Lez-Durance
FRANCE

Brandforsk
Attn: Tommy Arvidsson
S-115 87 STOCKHOLM, SWEDEN

Winfrith AEA Technology
Attn: Chris Fry
Heat Transfer Group, Bldg. B30
DORCHESTER, DORSET DT2 8DH UNITED KINGDOM

O. Keski-Rahkonen
VTT
Fire Technology Laboratory
Kivimiehentie 4
SF-02150 ESPOO, FINLAND

O. Sugawa
Center for Fire Science & Technology
Science University of Tokyo
2641 Yamasaki
NODA-SHI, 278
JAPAN

A. Strong
University of Waterloo
Dept. of Mechanical Engineering
Waterloo, ONTARIO CANADA N2L-3G1

K. Müller
Kernforschungszentrum Karlsruhe
HDR Sicherheitsprogramm
PO Box 3640
76021 KARLSRUHE, GERMANY

Petra Büttner
IGTS, mbH
Waldowallee 117
10318 BERLIN, GERMANY

Attn: C. Lebeda
U. Schneider
Tech. Universite Wien
Inst. fur Baustofflehre und Bauphysik
Karlsplatz 13/206
1040 WIEN, AUSTRIA

Bjorn Hekkelstrand
SINTEF/NTH
Division Thermodynamics
N-7034 TRONDHEIM, NORWAY

Lopez Marie-Claude
Institut de Protection et de Surete Nucleaire
Centre d'Etudes Nucleaires(CEN/G)
GRENOBLE, FRANCE

Internal SNL:

| no. | MS | Name | Org. |
|---|---|---|---|
| 1 | 0841 | P.J. Hommert, | 1500 |
| 1 | 0828 | P.J. Hommert (actg.), (route to 1511) | 1502 |
| 1 | 0441 | J.H. Biffle, (route to 1517,1518) | 1503 |
| 1 | 0828 | E.D. Gorham, (route to 1514, 1515) | 1504 |
| 1 | 0834 | A.C. Ratzel, (route to 1516) | 1512 |
| 1 | 0835 | R.D. Skocypec, | 1513 |
| 1 | 0835 | E.A. Boucheron, | 1513 |
| 1 | 1513 | L.A. Gritzo, | 1513 |
| 2 | 0835 | V.F. Nicolette, | 1513 |
| 1 | 0835 | S.R. Tieszen, | 1513 |
| 1 | 0825 | A.R. Lopez, | 1515 |
| 1 | 0825 | C.C. Wong, | 1515 |
| 1 | 1135 | J.L. Moya, | 2735 |
| 1 | 0739 | J. Tills, | 6429 |
| 1 | 0737 | M.P. Bohn, | 6449 |
| 15 | 0737 | S.P. Nowlen, | 6449 |
| 1 | 9018 | Central Technical Files, 8523-2 | |
| 5 | 0899 | Technical Library, | 13414 |
| 1 | 0619 | Print Media, | 12615 |

NRC FORM 335 (2-89) NRCM 1102, 3201, 3202

U.S. NUCLEAR REGULATORY COMMISSION

# BIBLIOGRAPHIC DATA SHEET

*(See instructions on the reverse)*

1. REPORT NUMBER (Assigned by NRC, Add Vol., Supp., Rev., and Addendum Numbers, if any.)
NUREG/CR-6017
SAND93-0528

2. TITLE AND SUBTITLE
Fire Modeling of the Heiss Dampf Reaktor Containment

3. DATE REPORT PUBLISHED
MONTH: September
YEAR: 1995

4. FIN OR GRANT NUMBER
L1330

5. AUTHOR(S)
V. F. Nicolette, Sandia National Laboratories
K. T. Yang, University of Notre Dame

6. TYPE OF REPORT
Technical

7. PERIOD COVERED *(Inclusive Dates)*

8. PERFORMING ORGANIZATION – NAME AND ADDRESS *(If NRC, provide Division, Office or Region, U.S. Nuclear Regulatory Commission, and mailing address; if contractor, provide name and mailing address.)*
Sandia National Laboratories
Albuquerque, NM 87185-0835

Notre Dame University
Notre Dame, IN 46556

9. SPONSORING ORGANIZATION – NAME AND ADDRESS *(If NRC, type "Same as above"; if contractor, provide NRC Division, Office or Region, U.S. Nuclear Regulatory Commission, and mailing address.)*
Division of Engineering Technology
Office of Nuclear Regulatory Research
U.S. Nuclear Regulatory Commission
Washington, DC 20555-0001

10. SUPPLEMENTARY NOTES
W. Gleaves, NRC Project Manager

11. ABSTRACT *(200 words or less)*

This report summarizes Sandia National Laboratories' participation in the fire modeling activities for the German Heiss Dampf Reaktor (HDR) containment building, under the sponsorship of the United States Nuclear Regulatory Commission. The purpose of this report is twofold: 1) to summarize Sandia's participation in the HDR fire modeling efforts and 2) to summarize the results of the international fire modeling community involved in modeling the HDF fire tests. Additional comments on the state of fire modeling and trends in the international fire modeling community are also included. It is noted that, although the trend internationally in fire modeling is toward the development of the more complex fire field models, each type of fire model has something to contribute to the understanding of fires in nuclear power plants.

12. KEY WORDS/DESCRIPTORS *(List words or phrases that will assist researchers in locating the report.)*
fire, Fire Modeling

13. AVAILABILITY STATEMENT
Unlimited

14. SECURITY CLASSIFICATION
*(This Page)*
Unclassified
*(This Report)*
Unclassified

15. NUMBER OF PAGES

16. PRICE


Federal Recycling Program

UNITED STATES
NUCLEAR REGULATORY COMMISSION
WASHINGTON, D.C. 20555-0001

OFFICIAL BUSINESS
PENALTY FOR PRIVATE USE, $300

SPECIAL FOURTH-CLASS RATE
POSTAGE AND FEES PAID
USNRC
PERMIT NO. G-67

120555139531 1 1AN
US NRC-OADM
DIV FOIA & PUBLICATIONS SVCS
TPS-PDR-NUREG
2WFN-6E7
WASHINGTON DC 20555